THE JOURNAL OF CHEMICAL PHYSICS

VOLUME 11 NUMBER 1

JANUARY, 1943

Published by the
AMERICAN INSTITUTE OF PHYSICS
Lancaster, Pa. and New York, N. Y.

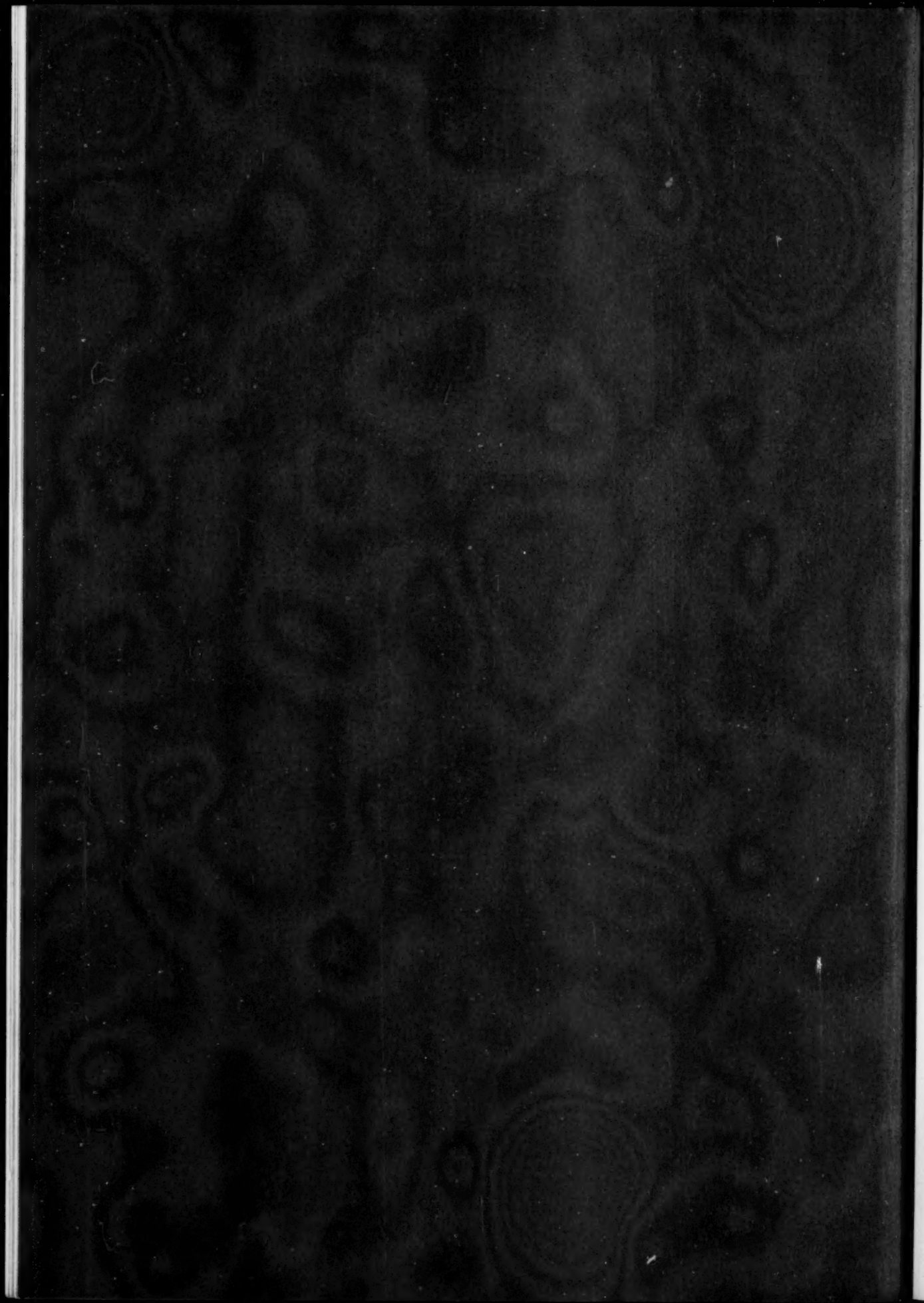

THE JOURNAL
OF
CHEMICAL PHYSICS

VOLUME 11, NUMBER 1 JANUARY, 1943

Raman Spectra of Hydrocarbons

I. 1-Octene, *cis*+*trans* 2-Octene, *trans*-3-Octene, *trans*-4-Octene, 4-Octyne, and 1-Octyne

FORREST F. CLEVELAND
Department of Physics, Illinois Institute of Technology, Chicago, Illinois

(Received September 22, 1942)

Raman frequencies, intensities and depolarization factors are reported for 1-octene, *cis*+*trans* 2-octene, *trans*-3-octene, *trans*-4-octene, 4-octyne, and 1-octyne. The experimental arrangement is described. The intensities were determined by use of a micro-densitometer. Comparison of the relative intensities obtained in the present investigation for 4-octyne with the estimated intensities obtained previously indicates that the so-called "estimated intensities" are in reality estimates of densities rather than of intensities. The relative intensities are based upon an arbitrary value of 1000 for the strongest line in the Raman spectrum. A high speed, Hilger E-518 glass spectrograph was used in obtaining some of the spectrograms. With this instrument, a spectrogram of carbon tetrachloride, from which eight lines could be measured, was obtained in one minute.

INTRODUCTION

HYDROCARBONS, especially those containing eight carbon atoms, are of commercial as well as scientific interest. The commercial interest arises primarily as a result of the promise of Raman spectra as a method of analysis of hydrocarbon mixtures. Before such an analysis can be carried out, it is necessary to secure accurate and reliable data for the pure hydrocarbons. The present paper reports Raman frequencies, intensities, and depolarization factors for 1-octene, *cis*+*trans* 2-octene, *trans*-3-octene, 4-octyne, and 1-octyne.

EXPERIMENTAL

Apparatus

Some of the spectrograms were obtained with previously described apparatus[1–3] and some were obtained with a Hilger E-518 spectrograph having a dispersion of 63A/mm at 4500A and a speed approximately 22 times that of the former spectrograph. Sharp lines could be measured to

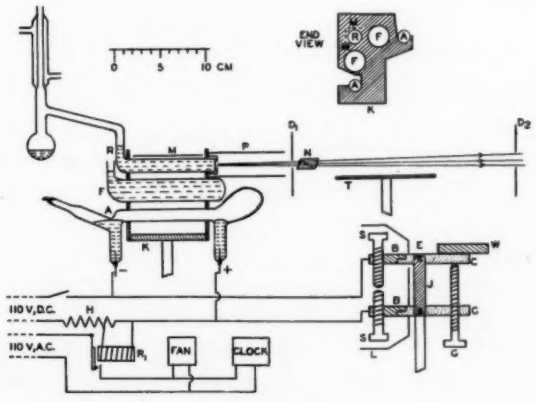

FIG. 1. Arrangement of the apparatus with the Hilger spectrograph.

[1] Forrest F. Cleveland and M. J. Murray, J. Chem. Phys. **7**, 396 (1939).
[2] Forrest F. Cleveland, M. J. Murray, H. H. Haney, and Julia Shackelford, J. Chem. Phys. **8**, 153 (1940).
[3] Forrest F. Cleveland, M. J. Murray, J. R. Coley, and V. I. Komarewsky, J. Chem. Phys. **10**, 18 (1942).

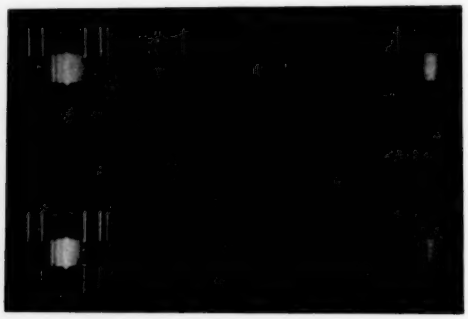

FIG. 2. Raman spectrum of *trans*-3-octene.

the nearest cm^{-1} and the over-all accuracy was 3 cm^{-1}. Excitation was by Hg 4358A. Trouble was experienced with motion of the film during the long exposures and it was therefore necessary to replace it with Eastman 103-J spectroscopic plates.

The arrangement of the apparatus is shown in Fig. 1. The letters represent the following: R_1—relay, *H*—600-watt heater element, *A*—mercury arc, *F*—filter tube, *R*—Raman tube, *M*—plane mirror, *P*, D_1, and D_2—light shields, *T*—table which supports ground glass plate and plane mirror for throwing light from the iron arc on to the slit, *N*—a Nicol prism used during polarization exposures, *S*—steel bolts, *B*—brass, *C*—Bakelite, *J*—metal strip, *W*—brass weight, *E*—pivot point, *L*—light shield, and *G*—screw for starting iron arc.

A typical spectrogram is shown in Fig. 2 and a typical polarization spectrogram is shown in Fig. 3, both made with the Hilger spectrograph.

Calibration of the Microdensitometer

The relative intensities and depolarization factors were obtained by use of a Gaertner microdensitometer. The scale reading on this instrument was proportional to the density. To calibrate the instrument, the Raman tube was removed and a white screen put in its place. A tungsten lamp, approximating a point source was placed at various distances from the screen in order to get known relative intensities of illumination on the screen. One-hour exposures were made for each position of the lamp. A calibration curve was then made by plotting the densities (at a wave-length corresponding to a Raman frequency of approximately 1400 cm^{-1}) against the relative intensities and finally a density-intensity table was prepared from this calibration curve.

To obtain the true intensity of a line, one must correct for the continuous background. This was done as follows: The density of the line D_l and the density of the background D_b were measured. Using the table, the corresponding intensities I_l and I_b were obtained. The true intensity of the line was then taken as $(I_l - I_b)$. In determining the relative intensities no correction was made for variation in the sensitivity of the plate with wave-length. Such a correction is unnecessary for the depolarization factors since the two lines of the polarization doublet correspond to light of the same wave-length. Tests showed that errors in relative intensities and depolarization factors due to inaccuracy in setting the densitometer were, in general, about 2 percent of the reported values. The errors for closely spaced lines may be considerably greater than this, however, since each line tends to spread and thus contributes to the density of the other. This is especially true of the closely spaced group of lines near 2900 cm^{-1}.

Materials

The compounds were prepared under the direction of Professor C. E. Boord, Department of Chemistry, Ohio State University. A brief summary of the methods used for the preparation of these materials is as follows:

1-Octene, $CH_3(CH_2)_5CH=CH_2$, C_8H_{16}: By

FIG. 3. Polarization spectrogram of 1-octyne.

TABLE I. The physical properties of the samples.

Compound	f.p. °C	b.p. °C	n_D^{20}	d_4^{20}
1-Octene	−102.11	121.6	1.4090	0.7150
cis+*trans* 2-Octene	− 94.04	125.2	1.4130	0.7192
trans-3-Octene	−110.0	123.2	1.4128	0.7146
trans-4-Octene	− 93.8	122.29	1.4119	0.7136
4-Octyne	−102.9	131.49	1.4247	0.7506
1-Octyne	− 79.5	126.17	1.4159	0.7457

TABLE II. Raman spectra of some octenes.

1-Octene			*cis*+*trans* 2-Octene			*trans*-3-Octene			*trans*-4-Octene		
$\Delta\nu$	I	ρ	$\Delta\nu$	I	ρ	$\Delta\nu$	I	ρ	$\Delta\nu$	I	ρ
289	10		*302*	8	0.55	289	vw		297	2	0.33
						322	22				
						397	4		372	2	0.18
433	vw		*480*	3		465	5				
[**633**]	vw					522	vw				
			762	2	0.73	745	vw		777	2	
813	4					815	12				
850	5		**835**	5	0.25	834	19		850	7	
886	11		*869*	4	0.39	873	14		871	11	
						898	20		891	27	0.26
909	11		**901**	6	0.25	929	8				
966	vw		**964**	3	0.80	962	3				
989	vw										
1014	6					1002	5		1008	4	
			1039	3	P	1040	15		1042	9	0.76
1067	12		**1057**	7	0.59	1062	37	0.56	1067	6	0.91
1079	13		**1077**	7	0.62						
1114	8		**1105**	4	0.25	1101	20	0.53	1091	13	0.39
						1154	4	0.59			
						1199	5	0.39	1204	vw	
			1253	7		1243	21	0.53	1230	13	0.56
						1281	52		1259	7	
1293	94	0.88						0.56	1290	41	0.54
			1300	40	0.64	1303	87		1304	7	
			1375	5	0.62	1375	vw				
1415	42	0.77									
1440	79	0.60	**1436**	59	0.82	1442	130	0.82	1439	69	0.81
1456	63	0.67	**1452**	58		1455	80		1451	50	0.82
1641	134	0.15	**1672**	47	0.23	1672	173	0.16	1672	150	0.19
2727	4		*2725*	4		2729	vw		2734	3	
2853	544	0.24	**2851**	351	0.18	2850	253	0.13	2838	121	0.11
2873	778	0.43	**2880**	682	0.23	2875	823	0.13	2871	68	0.17
2899	1000	0.50	**2908**	1000	0.18	2901	1000		2905	1000	0.22
2925	535	0.30	**2931**	1000		2932	861	0.13	2934	1000	0.17
2961	98	0.69	**2960**	222	0.43	2963	29	0.43	2963	193	0.50
2999	124	0.28	**3004**	37	0.34	2998	59	0.29	2997	27	0.36
3078	23	0.93									

TABLE III. Raman spectra of 1-octyne and 4-octyne.

1-Octyne			4-Octyne			1-Octyne			4-Octyne		
$\Delta\nu$	I	ρ	$\Delta\nu$	I	ρ	$\Delta\nu$	I	ρ	$\Delta\nu$	I	ρ
[*170*	14	0.37]				**1111**	9	0.36	**1095**	18	0.47
204	26	0.46							**1225**	2	
±*293*	9	0.95							**1261**	9	
±*310*	vw								**1280**	vw	
±**340**	41	0.53	**343**	vw		**1302**	15	0.69	**1295**	vw	
±*362*	vw		±**369**	52	0.68	**1323**	9	0.60	**1327**	28	0.42
403	vw								**1347**	vw	
437	vw					**1435**	48	0.68	**1440**	60	0.76
477	vw		**465**	3		**1453**	37	0.69	**1458**	47	0.87
532	vw		**549**	vw		*2066*	vw				
629	9	0.96	**670**	vw		**2118**	865	0.14			
805	2	0.16	**805**	2	P				**2234**	388	0.15
839	5	0.52							**2294**	65	0.10
882	3	0.21	**856**	13	0.47	*2726*	2	P	**2736**	3	P
			891	31	0.31	**2855**	309	0.14	**2839**	69	0.13
925	vw					**2876**	412	0.17	**2875**	465	0.06
979	1					**2908**	1000	0.16	**2906**	1000	0.06
1013	4	0.55	**1018**	vw		**2930**	614	0.18	**2936**	869	0.23
			1036	6		**2959**	62	0.76	**2965**	101	0.42
1070	6	0.72	**1070**	6		**3302**	2	P			

condensation of normal amyl magnesium bromide with allyl chloride, in 70 to 80 percent yields.

cis+*trans* **2-Octene,** $CH_3(CH_2)_4CH=CHCH_3$, C_8H_{16}: By condensation of crotyl chloride with butyl magnesium chloride to give a mixture of 2-octene (60 percent) and 3-methyl-1-heptene (10 percent).

trans-**3-Octene,** $CH_3(CH_2)_3CH=CHCH_2CH_3$, C_8H_{16}: By reduction of 3-octyne with Na in liquid NH_3 with 98 percent yield.

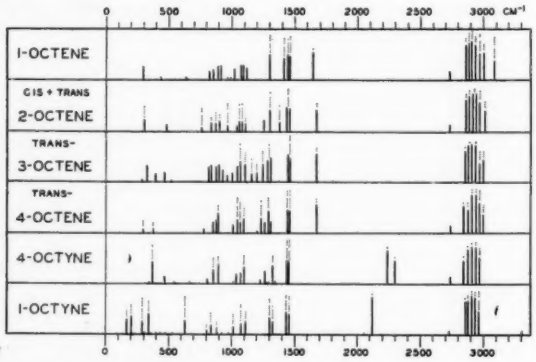

FIG. 4. Raman spectra of some octenes and octynes.

trans-**4-Octene,** $CH_3(CH_2)_2CH=CH(CH_2)_2CH_3$, C_8H_{16}: By reduction of 4-octyne by Na in liquid NH_3 with a 98 percent yield.

1-Octyne, $CH_3(CH_2)_5C\equiv CH$, C_8H_{14}: By reacting hexyl bromide and sodium acetylide in liquid NH_3 with a 70 percent yield.

4-Octyne, $CH_3(CH_2)_2C\equiv C(CH_2)_2CH_3$, C_8H_{14}: By reacting propyl bromide and $HC\equiv CNa$ in liquid NH_3 to give 1-pentyne with a 99 percent yield. The sodium derivative of the crude pentyne treated with propyl bromide in liquid NH_3 to give a 73 percent yield of 4-octyne.

The physical properties of the samples are listed in Table I.

RESULTS

The Raman data for the octenes are given in Table II and those for the octynes are given in Table III. $\Delta\nu$ is the Raman frequency in cm^{-1}, I is the intensity, and ρ is the depolarization factor. Previously observed frequencies are set in **bold face type,** brackets enclose data in regard to which there is some uncertainty, and the braces join lines which were unresolved on the polarization spectrograms. The relative intensities are based upon an arbitrary value of 1000 for the strongest line on the spectrogram, the weaker lines being rounded off to the nearest whole number because of the uncertainty introduced by the continuous background for such lines. Lines that were just visible but for which no densitometer reading could be obtained are designated by the symbol vw (very weak). Polarized lines for which the weaker component of the polarization doublet was too weak to obtain a densitometer reading are designated by the letter P. The symbol ± means that the line was observed both as a Stokes and as an anti-Stokes line. All of the relative intensities reported here were obtained from spectrograms made on the Agfa Superplenachrome Press film.

A graphical over-view of the results is given in Fig. 4. In this figure, the height of the line represents, to scale, the logarithm of the intensity and the number of dots above the line indicates, to the nearest tenth, its depolarization factor.

DISCUSSION

The Octynes

The Raman spectrum of 4-octyne has been measured previously in this laboratory.[4] All the frequencies reported here were found in the previous investigation, but four lines, two listed as doubtful and two as of very low intensity, were not found in the present study. The mean deviation in the values of the frequencies for the two investigations is 2.2 cm^{-1}. It is interesting to compare the estimated intensities reported in the previous paper with the intensities obtained

TABLE IV. Comparison of estimated intensities for 4-octyne with those obtained with the aid of the densitometer.

$\Delta\nu$	I_d	3.3 log I_d	I_e	$\Delta\nu$	I_d	3.3 log I_d	I_e
369	52	6	5	1327	28	5	5
465	3	2	2	1440	60	6	5
805	2	1	3	1458	47	6	4
856	13	4	4	2234	388	9	10
891	31	5	5	2294	65	6	6
1036	6	3	2	2736	3	2	2
1070	6	3	1	2839	69	6	5
1095	18	4	4	2875	465	9	8
1225	2	1	2	2906	1000	10	9
1261	9	3	3	2936	869	10	9
				2965	101	7	6

[4] Forrest F. Cleveland, M. J. Murray, and H. J. Taufen, J. Chem. Phys. **10**, 172 (1942).

with the aid of the densitometer in the present investigation. This is done in Table IV. The first column gives the Raman frequency $\Delta\nu$, the second column the intensity obtained with the densitometer I_d, the third column the values of $3.3 \log I_d$ (the factor 3.3 being introduced to give a value of 10 for the most intense line), and the fourth column the estimated intensities from the previous paper. As might have been expected, if it is remembered that the density is proportional to the logarithm of the intensity, it is found that the *estimated intensities* are not really estimates of the intensities but rather of the densities of the lines. The agreement between the values of I_e and $3.3 \log I_d$ is quite remarkable, the mean deviation being only 0.76.

Raman frequencies and qualitative estimates of the relative intensities for 1-octyne have been reported by Courtel[5] and by Bourguel and Daure.[6] The average deviation between the values of the fifteen frequencies reported by Bourguel and Daure and the values found in the present study is 5.7 cm^{-1}. Sixteen new frequencies were observed and the 2862 line was resolved into the doublet 2855, 2876. The weak line at 2066 cm^{-1} is probably due to the C^{13} isotope.[7] The infra-red spectrum has been investigated by Lambert and Lecomte.[8]

The Octenes

The Raman spectrum of 1-octene has been studied by several investigators[5, 9, 10] and the infra-red spectrum has been reported in graphical form by Kettering and Sleator.[11] All of the lines found by Bourguel and Piaux, except the very weak line at 362, were found in the present investigation, the average deviation being 2.5 cm^{-1}. The line at 1001 was resolved into the doublet 989, 1014.

The Raman spectrum of *cis*+*trans* 2-octene has been reported by Bourguel, Gredy, and Piaux[12] and by Gredy.[13] Bourguel, Gredy and Piaux list the frequencies 1256(aF), 1376(f), and 1658(F) as characteristic of *cis*-2-octene and 1305(aF), 1379(aF), and 1673(F) as characteristic of *trans*-2-octene. The sample used in the present investigation was supposed to be a mixture of the *cis* and *trans* isomers, but the failure to observe any trace of a line at 1658 cm^{-1} suggests that the *cis* isomer, if present, must constitute an exceedingly small percentage of the total. All of the frequencies reported by Gredy were found for the sample used in the present study, with an average deviation of 5.0 cm^{-1}. However, the double bond line was reported by Gredy as 1658, rather than the value of 1672 found here. Apparently Gredy's sample was predominantly the *cis* form, while the sample used in the present study was predominantly the *trans* form. In fact, the *trans* form in Gredy's sample and the *cis* form in the present sample must have been present in negligible percentages since the double bond line is so intense and sharp that the presence of a very small amount would be sufficient to give a line. The lines reported by Gredy at 1067 and 1447 have here been resolved into the doublets 1057, 1077 and 1436, 1452 while the line reported here at 2931 cm^{-1} was reported by Gredy as the doublet 2921, 2940. Four new lines were found in the present investigation.

No previous data seem to exist for *trans*-3-octene or *trans*-4-octene and depolarization factors have apparently not been determined for any of the six compounds, with the exception of 4-octyne.[4]

The spectrum of 1-octene contains strong lines at 1293, 1415, and 3078, which are not present in the spectra of the other octenes studied. Also, the double bond line appears at 1641, rather than at 1672 as with the other three octenes. The strong line observed near 3000 cm^{-1} for the octenes corresponds to the ethylenic C−H frequency and the weak line observed at 3302 cm^{-1} for 1-octyne corresponds to the acetylenic C−H frequency.

[5] R. Courtel, Diplôme d'études supérieures (Paris, 1932).
[6] M. Bourguel and P. Daure, Comptes rendus **190**, 1298 (1930); Bull. Soc. Chim. **47**, 1349 (1930).
[7] Cf. Forrest F. Cleveland and M. J. Murray, J. Chem. Phys. **9**, 390 (1941).
[8] P. Lambert and J. Lecomte, Ann. de physique **10**, 503 (1938).
[9] M. Bourguel, Comptes rendus **193**, 934 (1931); **194**, 1736 (1932).
[10] M. Bourguel and L. Piaux, Bull. Soc. Chim. **2**, 1958 (1935).
[11] C. F. Kettering and W. W. Sleator, Physics **4**, 39 (1933).
[12] M. Bourguel, B. Gredy, and L. Piaux, Comptes rendus **195**, 129 (1932).
[13] B. Gredy, Bull. Soc. Chim. **2**, 1029 (1935); **3**, 1101 (1936).

ACKNOWLEDGMENTS

The hydrocarbons used in this work were prepared under the direction of Professor C. E. Boord of the Department of Chemistry of the Ohio State University as part of the American Petroleum Institute Hydrocarbon Research Project in the Industrial Research Foundation of the University. The micro-densitometer used in the intensity measurements was obtained with a grant made to the author from the Penrose Fund of the American Philosophical Society. The Hilger spectrograph was obtained, in part, with a grant made to the author from the Permanent Science Fund of the American Academy of Arts and Sciences. The author wishes to express his appreciation for this assistance. He also wishes to thank Professor W. W. Colvert, of the Department of Physics, for making the enlargements used in Figs. 2 and 3.

JANUARY, 1943 JOURNAL OF CHEMICAL PHYSICS VOLUME 11

The Activation Energy of the Reaction $CH_3+HBr=CH_4+Br$ and the Carbon-Hydrogen Bond Strength in Methane

HOLGER C. ANDERSEN* AND G. B. KISTIAKOWSKY
The Department of Chemistry, Harvard University, Cambridge, Massachusetts

(Received October 1, 1942)

Mixtures of hydrogen bromide, methyl iodide, and iodine have been illuminated with ultraviolet light, and the rate of formation of methane as a function of the relative concentrations has been determined. With iodine absent from the system, a maximum amount of methane is formed, due to the absence of recombining reactions of methyl radicals and iodine. A comparison of the amount of methane produced with iodine present in various amounts with that produced when iodine is absent enables one to calculate the relative rates of the reactions

$$CH_3+HBr=CH_4+Br,$$

$$CH_3+I_2=CH_3I+I,$$

when the relative steric factors of the two reactions are assumed to be approximately the same as for the reactions

$$H+HBr=H_2+Br,$$
$$H+Br_2=HBr+Br.$$

This leads to an activation energy of 1.5 kcal. for the methyl-hydrogen bromide reaction, which, combined with the activation energy of the reverse reaction as determined by Van Artsdalen, yields a binding energy of 102 kcal. for CH_3-H.

VAN ARTSDALEN[1] has recently studied exhaustively the kinetics of the methane-bromine reaction, and his results show conclusively that the formation of methyl bromide proceeds according to a chain mechanism:

$$Br_2+h\nu=2Br \quad \text{or} \quad Br_2+M=2Br+M, \tag{1}$$

$$Br+CH_4=CH_3+HBr, \tag{2}$$

$$CH_3+Br_2=CH_3Br+Br, \tag{3}$$

$$CH_3+HBr=CH_4+Br, \tag{4}$$

$$Br+Br+M=Br_2+M. \tag{5}$$

The over-all temperature dependence of the reaction is that of the slowest step, namely (2), and the activation energy of (2) was determined as 17.8 kcal., with a considerable degree of precision. A knowledge of the activation energy of the reverse reaction would then yield the over-all energy of reaction. The method and results of a series of experiments designed to measure this quantity have already been alluded to in a preliminary note,[2] and will be described more fully in this paper.

The method we have employed in seeking the activation energy of

$$CH_3+HBr=CH_4+Br \tag{4}$$

* Present address: Distillation Products, Inc., Rochester, New York.

[1] E. R. Van Artsdalen, to be published shortly.

[2] Andersen, Kistiakowsky, and Van Artsdalen, J. Chem. Phys. **10**, 305 (1942).

consists in the production of methyl radicals in a hydrogen bromide atmosphere, followed by an analysis of the gaseous products, with special emphasis on the methane yield. In considering the possible sources of methyl radicals, the simplest and best-studied case seemed to be that of the photolysis of methyl iodide, and this was accordingly chosen.

The photolysis has been studied by Emschwiller,[3] Spence and Wild,[4] and most recently by West and Schlessinger,[5] whose proposed mechanism is well supported by a considerable amount of analytical data. The low quantum yield of decomposition, which was found by most of the workers, is explained on the basis of a primary dissociation

$$CH_3I+h\nu=CH_3+I,$$

followed by a rapid recombination.

The photochemical production of methyl radicals in the system chosen by us unfortunately involves the production of hydrogen atoms as well, *viz.*,

$$HBr+h\nu=H+Br,$$

and the fate of the very active hydrogen atoms must be considered. However, Chadwell and Titani[6] have shown that hydrogen atoms react with alkyl halide molecules on every collision:

$$H+RX=R+HX.$$

The effect is therefore equivalent to increasing the methyl radical concentration, and consequently no real difficulty is encountered from this source. The decomposition of hydrogen bromide was utilized to measure the relative light intensities in various experiments.

The formation of methane by step (4) being only one possibility among a number of methyl radical reactions, it was necessary to relate it always to some known reaction. The most convenient choice appears to be the combination of methyl radicals and iodine:

$$CH_3+I=CH_3I, \quad (6)$$

$$CH_3+I_2=CH_3I+I, \quad (7)$$

$$CH_3+I+M=CH_3I+M, \quad (8)$$

any of which proceeds with essentially zero activation energy, a statement which we shall attempt to justify later. Deferring proof that the second of these is the preponderant methyl-removing reaction, we then see that the competitive reactions are, in the main

$$CH_3+HBr=CH_4+Br, \quad (4)$$

$$CH_3+I_2=CH_3I+I, \quad (7)$$

and that a knowledge of the rate of methane formation as a function of the hydrogen bromide: iodine ratio will lead directly to a ratio of the type

$$\frac{\text{Rate of formation of methane}}{\text{Rate of formation of methyl iodide}}=\frac{A_4e^{-E_4/RT}}{A_7e^{-E_7/RT}}.$$

Since the ratio of A factors is known from highly plausible analogies with the hydrogen-bromine reactions, the only unknown remaining is E_4.

EXPERIMENTAL

Paragon Testing Laboratory methyl iodide was fractionated in a 3-foot glass-packed column; the middle third, boiling at 42.0–42.1° (755 mm) was collected, dried over anhydrous calcium sulfate, and given two bulb-to-bulb distillations in high vacuum. It was kept under an Apiezon-greased stopcock; in ice, and protected from the stray room light, it remained colorless for about two months. Hydrogen bromide was prepared from electrolytic hydrogen and reagent bromine, by direct combination, according to the method of *Organic Syntheses*, Vol. XV, p. 35. This was stored in a 6-liter flask, after removal of non-condensable gases with the usual high vacuum treatment. Iodine was of Mallinckrodt Analytical Reagent grade, used without purification.

The photolysis cells were simple quartz tubes (volume 93 cc) with a graded seal to 12-mm Pyrex tubing having two side tubes: one leading to the system for filling with the vapors, the other being a "breakoffsky" (thin bulb breakable with magnetic hammer). In general, a crystal of

[3] G. Emschwiller, Ann. d. Chimie **17**, 413 (1932).
[4] R. Spence and W. Wild, Proc. Leeds Phil. Soc. **3**, 141 (1936).
[5] W. West and L. Schlessinger, J. Am. Chem. Soc. **60**, 961 (1938).
[6] H. M. Chadwell and T. Titani, J. Am. Chem. Soc. **55**, 1363 (1933).

iodine was placed in the bottom of the cell, and after evacuation and flaming, the desired pressures of hydrogen bromide and methyl iodide were admitted, as measured on a quartz spiral null manometer. The gases were condensed in liquid air, and the cells sealed away. The cells were then placed in an oven at 60°, and allowed to equilibrate for several hours (several blank runs showed complete absence of dark reaction under these conditions). After temperature equilibration had been assured, the cells were illuminated, through a hole in the oven door, by a Hanovia high pressure mercury arc (S55), for a specified period of time. The cells were usually illuminated four at a time, in a holder, each at a distance of 20 cm from the lamp. The relative amounts of light reaching each cell were measured by placing a cell containing only hydrogen bromide and iodine in the same positions, and measuring the volume of hydrogen produced. In a few of the experiments, a different light intensity was required; for this purpose a simple screen was placed over the hole in the oven door, and again use was made of the hydrogen bromide actinometers to measure the relative light intensity.

TABLE I.

Experiment no.	Intensity in arbitrary units as measured by hydrogen bromide actinometer	Vol. CH_4 formed, cu. mm (NTP) per hour	R/In
13	1	742	729
14	1	715	702
32	0.070	46	660
29	0.055	37	670

(In computing the values in the fourth column, the gross yield of methane has been corrected for methane produced in reaction (9), as determined in an independent experiment, in which methyl iodide alone was photolyzed.)

After illumination, the cells were removed and blown onto the analytical system, which consisted of a small liquid-air trap, a Töpler pump, and a microanalysis system of the Blacet and Leighton type, designed and constructed by Dr. S. W. Benson of this laboratory. After evacuation and breakage of the breakoffsky, the liquid-air non-condensables were transferred by means of the Töpler pump into the microanalytical system, where the total volume was measured, and then an analysis for methane and hydrogen, usually in duplicate, was conducted. The volume collected varied from 40 to 1000 cu mm. A typical analysis was: 94 percent methane, 4 percent hydrogen, 2 percent inert, on a sample of 374 cu mm (NTP), obtained by illuminating 93 cc of a vapor mixture of methyl iodide (151 mm Hg, reduced to 0°C), hydrogen bromide (41 mm), and iodine (3.9 mm). Most of the analyses were by combustion, although a few hydrogen determinations with copper oxide were also performed.

RESULTS

A few preliminary experiments were performed to check, if only qualitatively, the low quantum yield of methyl iodide photodecomposition. This was done by comparing the volume of methane found from methyl iodide photolysis to the volume of hydrogen from hydrogen bromide photolysis, and making use of Warburg's value of 2 for the quantum yield of the latter. Methyl iodide was taken as absorbing completely in the region 2400–2550A, and hydrogen bromide as absorbing completely below 2300A, and limited by the transmission of quartz at 2000A. The relative light intensities in these two regions were taken from the spectral energy distribution supplied by the Hanovia Manufacturing Company. In the two experiments made, the values thus found were 0.025 and 0.021 for the quantum yield of methane formation, or about 0.05 for the quantum yield of methyl iodide decomposition, making use of West and Schlessinger's analysis of all the decomposition products (of which methane represents about 50 percent). This figure —0.05 at about 2500A—is to be compared with 0.02 and 0.06 by Emschwiller and Spence and Wild, and 0.002 (2026A) by West and Schlessinger. The significance of the low quantum yield is that the methyl radicals recombine rapidly with iodine, according to steps (6), (7), or (8), methane being formed by reactions of the type

$$CH_3+CH_3I=CH_4+CH_2I, \qquad (9)$$

as suggested by West and Schlessinger. This is fortunate for the method we have employed, as it means that the methane formed in an experiment with hydrogen bromide arises almost solely from reaction (4), with essentially none from reaction (9).

The next step was to establish the nature of

the recombination of methyl radicals and iodine, so that the relative A factors (A_4/A_7) could be computed. This was done by varying the light intensity. Consider the methyl radicals, which can disappear mainly by reactions (4), (6), and (7). [(8) may be considered equivalent to (7) in most of these experiments, the total pressure being roughly the same in all experiments.] The total rate of disappearance of methyl radicals is

$$r=k_4(\mathrm{HBr})(\mathrm{CH_3})+k_6(\mathrm{CH_3})(\mathrm{I})+k_7(\mathrm{CH_3})(\mathrm{I_2}),$$

and the fraction ultimately appearing as methane would be

$$k_4(\mathrm{HBr})/[k_4(\mathrm{HBr})+k_6(\mathrm{I})+k_7(\mathrm{I_2})].$$

The absolute rate of formation of methane would be

$$R=[k_4(\mathrm{HBr})\cdot In]/[k_4(\mathrm{HBr})+k_6(\mathrm{I})+k_7(\mathrm{I_2})],$$

where In is a factor including the light intensity. Now if (6) is the principal recombining reaction, the ratio R/In should be dependent on light intensity, since I, the iodine atom concentration, would depend on the amount of absorbed light. Within the experimental error, however, there was no dependence of this ratio on the light intensity, as shown in Table I.

TABLE II.

Exp. no.	Reactants, pressure in mm Hg, reduced to 0°C HBr	I_2*	Intensity, arbitrary units	Vol. CH_4 per hour, corrected for (9) $=R'$	R'/R_{max} ($R_{max}=716$, from Table I)	k_4/k_7
11	9.3	3.8	1.95	184 mm³	0.132	0.062
12	2.6	3.8	1	20	.028	.042
9	41	3.9	1	339	.473	.085
16	41	(0.30)†	1	572	.798	.029
25	40.3	3.5	0.82	290	.493	.084

In all of these experiments, pressure of methyl iodide was 150±2 mm.
* Taken as the vapor pressure of iodine at the furnace temperature (60°C).
† Calculated from the methane found, by means of West and Schlesinger's analyses, which indicate a final ratio $I_2/CH_4=0.38\pm0.05$ (their experiments 3, 4, and 1).

The experiments listed in this table were performed without added iodine, and hence correspond to conditions under which the methane formation is a maximum, i.e.,

$$R=R_{max}=In.$$

This formulation now leads to the simple relation

$$R/R_{max}=k_4(\mathrm{HBr})/[k_4(\mathrm{HBr})+k_7(\mathrm{I_2})],$$

which indicates the possibility of determining the ratio of k_4 to k_7 in a series of experiments with different amounts of hydrogen bromide and iodine. The R_{max} value was determined by photolyzing in the absence of added iodine for very short periods of time, so that there was essentially no competition between reactions (4) and (7), all the methyl radicals reacting with the hydrogen bromide because of the exceedingly low concentrations of other reacting substances.

TABLE III.

k_4/k_7	E_4-E_7
0.062	0.7 kcal.
.042	1.0
.085	0.5
.029	1.2
.084	0.5
	Average 0.8±0.3 kcal.

Table II lists the experiments with various ratios of hydrogen bromide: iodine, together with the computed value of the rate constant ratios, from the expression just developed.

The values in the final column may now be related to the simple bimolecular reaction expression $k=Ae^{-E/RT}$, whence

$$\frac{k_4}{k_7}=\frac{s_4\sigma_4^2[M_{\mathrm{I_2}}(M_{\mathrm{CH_3}}+M_{\mathrm{HBr}})]^{\frac{1}{2}}}{s_7\sigma_7^2[M_{\mathrm{HBr}}(M_{\mathrm{CH_3}}+M_{\mathrm{I_2}})]^{\frac{1}{2}}}e^{-(E_4-E_7)/RT},$$

where the s's represent steric factors. It is now necessary to introduce certain assumptions in regard to these steric factors, and the work of Bodenstein and Jung[7] suggests itself immediately. They found as values of the relative steric factors for the completely analogous set of reactions with hydrogen atoms

$$\mathrm{H+Br_2=HBr+Br}, \qquad (A)$$

$$\mathrm{H+HBr=H_2+Br}, \qquad (B)$$

the value $k_A/k_B=8.6$. We performed one experiment with iodine as the inhibitor of hydrogen bromide decomposition instead of bromine, and found the value 6.3, which may be considered good agreement. Although it seems unlikely that the absolute steric factors are the same for the two reaction sets, it is not unreasonable to

[7] M. Bodenstein and G. Jung, Zeits. f. physik. Chemie **121**, 127 (1926).

assume that the relative steric factors are the same. Taking the average figure 7.5, and using the numbers 3.12A and 3.7A for the kinetic theory molecular diameters of methyl and iodine, as suggested by Spence and Wild, and 3.0 for the corresponding value of hydrogen bromide,[8] the equation involving rate constants and activation energies becomes

$$E_4-E_7=2.30\,RT\log\left[(0.018)/(k_4/k_7)\right].$$

The values of E_4-E_7 calculated from the rate constant ratios of Table II are reproduced in Table III.

The approximate value of E_7 is indicated qualitatively by Gorin,[9] Bates and Spence,[10] and Ogg,[11] all of whom operate on the tentative assumption that it is zero. Again analogy may be of some use: The reaction

$$H+I_2=HI+I \qquad (10)$$

has zero activation energy.[12] The first of the following reactions, which is the ortho-para hydrogen conversion, has an activation energy equal to 7.8 kcal.,[13] while the second reaction has an activation energy variously estimated[14] as 5.5–6.3, 8, ≦9, 11±2 kcal.:

$$H+H_2=H_2+H,$$

$$CH_3+H_2=CH_4+H.$$

Rather than evaluate critically the results for the latter case, we may say that 9 kcal. is within the experimental error of all the reported values. This is only 1 kcal. different from the hydrogen atom reaction, and by extension it would seem probable that reaction (7) should have a value within about 1 kcal. of that of (10). Taking this view, we have $E_7=0.5\pm0.5$ kcal., whence E_4 is 1.3 ± 0.8, or more conservatively 1.5 ± 1 kcal., in excellent agreement with Van Artsdalen's value of 2 kcal. from measurements of the temperature dependence of hydrogen bromide inhibition of the photobromination of methane.

The energy changes of the two reactions may then be given as

$$\begin{aligned} CH_4+Br&=CH_3+HBr-(17.8-1.5),\\ HBr&=H+Br-85.8,\\ \hline CH_4&=CH_3+H-102\pm1\text{ kcal.} \end{aligned}$$

The energy of dissociation of hydrogen bromide into the elements was determined from the thermal heat of dissociation, the heat of dissociation of bromine, and that of hydrogen, as summarized by Gordon and Barnes.[15]

A comparison and critical survey of other values will be given by Van Artsdalen in his forthcoming paper.

We are indebted to Dr. R. S. Halford for many helpful suggestions in this work.

[8] L. B. Loeb, *Kinetic Theory of Gases* (McGraw-Hill, New York, 1936).
[9] E. Gorin, Acta Physicochimica **8**, 513 (1938).
[10] J. R. Bates and R. Spence, J. Am. Chem. Soc. **53**, 1689 (1931).
[11] R. A. Ogg, J. Am. Chem. Soc. **56**, 526 (1934).
[12] J. C. Morris and R. N. Pease, J. Chem. Phys. **3**, 796 (1935).
[13] W. A. Noyes and P. A. Leighton, *The Photochemistry of Gases* (Reinhold, 1940), p. 168.
[14] G. K. Rollefson and M. Burton, *Photochemistry and the Mechanism of Chemical Reactions* (Prentice-Hall, New York, 1939), Appendix III. See also F. Patat, Zeits. f. physik. Chemie **B32**, 290 (1936).
[15] A. R. Gordon and C. Barnes, J. Chem. Phys. **1**, 692 (1933).

Exchange of Radioactive Silver and Bromide with Silver Bromide Suspensions

A. LANGER
Westinghouse Research Laboratories, East Pittsburgh, Pennsylvania
(Received September 11, 1942)

The exchange of radioactive silver and bromide ions with aqueous silver bromide suspensions was studied. It was observed that both constituents of the silver bromide lattice exchange with the ions in solution. A strong dependence of the exchange rate on the amount of surface of the precipitates used, for both the silver and the bromide was observed. A pronounced difference was found in the exchange rate for bromide if dye molecules were adsorbed on the precipitate prior to the exchange experiment. The rate for silver was not affected by the presence of the adsorbed dye molecules. A discussion of these results is included.

IN a previous paper[1] it was shown that the radioactive silver exchange with silver chloride suspensions could be simply explained by assuming that the exchange mechanisms are governed mainly by a diffusion process of the radioactive silver into the lattice of the precipitate. The radioactive exchange apparently stops when a homogeneous distribution of the radioactive atoms in the solid phase is achieved. Assuming simple, idealized conditions, it was derived that for a given amount of any precipitate for a chosen fraction of complete exchange the quantity $D_T t/a^2$ or $D_T t S^2$ should be constant, where D_T is the diffusion coefficient at the temperature T, t is the time to attain the given fraction of exchange, a is the radius of the particles, and S is the surface area of the precipitate.

It is of some interest to study the exchange of both constituent ions in silver halides, since, if diffusion is the main factor determining the rate of exchange one can expect that this rate might be different for the different ions if the particular diffusion coefficients (D_T) of the ions differ. A difference in rate would result, even with the same precipitate under the same conditions. The experiments to be described are in close agreement with this line of thought and also give us a new possible explanation of similar phenomena observed in silver bromide by other investigators.

APPARATUS AND PROCEDURE

The experiments were done with the same apparatus and under the same conditions as already described.[1] The radioactive silver was prepared in the same manner as before. The radioactive bromine was produced by proton bombardment of selenium at the Rochester cyclotron.[2] The selenium thus obtained was oxidized with concentrated nitric acid and the radioactive bromine distilled over into water, with a small amount of bromine added as carrier. From the water it was extracted with chloroform

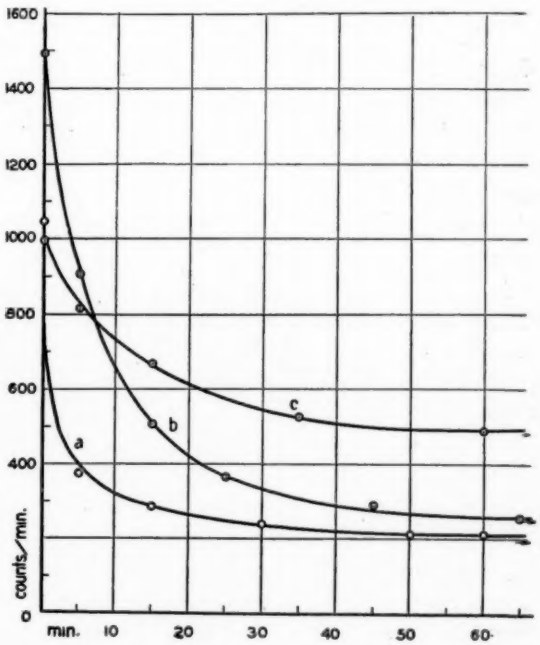

FIG. 1. Radioactive silver and bromide exchange-time curves for fresh silver bromide with different amounts of total silver or bromide in the precipitate (M_p) and in the solution (M_s) at a temperature around 25°C.

Curve:	*a*	*b*	*c*
M_p mg	107.9 Ag	79.9 Br	32.0 Br
M_s mg	24.4 Ag	16.0 Br	32.0 Br

[1] A. Langer, J. Chem. Phys. **10**, 321 (1942).

[2] J. H. Buck, Phys. Rev. **54**, 1025 (1938).

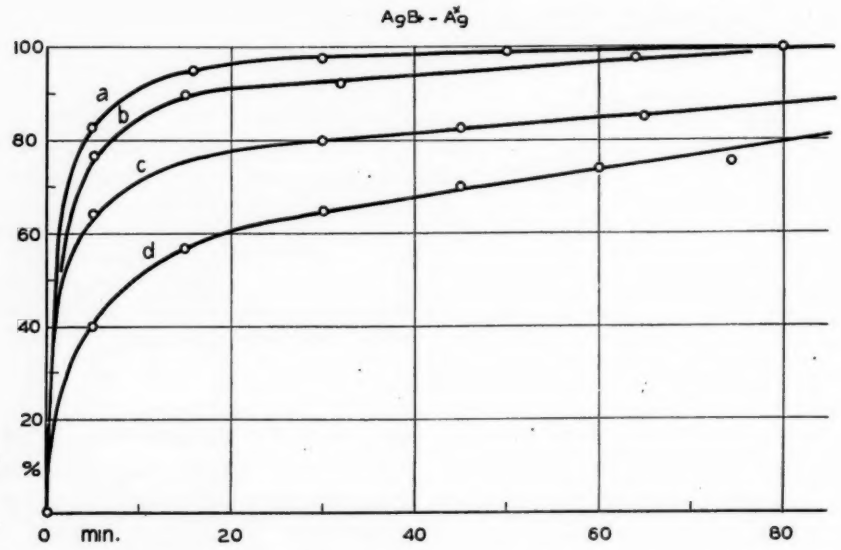

FIG. 2. Radioactive silver exchange-time curves for silver bromide of different treatments. Curves: (a) Precipitate shaken with mother liquid for 5 minutes; (b) Precipitate shaken for 2 hours; (c) Precipitate boiled in dilute nitric acid solution for 15 minutes; (d) Precipitate recrystallized from ammonia by heating and stirring. $M_p = 107.9$ mg Ag, $M_s = 23.4$ mg Ag. Temperature = 25°C.

and then reduced by shaking with a weak solution of sodium bisulfite in water. One drop of the extremely strong radioactive bromide solution in water was added to the standard sodium bromide solution used for the experiments. The starting counting rates were under $2 \cdot 10^3$ counts/minute, so that no resolving time corrections were necessary for the counter system used. Since the half-life of the bromine isotope present was 34 hours, correction for decay was applied only if it markedly affected the result. All other reagents were prepared from C.P. chemicals.

The silver bromide was prepared for most of the experiments from 10 ml 0.10 M sodium bromide containing 0.5 ml 0.1 M nitric acid. Sodium salts were used to avoid a possible interference with the detectable radioactivity of potassium. To this solution 10.1 ml of 0.10 M silver nitrate was added with slow stirring of the liquid. All the manipulations were done in photographically inactive light. The coagulated precipitates were subsequently treated as indicated in the captions of Figs. 2 and 3.

The "aged" precipitates so obtained were centrifuged at low speed for 2 minutes, the mother liquid decanted, the solids washed by shaking with 15 ml 10^{-3} M nitric acid twice, then recentrifuged and partly dried by applying a vacuum for a short time. To the still damp precipitates, 40 ml of radioactive silver nitrate or radioactive sodium bromide of known radioactive strength and silver and bromide concentrations were added and shaken. After arbitrary times, the radioactivity of the liquid was determined by filling a 6-ml volume liquid-jacketed pipette counter and counting for 4 minutes before the liquid was returned.

After the radioactive exchange experiments, the precipitates were centrifuged, washed twice with 20 ml of water, and again damp dried. They were then shaken with 10 ml of 0.01 percent solution of methylene blue for 2 hours and the amount of dye adsorbed was determined by comparison of the centrifuged clear solution with the original dye solution by means of a photometer.

To coat the surface of the precipitate with the dyes, fresh silver bromide was shaken with 1 percent water solution of methylene blue or eosin for an hour. After that the precipitate was centrifuged and the exchange experiments made with the radioactive solution.

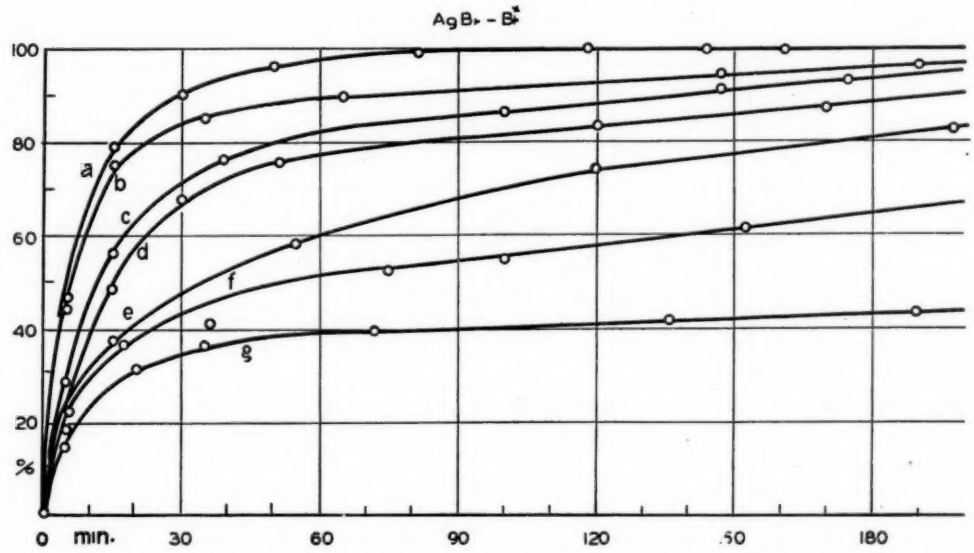

FIG. 3. Radioactive bromide exchange-time curves for silver bromide of the following origin. Curves: (a) Precipitate shaken with mother liquid for 5 minutes; (b) Precipitate boiled in the mother liquid for 5 minutes; (c) 5 ml conc. nitric acid added to mother liquid and boiled for 10 minutes; (d) The same as (c) only boiled for 20 minutes; (e) and (f) Precipitate prepared by dropping silver nitrate at different rates into dilute nitric acid solution while boiling and stirring; (g) Precipitate recrystallized from ammonia by heating and stirring the solution.

EXPERIMENTAL RESULTS

From the activity-time curves obtained with precipitates shaken with the mother liquid for 5 minutes and with a given ratio of the silver or bromide in solution and in the precipitate as are indicated in Fig. 1, it can be deduced: First, that both the silver and the bromide in the silver bromide lattice are exchanging with the silver and bromide in the solution and that similar mechanisms are probably causing both. Second, that the final radioactivity of the solution is attained after a homogeneous distribution of the

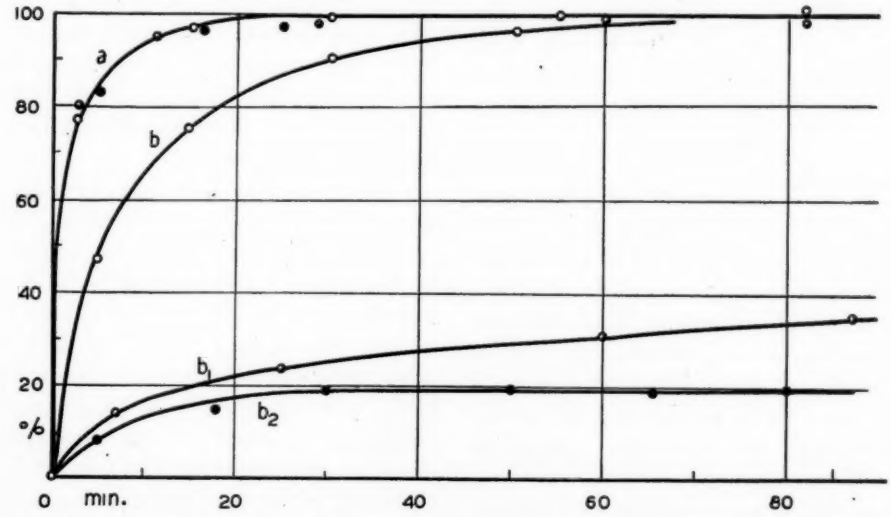

FIG. 4. Radioactive silver and bromide exchange-time curves for fresh silver bromide with dye coated surface. ○, without dye; ◑, eosin; ●, methylene blue. Curve (a) for silver $M_p = 107.9$ mg; $M_s = 23.4$ mg. Curves (b) for bromine $M_p = 79.9$ mg; $M_s = 16.0$ mg. Temperature around 25°C.

radioactive silver or the radioactive bromide is achieved, since the final activity C_∞ is given by the relation $C_\infty = C_0(M_s/M_t)$, where C_0 is the original activity of the solution and M_s/M_t is the ratio of the atoms of silver or bromide in solution to the total amount of silver or bromide atoms present in the particular experiment.

From Figs. 2 and 3 it can be deduced that the rate of exchange, under identical conditions, temperature, and amounts of precipitates, is strongly dependent on the previous treatment "age" of the used precipitates. In general, fresh precipitates exchange more rapidly than the precipitates which had a chance to mature. Dye adsorption measurement shows that the exchange is related to the amount of dye adsorbed and therefore to the surface of the precipitate used. Figure 5 indicates that the same dependence on surface area was found for the silver as for the bromide.

Quite a different picture was obtained if the fresh precipitates were first coated with methylene blue or with eosin. As seen in Fig. 4, no noticeable difference was found in the exchange of silver compared with the uncoated precipitate. In the case of bromide, however, the layer of adsorbed dye has a very pronounced effect, slowing down the rate of exchange in the case of eosin, and almost stopping the exchange when methylene blue was adsorbed after only a small fraction of bromide was exchanged. From the color of the coated precipitates it was clear that the amount of dye adsorbed was about the same in each experiment.

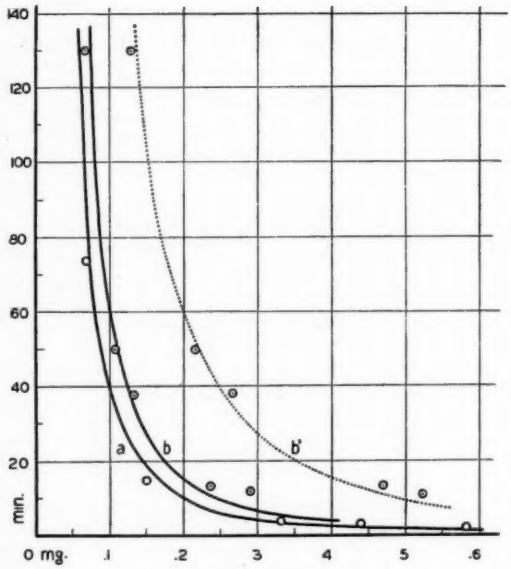

FIG. 5. Curves indicating the relation between the amount of adsorbed methylene blue in mg of dye per millimole of silver bromide and the times required to obtain 75 percent of total radioactive exchange. ○ for silver, ⊙ for bromide. The dotted curve is obtained by taking into account the difference in dye adsorption for sodium bromide and silver nitrate treated precipitates.

DISCUSSION

Returning now to experiments on precipitate uncoated with dye, if we plot the amount of dye adsorbed after the exchange process for a given constant amount of precipitate against the time to reach, for example, 75 percent total exchange as indicated in Fig. 5, we can see that here as was for silver chloride, the relation $S^2t = \text{const.}$ is quite well realized for silver as well as for the bromide. Therefore, also here the "aging" of silver bromide as observed on the exchange rates of radioactive silver or radioactive bromide can be simply explained as a crystal growth.

A strong dependence of the speed of exchange of radioactive bromide on the "age" of the silver bromide has already been noted by Polessitsky[3] and by Kolthoff and O'Brien.[4]

Polessitsky observed almost no exchange of the active bromide during two days if the silver bromide was previously melted, although fresh silver bromide exchanged rapidly. This can be expected for since the particle size, in the case of the melted silver bromide, must be very large in comparison with that of a fresh precipitate, the time to obtain a noticeable exchange may be increased enormously.

From Fig. 5 it can also be seen that for a given amount of dye adsorbed, the time to reach the same percentage of exchange is longer in the case of bromide. This difference is not very large and below a factor of two, but because of the uncertainty in the nature of the dye adsorption measurement, no quantitative significance can at present be associated with this result, which would give us otherwise the difference in the exchange rates of the silver and bromide. In one case the dye was adsorbed after

[3] A. Polessitsky, Comptes rendus Acad. Sci. U. S. S. R. **24**, 668 (1939).
[4] I. M. Kolthoff and A. S. O'Brien, J. Am. Chem. Soc. **61**, 3409 (1939) and J. Chem. Phys. **7**, 401 (1939).

shaking the precipitate with silver nitrate and in the second case with sodium bromide. From other experiments it was found that the adsorption of methylene blue on a precipitate shaken with silver nitrate is about 1.8 times larger than that of a similar precipitate shaken with sodium bromide. A factor of two was observed by Kolthoff and O'Brien.[4] This effect is probably attributable not to a change in crystal size, but to adsorption phenomena, for it is observed also after a short time of shaking.

Taking this factor into account, the rate of exchange of silver would be around six times greater than that of bromide. Whatever the uncertainty in the exact relative rates of exchange for the silver and bromide might be, these results lead to the conclusion that in the lattice of silver bromide the silver as well as the bromide is mobile and for crystals of the size used in this work, exchange rapidly with ions in solution even at room temperatures, with the silver exchanging the faster. This result apparently contradicts the observations of Tubandt[5] who, from analysis of solid silver bromide disks through which current was passed, gained the impression that only the positive silver ions move under the potential gradient through the crystal while the bromine is completely immobile. This discrepancy might involve questions of a more fundamental nature, as has been anticipated by Mott and Gurney.[6] Boundary conditions of the grains and disks might have to be considered also.

The pronounced difference in the rates of exchange of bromide for precipitates coated with methylene blue or eosin can probably be accounted for partly on the basis of the difference in the sizes of these ions, silver having an ionic radius[7] of 1.26A and bromine of 1.95A, along with a protective action of the adsorbed dye layer which impedes the passage of the larger ions to the surface of the crystal. That such a difference in the exchange rate of bromide between the dye-coated and uncoated precipitates of silver bromide exists has already been shown by Kolthoff and O'Brien.[4] They suggested that the adsorbed dye prevented the crystal from recrystallizing since they assume that a certain kind of recrystallization[8] is the necessary mechanism by which the radioactive material is incorporated into the lattice of the precipitate. Although such a mechanism of recrystallization could be quite possible, it is not a too satisfactory explanation in this case, because if the cessation of recrystallization is the only factor preventing the exchange of bromide, there is no reason why it should not equally prevent the exchange of silver; as already stated, this phenomenon was not observed. Furthermore, in a mechanism of recrystallization alone the exchange of the silver and bromide with uncoated crystals should proceed at the same rate, but the evidence here presented shows that the silver exchanges more rapidly than bromide does under otherwise identical conditions. On the other hand, the consideration of a diffusion mechanism may help to interpret more adequately the observed exchange phenomena.

[5] C. Tubandt, Zeits. f. anorg. allgem. Chemie **115**, 112 (1921).

[6] N. F. Mott and R. W. Gurney, *Electronic Processes in Ionic Crystals* (Oxford, 1940), p. 52.

[7] L. Pauling, *The Nature of the Chemical Bond* (Cornell University Press, 1940), p. 346.

[8] For details see I. M. Kolthoff and C. Rosenblum, Phys. Rev. **47**, 631 (1935) and I. M. Kolthoff, Osterreich. Chem. Zeits. No. 6 (1938).

The Specific Heat of Pure Iron at Low Temperatures[1]

K. K. KELLEY[2]
Western Region, Bureau of Mines, United States Department of the Interior

(Received October 26, 1942)

Specific-heat measurements of iron of 99.94 percent purity were determined throughout the temperature range 52° to 298°K. These measurements were undertaken because of the five sets of determinations in this region previously recorded in the literature are in disagreement, with the exception of those of Eucken and Werth and of Simon and Swain, although even these differ on an average of 1.8 percent. Present results are considered accurate on the average to within 0.3 percent, and they confirm the work of the investigators just mentioned rather than that of Rodebush and Michalek and of Griffiths and Griffiths. The entropy of iron was computed as $S_{298.16}=6.49\pm0.03$ cal./deg. (gram atom), of which only 4×10^{-4} is extrapolation below 1°K.

THE specific heat of iron at low temperatures has already been investigated by Duyckaerts[3] (1.5°–20°K), Eucken and Werth[4] (16°–206°K), Griffiths and Griffiths[5] (50°–310°K), Günther[6] (32°–95°K), Keesom and Kurrelmeyer[7] (1°–20°K), Rodebush and Michalek[8] (72°–200°K), and Simon and Swain[9] (30°–220°K). The results below 20°K, i.e., those of Duyckaerts and of Keesom and Kurrelmeyer, are in good agreement, but this is by no means true of the higher temperature measurements. Only two sets of the latter can be considered as agreeing at all satisfactorily, namely, those of Eucken and Werth and of Simon and Swain; but even these differ by as much as 3.9 percent and on the average by 1.8 percent. Then, too, measurements of true specific heat are lacking in the temperature range 220° to 298°K, except for the result of Griffiths and Griffiths at 250°K, which apparently is inaccurate. For these reasons another set of data above 20°K is not to be considered superfluous. The present paper presents such data for pure iron in the temperature range 52° to 298°K.

MATERIAL

The material used in these measurements was carbonyl iron furnished by Professor John Chipman of Massachusetts Institute of Technology five years ago while he was in the employ of the American Rolling Mill Company. It had been annealed at 1190°C in dry hydrogen until the oxygen content was reduced below 0.001 percent. The analysis furnished with the sample follows: C<0.005 percent; S<0.004 percent; Si<0.008 percent; Mn, 0.003 percent; P, 0.002 percent; Cu, 0.004 per cent; Ni, 0.031 percent; O<0.001 percent; and N nil. It was stated that several batches of material from the same source had been analyzed from time to time and were never found to contain more than the faintest trace of elements other than those reported. The purity, therefore, is very nearly 99.94 percent.

As received, the iron was in the form of strips of about 0.16×3.1×50 cm. These were cut into pieces of about 0.16×0.2×0.2 cm for filling the calorimeter. The cut material was washed several

TABLE I. Specific heat of iron (at. wt. = 55.85 grams).

T, °K	C_p cal./g atom	T, °K	C_p cal./g atom	T, °K	C_p cal./g atom
54.6	0.924	115.3	3.413	216.0	5.306
57.8	1.057	125.5	3.725	225.9	5.410
61.4	1.213	135.5	3.993	236.6	5.508
65.6	1.407	145.9	4.237	246.3	5.604
69.4	1.583	155.8	4.443	256.2	5.681
73.7	1.781	166.0	4.635	266.1	5.765
82.2	2.154	176.3	4.798	276.1	5.839
86.2	2.326	186.0	4.942	285.8	5.897
95.1	2.694	196.5	5.092	295.1	5.952
105.0	3.062	206.2	5.204		

[1] Published by permission of the Director, Bureau of Mines, U. S. Department of the Interior.
[2] Senior chemist, Western Region, Bureau of Mines.
[3] G. Duyckaerts, Comptes rendus **208**, 979 (1939); Physica **6**, 401 (1939).
[4] A. Eucken and H. Werth, Zeits. f. anorg. allgem. Chemie **188**, 152 (1930).
[5] E. H. Griffiths and E. Griffiths, Proc. Roy. Soc. London, **90A**, 558 (1914).
[6] P. Günther, Ann. d. Physik [4] **51**, 828 (1916).
[7] W. H. Keesom and B. Kurrelmeyer, Physica **6**, 364 and 633 (1939).
[8] W. H. Rodebush and J. C. Michalek, J. Am. Chem. Soc. **47**, 2119 (1925).
[9] F. Simon and R. C. Swain, Zeits. f. physik. Chemie **B28**, 189 (1935).

times with reagent-quality benzene and reannealed in vacuum (5×10^{-4} mm of Hg) in small batches in an Alundum thimble inside a porcelain tube. The annealing was accomplished by heating slowly to 890°C, the material being kept in the range 790° to 890° for over an hour, and then slowly cooling to 500°.

A large sample, 491.76 grams or 8.805 gram atoms, was used in the measurements.

SPECIFIC HEATS

The previously used method and apparatus[10] again were employed. The results, expressed in defined calories (1 calorie = 4.1833 int. joules), are reported in Table I and shown graphically in Fig. 1. The atomic weight of iron (55.85 grams) is in accordance with the 1941 International Atomic Weights.

These specific-heat measurements are considered accurate, on the average, to within 0.3 percent, but the relative agreement of the data is much better than this. No correction for impurities has been made, as the only impurity of consequence, Ni—0.031 percent, would involve a correction of only 0.01 percent at the lowest temperature studied and even less at higher temperatures.

TABLE II. Comparison of specific heat values (cal./g atom).

T, °K	Eucken and Werth	Simon and Swain	This research
50	0.71	0.73	0.72
60	1.13	1.15	1.15
70	1.58	1.62	1.61
80	2.02	2.10	2.06
90	2.44	2.51	2.49
100	2.84	2.91	2.88
110	3.21	3.30	3.24
120	3.54	3.62	3.56
130	3.84	3.88	3.85
140	4.11	4.14	4.11
150	4.34	4.34	4.33
160	4.54	4.50	4.52
180	4.88	4.82	4.86
200	5.16	5.13	5.13

In Fig. 1 also are plotted the results of previous work with the exception of the values of Duyckaerts and of Keesom and Kurrelmeyer, all of which are at temperatures below 20°K, where the specific heat is too small to be shown on a plot of these dimensions. The present work confirms the measurements of Eucken and Werth and Simon and Swain as against those of Rodebush and Michalek and Griffiths and Griffiths. The results of Günther are lower than any obtained by other workers and obviously are rather crude.

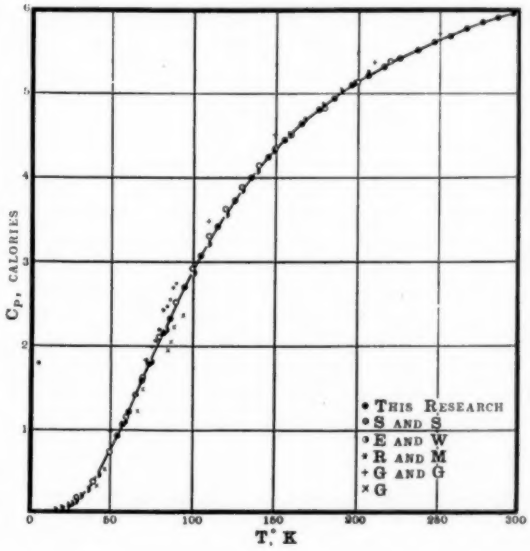

FIG. 1. Specific heat of iron.

It may be seen from Table II, wherein values at rounded temperatures are compared, that the present results average about 0.02 calorie per gram atom higher than those of Eucken and Werth and about 0.02 calorie per gram atom lower than those of Simon and Swain and that they intermediate the figures of these workers except at 150°K.

ENTROPY AT 298.16°K

The entropy of iron at 298.16°K, computed from the present measurements and those of Duyckaerts and of Keesom and Kurrelmeyer at lower temperatures, is $S_{298.16}=6.49\pm0.03$ cal./deg. (gram atom), of which only *ca.* 4×10^{-4} is extrapolation below 1°K. There is but little dif-

[10] K. K. Kelley, J. Am. Chem. Soc. **63**, 1137 (1941)

ference between this value and the previously calculated result,[11] $S_{298.16}=6.47\pm0.1$, for which the combined specific heats of Eucken and Werth and Simon and Swain were employed.

[11] K. K. Kelley, Bureau of Mines Bulletin **434** (1941), 115 pp.

SUMMARY

The specific heat of carbonyl iron of 99.94 percent purity has been measured in the temperature range 52° to 298°K.

The entropy of iron was computed as $S_{298.16}=6.49\pm0.03$ cal./deg. (gram atom).

JANUARY, 1943 JOURNAL OF CHEMICAL PHYSICS VOLUME 11

The Conductance of Aqueous Solutions of Potassium Bromide at Temperatures from 15° to 45°C, and the Limiting Mobility of Bromide Ion

H. E. GUNNING AND A. R. GORDON
Chemistry Department, University of Toronto, Toronto, Canada

(October 19, 1942)

The conductance of aqueous solutions of potassium bromide at concentrations from 0.0005 *N* to 0.01 *N* for temperatures from 15° to 45° C has been measured by the direct-current method previously employed for potassium and sodium chlorides. At 15°, there is a small logarithmic term required to represent the Shedlovsky function Λ'_0, but for 25° and higher temperatures, Λ'_0 is linear in the concentration. The limiting mobility of bromide ion is obtained from the limiting conductance and the known mobility of potassium ion; the temperature coefficients of the limiting bromide ion mobility are uniformly about 2 percent less than the corresponding values for chloride ion.

A RECENT paper[1] from this laboratory reported the conductances and ionic mobilities for aqueous solutions of potassium and sodium chlorides at temperatures from 15° to 45°C; this paper gives the corresponding conductances for potassium bromide and thus provides information as to the variation of the mobility of bromide ion with temperature. One reason for selecting this electrolyte was the fact, previously reported,[1] that potassium ion, although slightly slower than chloride ion, had the smaller temperature coefficient; bromide ion, which is slightly faster than chloride ion and is, like chloride, an anion, provides a fairer test of the often-quoted rule that the faster an ion the smaller is the temperature coefficient of its mobility.

The measurements were carried out with same direct-current apparatus used for the chlorides. The method of eliminating bias potential between the probe electrodes by current reversal, the determination of the temperature, and the general experimental technique have been previously described.[1] The probe electrodes were bromidized anodically after silver plating by electrolyzing for 30 minutes in a tenth normal potassium bromide solution at 1 ma/cm²; the "current" electrodes were covered with fused silver bromide. The potassium bromide was British Drug Houses "Analar" twice recrystallized from conductivity water; the solutions were made by gravimetric dilution with conductivity water of stock solutions; the latter were made gravimetrically from the salt, which had been rapidly fused in platinum in an atmosphere of dry CO_2-free nitrogen and conductivity water. In converting from mass to volume concentrations, density data[2] from *International Critical Tables* were employed and all weights were reduced to vacuum. As in the previous work, all conductances are based on Jones and Prendergast's "0.01 *N*" potassium chloride standard[3] at 25°C.

[1] H. E. Gunning and A. R. Gordon, J. Chem. Phys. **10**, 126 (1942).

[2] *International Critical Tables*, Vol. 3, p. 87.

[3] Grinnell Jones and M. J. Prendergast, J. Am. Chem. Soc. **59**, 731 (1937).

Table I gives the observed equivalent conductance Λ as a function of C, the concentration in moles per liter. The theoretical coefficients[4] ϑ and σ used in the calculation of the function $\Lambda'_0=(\Lambda+2\sigma\sqrt{C})/(1-\vartheta\sqrt{C})$ are given in Table II, as are also the values of Λ_0, B, and (for 15°) D involved in the Onsager-Shedlovsky equation $\Lambda'_0=\Lambda_0+BC+DC\log C$. The numbers in brackets after the entries in Table I give for comparison the difference Λ, calculated by the Onsager-Shedlovsky equation with the constants of Table II, minus Λ of Table I; it is evident that the equation gives an entirely satisfactory representation of the data. Table III gives Λ, calculated by the equation, for a few round values of the concentration.

It is interesting to note that for 25°, 35°, and 45° Λ'_0 is, within the limit of error of the measurements, linear in the concentration, and gives no hint of a $C\log C$ term; even for 15°, a linear representation of Λ'_0 would not do serious violence to the data. Potassium bromide is thus quite different from potassium and sodium chlorides; with both chlorides at 15°, there is a minimum in Λ'_0 near 0.0005 N, and Λ'_0 does not equal Λ_0 until the concentration has risen to approximately 0.0015 N. As the temperature rises, the logarithmic term becomes steadily less important, especially for the sodium salt, but for potassium chloride it has not entirely disappeared even at 45°.

Jones and Bickford[5] have reported conductances for potassium bromide solutions at 25°C, determined by means of the alternating-current bridge. Where our measurements and theirs overlap, the agreement[6] is highly satisfactory, thus providing additional evidence for the reliability of the direct current method when properly employed.

Even in the absence of complete transference data for potassium bromide solutions, it is nevertheless possible to obtain values of the limiting mobility of bromide ion from the conductance measurements of Table III and the limiting mobilities of potassium ion—59.67, 73.52, 88.25, and 103.53 at 15°, 25°, 35°, and 45°, respectively (see Tables V and VI of reference 1). It must be recognized of course that the accuracy of the resulting $\lambda_-°$ of Table IV below depends essentially on the reliability of the transference and conductance measurements previously reported.[1] The excellent agreement of our results with the best existing data for both potassium and sodium chloride solutions at 25°C and with those for potassium chloride solutions at 15°C. and the self-consistency of the conductance and transference measurements for both salts at all temperatures argued strongly in favor of their accuracy. Nevertheless, Li and Fang[7] have recently reported conductances for potassium chloride which disagree with ours at their higher temperatures by more than the rather

TABLE I.

$10^4\cdot C$	Λ	$10^4\cdot C$	Λ
15°C		25°C	
5.1236	121.22(−2)	4.9837	149.60(+1)
10.5567	120.50(+1)	10.8425	148.66(0)
20.727	119.61(+2)	21.043	147.54(0)
33.380	118.86(−2)	34.815	146.43(+1)
53.399	117.87(+1)	51.481	145.43(−2)
76.756	117.03(−2)	72.021	144.38(0)
100.774	116.26(+2)	97.851	143.33(−1)
35°C		45°C	
4.6538	179.86(−2)	4.7587	211.16(−1)
9.9127	178.76(−1)	10.6113	209.71(0)
19.693	177.36(+1)	20.146	208.07(+4)
32.977	176.01(+1)	33.843	206.44(+1)
49.427	174.72(+2)	50.922	204.87(−4)
75.139	173.17(−1)	74.341	203.10(−1)
100.285	171.94(−1)	100.955	201.47(+1)

TABLE II.

	15°	25°	35°	45°
Λ_0	0.2249	0.2289	0.2335	0.2387
ϑ	23.38	30.09	37.60	45.72
σ	122.84	151.67	182.32	214.18
B	104.5	108	143	165
D	6.5	0	0	0

[4] See footnote 13, reference 1.

[5] Grinnell Jones and C. F. Bickford, J. Am. Chem. Soc. 56, 602 (1934).

[6] The second line of the table below gives Jones and Bickford's observed equivalent conductance, increased by 0.021 percent to conform with Jones and Prendergast's calibration (see footnote 14 of reference 1). The third line gives Λ calculated from Table II.

$10^4\cdot C$	2.5	3.6	5.0	7.5	10.0	16.0
Λ (J. and B.)	150.19	149.90	149.58	149.15	148.81	148.05
Λ calc.	150.20	149.91	149.60	149.15	148.78	148.05
$10^4\cdot C$	20	50	100			
Λ (J. and B.)	147.67	145.50	143.18			
Λ calc.	147.64	145.49	143.23			

[7] N. C. C. Li and H. Fang, J. Am. Chem. Soc. 64, 1544 (1942).

large apparent error of their experiments.[8] In view of the importance of having a well-established temperature scale for ionic mobilities so that temperature coefficients for other ions can be obtained simply from conductance measurements on an appropriate electrolyte, it would seem desirable to consider briefly the possible cause of the discrepancy. The only error which could affect all our data—both conductance and transference—for both salts would be some

TABLE III. Λ.

$10^4 \cdot C$	0	5	10	20	50	100
15°	122.84	121.22	120.57	119.69	118.02	116.30
25°	151.67	149.60	148.78	147.64	145.49	143.23
35°	182.32	179.76	178.74	177.34	174.70	171.94
45°	214.18	211.07	209.84	208.13	204.91	201.53

gross error in our higher temperatures. This seems most improbable as all temperatures were fixed by means of a platinum resistance thermometer with National Bureau of Standards certificate; moreover, there is, fortunately, independent evidence that our temperatures in this range are accurate within very narrow limits.

In the course of their determination of the ionization constant of carbonic acid, Shedlovsky and MacInnes[9] measured the conductance of 0.001 *N* KCl and 0.001 *N* HCl solutions at 38°C. Their method consisted in placing the cell in a bath at 25°, measuring the conductance, then transfering it to a bath at 38°, and measuring the conductance again. Since they were concerned primarily with conductance ratios, it was unnecessary for them to take account of the change with temperature of the volume concentration and of the cell factor since these canceled for such dilute solutions in the ratio. Thus although their absolute values of Λ at 38° are subject to correction, their ratio $\Lambda_{KCl}/\Lambda_{HCl}$ at this temperature, *viz.*, 185.0/498.7, should be accurate within their estimated limit of error—0.05 percent. More recently, Owen and Sweeton[10] have made an extensive investigation of the conductance of hydrochloric acid solutions at temperatures from 5° to 65°C; their measurements correspond[11] to Λ = 501.8 for 0.001 *N* HCl at 38°. If this be combined with Shedlovsky and MacInnes' value of the ratio, Λ for 0.001 *N* KCl at 38° is 186.2; this may be compared with 186.15, the result obtained by interpolation, using mean second differences, in Table V of reference 1. It would therefore seem safe to conclude that there is some systematic error in Li and Fang's 30° and 40° measurements, and that our Tables V and VI may be used with confidence to determine the limiting mobilities of other ions.

A comparison of the limiting mobilities of bromide ion with those for chloride ion shows that bromide is definitely faster at all temperatures—roughly 3 percent greater mobility at 15°, 1.5 percent greater mobility at 45°. The temperature coefficients, also listed in Table IV, were obtained from the mobilities by the method previously described;[1] they are about 2 percent less than the corresponding $d \ln \lambda_-^\circ/dT$ for chloride, and thus conform with the rule that bromide, the faster ion, should have the smaller temperature coefficient.

TABLE IV.

	15°	25°	35°	45°
$(\lambda_-^\circ)Br_-$	63.17	78.15	94.07	110.65
$d \ln \lambda_-^\circ/dT$	0.0231	0.0199	0.0173	0.0153

In conclusion, we wish to express our thanks to Mr. G. C. Benson of this department for his assistance in making some of the measurements.

[8] This has already been pointed out by one of us, J. Am. Chem. Soc. **64**, 2517 (1942). The discrepancy is about 0.3 percent at 30° and 1.1 percent at 40°.

[9] T. Shedlovsky and D. A. MacInnes, J. Am. Chem. Soc. **57**, 1705 (1935).

[10] B. B. Owen and F. H. Sweeton, J. Am. Chem. Soc. **63**, 2811 (1941).

[11] From Owen and Sweeton's Table II, Λ'_0 for 0.001 *N* is 426.4, 489.4, 550.6, and 609.8 at 25°, 35°, 45°, and 55°, respectively; interpolation, using mean second differences, gives $\Lambda'_0 = 508.0$ for 38°. From their Table I, the theoretical coefficients for this temperature are 0.2337 and 79.56; hence Λ = 501.7, which must be increased by 0.021 percent to make it consistent with Jones and Prendergast's calibration on which our measurements are based.

Phosphorescence of Adsorbed Trypaflavine and Its Quenching by Oxygen

JAMES FRANCK AND PETER PRINGSHEIM
Department of Chemistry, University of Chicago, Chicago, Illinois

(Received September 24, 1942)

Dyes adsorbed at, or imbedded in, solids have a greater yield of fluorescence and phosphorescence than they do in liquid solutions. As an hypothesis, it is suggested that hindrance of the natural movement of the atoms in the dye molecule causes a delay in the internal conversion of excitation energy into molecular oscillation energy, thus favoring the re-emission of light. The green phosphorescence of trypaflavine adsorbed on silica gel, is half quenched by oxygen at 5×10^{-5} mm pressure; the quenching at higher oxygen pressures is much smaller than would be expected. This fact indicates that two long-lived excitation states (tautomers of trypaflavine) share in causing the green phosphorescence. The first (M_1) is very sensitive to oxygen, whereas the second (M_2) is insensitive. The phosphorescence still visible at the higher oxygen pressures owes its origin entirely to M_2. The quenching in this pressure range is due to the oxygen sensitivity of F, the unstable state responsible for the green fluorescence. Water vapor does not quench the phosphorescence. The quenching described by Kautsky is due to oxygen liberated from the gel by a process in which strongly adsorbed oxygen molecules are dislodged by water molecules.

MANY dyestuffs, trypaflavine for example, exhibit strong phosphorescence when adsorbed on silica gel. Kautsky[1] has shown that this phosphorescence is exceedingly sensitive to the quenching action of traces of oxygen. He suggests that this phenomenon might be applied to the study of the gas exchange occurring in photosynthesis. Since it is sometimes important to measure the minute amount of oxygen released by plants irradiated by a single light flash, we decided to determine whether the phenomenon observed by Kautsky was sensitive enough for our purposes. The data available in the literature are only qualitative. We therefore measured quantitatively the quenching of the trypaflavine phosphorescence, and also used the opportunity to study in a more general way some questions connected with the quenching problem. The following paper reporting these results is a contribution to the problem of the fluorescence and phosphorescence of adsorbed dyes.

PHOSPHORESCENCE OF ADSORBED DYESTUFFS

As early as 1896, Wiedemann and Schmidt[2] discovered that dyestuffs which, in liquid solutions, show only fluorescence, can, when imbedded in solid solvents like sugar or adsorbed on solid gels like gelatine, be excited to phosphorescence visible for several seconds. These authors found, moreover, that many dyestuffs which are not fluorescent in liquid solutions become not only fluorescent but even phosphorescent in solid solutions. They were of the opinion that there is a smooth transition from fluorescence to phosphorescence accompanied by gradual increase in the lifetime of the excited states. Vavilov and Levschin[3] proved that the phosphorescence is a distinct slow decay phenomenon superimposed upon the emission of light by fluorescence which even in solid solutions endures for only about 10^{-8} second. Jablonski[4] explained this behavior by the simple energy level diagram of Fig. 1 in which M is a "metastable state." By light absorption, the molecules are raised to the excited state F from which (after the loss of some vibrational energy)

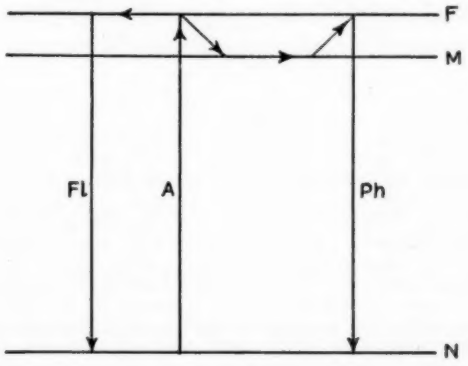

FIG. 1.

[1] H. Kautsky and A. Hirsh, Zeits. f. anorg. allgem. Chemie **222**, 126 (1935).
[2] E. Wiedemann and G. C. Schmidt, Ann. d. Physik **58** 103 (1896).
[3] S. I. Vavilov and V. L. Levschin, Zeits. f. Physik **35**, 920 (1926).
[4] A. Jablonski, Zeits. f. Physik **94**, 38 (1935).

they return to the ground state N by emission of fluorescence. Some of the molecules, however, pass from F to M; in liquid solutions they are somehow "quenched" during their stay in M, but in solid solutions they are more effectively "protected" against quenching influences. Thus they can return to F, when the energy difference F–M is provided by the thermal fluctuations; the subsequent passage F–M produces a phosphorescence emission of the same wave-lengths as in the fluorescence.

By chemists the term "metastable state" has long been used with a rather general meaning. In the terminology of spectroscopists, however, metastable states are defined as atomic or molecular states from which transitions to all lower electronic levels are forbidden by the well known selection rules.

According to Franck and Livingston,[5] the existence of long-lived excited states in dyestuff phosphorescence is due to quite a different cause. These authors regard the metastable states in question as unstable tautomeric forms of the original compound. The transition of the tautomeric form to the original one by light emission is then "forbidden" by the nuclear configuration (Franck-Condon principle)* and not by the normal selection rules. To emphasize the different cause of this metastability we propose to use the name "quasistability." This term was applied by Pringsheim[6] to long-lived excitation states in some crystal phosphors where the longevity can also be explained by the Franck-Condon principle.

The increase in fluorescence yield and the appearance of phosphorescence observed when dyestuffs are adsorbed on or imbedded in solids has been ascribed by different authors[7] to a loss of natural mobility of the atoms within the molecules. But so far, there is no satisfactory explanation why loss of mobility should have such an effect. We propose an interpretation based on the tautomer hypothesis mentioned above. An excited dye molecule, like all other complicated molecules, can either re-emit light by fluorescence or else transfer its total excitation energy into oscillation energy of the molecule in the electronic ground state by a process called "internal conversion." This radiationless transition occurs as soon as the atoms composing the molecule, by virtue of their heat motions, reach a certain configuration. The excessive oscillation produced by the internal conversion is either quickly dissipated by interaction with the surrounding molecules or else partially stored by the transition of the dye molecule to some tautomeric form with a higher energy content. In the first case the light emission is quenched by the internal conversion in the second, the tautomeric states cause phosphorescence, just as do the metastable states in Jablonski's energy scheme. Whether the phosphorescence is quenched by oxygen or other gases depends upon the reactivity of the particular tautomer towards the gas molecules. The quasistable states are of course subject to internal conversion, just as are the normal excitation states. According to this interpretation, all the factors which influence the system of proper frequencies of the original dye molecules must obviously alter the fluorescence yield and the duration of the phosphorescence by changing the average time lapse between the moment of excitation and the moment of internal conversion. Every influence which hinders the natural movement by reducing the amplitudes of certain proper modes of oscillation is apt to prolong this time lapse, and thus to increase the intensity of fluorescence and the duration of phosphorescence. It may be mentioned that we are here using the word tautomerism in a broader sense than that in which it is usually employed. The great amount of energy involved in the processes under discussion may cause intramolecular rearrange-

[5] J. Franck and R. Livingston, J. Chem. Phys. **9**, 184 (1941).

* The term "forbidden," as in the electronic selection rules, does not mean that the corresponding radiating transition never occurs under any conditions. The transition becomes possible, if the "tautomer" is brought by temperature fluctuations into a configuration which can also be reached in the ground state of the normal molecule. If such a configuration has a very small probability it is attained only after a long time; the corresponding transition is then "forbidden." If the tautomerism involves only the usual hydrogen atom shift, then the indeterminacy of position prevalent at absolute zero may suffice to bring the molecule into the critical configuration. We ascribe the long wave luminescence bands observed at low temperatures in the after glow of almost every dyestuff to this type of forbidden transition. The yellow trypaflavine band mentioned in a later paragraph is an example.

[6] P. Pringsheim, Rev. Mod. Phys. **14**, 132 (1942).

[7] For instance G. N. Lewis and M. Calvin, Chem. Rev. **25**, 273 (1939), and G. N. Lewis, D. Lipkin, and T. T. Magel, J. Am. Chem. Soc. **63**, 3005 (1941).

ments more extensive than the mere shift of hydrogen atoms; heavier radicals may also be transferred to new positions.

The main facts known about the phosphorescence of trypaflavine are the following. This dye shows fluorescence but no phosphorescence in aqueous solution. If adsorbed on silica gel, paper, gelatine, etc., it becomes phosphorescent. Pringsheim and Vogels[8] found that the afterglow of trypaflavine is connected with the presence of two separate quasistable states M_1 and M_2. The main green phosphorescence is caused by the return from M_1 to F_1, whereas a forbidden transition from M_2 to the ground state gives rise to a yellow afterglow which is relatively weak at room temperature but prevalent at low temperatures. The half-life of M_1 is about 0.3 sec. at room temperature, whereas that of M_2 is 1.2 sec. under the same conditions. All observers agree that the green phosphorescence is very sensitive toward oxygen; the yellow afterglow (according to Pringsheim and Vogels) is insensitive.

The order of magnitude of the oxygen pressure which can be detected by its quenching influence on phosphors was determined by Kautsky[1] and by Meyer and Ronge.[9] Kautsky states that, in one of his phosphors, the phosphorescence was entirely suppressed by oxygen at 3×10^{-3} mm pressure; at 5×10^{-4} mm the intensity of the phosphorescence was considerably reduced. Meyer and Ronge measured the time during which the afterglow could be visually perceived after the exciting radiation was cut off. They detected a shortening of this period by oxygen at a partial pressure of only 3×10^{-4} mm. The quenching process is connected with a photochemical reaction by which oxygen is consumed and the dyestuff oxidized.

Kautsky also studied the quenching action of other gases and found that the phosphorescence is strongly quenched by both water and ammonia. This result is surprising, since it is difficult to imagine that the excited dye molecule can react with water or ammonia if only 60 kcal. are available as excitation energy.

[8] P. Pringsheim and H. Vogels, J. de Chim. Physique **33**, 395 (1936).

[9] F. R. Meyer and G. Ronge, Zeits. f. angew. Chemie **52**, 637 (1939). Compare also K. P. Meyer, Helv. Phys. Acta **15**, 3 (1942).

EXPERIMENTAL METHOD

The trypaflavine silica gel phosphors were prepared exactly according to Kautsky's directions.* As a rule, aqueous solutions of trypaflavine somewhat less concentrated than those mentioned by Kautsky (only 0.5 to 2×10^{-5} molar instead of 5 to 25×10^{-5} molar) were used, because the gels seemed to have stronger phosphorescence when prepared under these conditions. It proved to be very important to keep the solution containing the gels in the dark during the adsorption process, in order to get homogeneously colored preparations. When a gel, immersed in the dye stuff solution is exposed to daylight, many of its grains acquire a brownish color due to a chemical reaction (oxidation). The dye solution itself (without gel), and the dried gel with the adsorbed dye on it are much less sensitive to such photochemical influences.

The gel (average grain size 0.5 mm) was introduced into small glass bulbs 1 cm in diameter. These bulbs, after having been evacuated and heated to 150°C for 2 to 4 hours, remained either attached to the mercury diffusion pump or else were sealed off. Various gases (air, tank oxygen, water vapor) were admitted through side tubes. The gas pressure was measured in the range from 10^{-5} to 10^{-1} mm by means of a McLeod manometer, in the range from 0.01 to 0.75 mm by a Pirani gauge, and in the interval between 1 mm and atmospheric pressure by a Hg column.

A simple phosphoroscope and a photoelectric cell served to determine the phosphorescence intensity. The phosphoroscope consisted of a single metal disk with a 90° open segment for light transmission. This disk rotated at a speed of 3 revolutions per second. The primary light source (a 6 v 108 watt filament lamp) and the photoelectric cell were placed on the same side of the disk. During $\frac{1}{4}$ of each rotation the parallel beam of primary light was allowed to fall through the open segment onto a mirror, from which it was

* Kautsky and all other workers with silica gel phosphors have used only the gel prepared by I. G. Farben Industrie. We, on the contrary, used a gel manufactured by the Davison Chemical Corporation (Dayco); it gave very satisfactory results. Nevertheless certain discrepancies between our observations and those of Kautsky may possibly be due to the differences between the materials used. (For details of the preparation see Kautsky.)

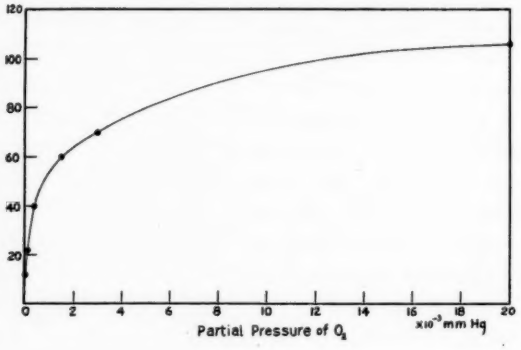

FIG. 2.

reflected; it was then focused upon the surface of the gel by a lens. Immediately after the incident light was cut off by the rotating disk, the photo-cell was exposed to the now luminescent phosphor. This photo-cell was an all glass sodium cathode cell enclosed in an air-tight metal box with a small glass window. The photo-currents were measured by observing the time T, necessary to charge a string electrometer connected with the photo-cathode up to a certain voltage (0.5 volts in some cases, 2 volts in others). T is inversely proportional to the photoelectric current, i. Any dark currents due to leakage were negligible in comparison to the photo-currents under investigation.

RESULTS AND DISCUSSION OF THE QUENCHING BY OXYGEN

The quenching influence of oxygen is shown by the curves in Figs. 2 and 3, where the values of T are plotted against the oxygen pressure. The curve in Fig. 2 contains the results up to 2×10^{-2} mm; the curve in Fig. 3 (plotted on a reduced scale) covers the range up to 150 mm which is the partial pressure of oxygen in the atmosphere under standard conditions. The curves given are examples of the results obtained. Their general shape remains constant for different gel preparations, but the absolute value of the intensity of the phosphorescence varies somewhat with the gel sample used. The high sensitivity to oxygen at low pressures shown by the intensity of the phosphorescence agrees with the results of Kautsky and of Meyer and Ronge. In the apparatus here used, the measured phosphorescence decreased to $\frac{1}{2}$ of its original intensity when 5×10^{-5} mm of oxygen was admitted; less than 10^{-5} mm of oxygen could be detected. This sensitivity seems sufficient to allow measurement of the oxygen production of plants illuminated by a single light flash. The slope of the curves decreases rapidly with increasing oxygen pressure; finally the curves become straight lines with rather small slopes. Between pressures of 10 and 150 mm the intensity of the phosphorescence changes by a factor of less than two; about four percent of the intensity in vacuum remains at 150 mm pressure. Even in air at atmospheric pressure, phosphorescence was easily visible in all the samples tested, a finding which seems to contradict Kautsky's statement that the phosphorescence is completely extinguished by oxygen at a pressure of 4×10^{-3} mm.

The shape of the quenching curves were found to be incompatible with the assumption that only one quasistable state is responsible for the occurrence of the green phosphorescence. For a phosphor with a single quasistable state, the following theory must be applied: The quenching effect of gases on fluorescence is given by the well known Stern Volmer formula

$$I=I_0/(1+cp). \tag{1}$$

I is the intensity at the pressure p of the quenching gas; I_0 is the intensity in the absence of a quencher. Thus a straight line represents either $1/I$ or T when these quantities are plotted against pressure. The same formula holds for the phosphorescence as measured by the maximum intensity which the phosphor, if excited to its equilibrium, exhibits at the beginning of its decay period. In order to fulfill this condition the illumination period must be several times as long as the lifetime of the quasistable state, whereas the period during which the phosphorescence reaches the photo-cell must be small as compared with this lifetime. If, on the other hand, the observation period is several times as long as the lifetime, then what is measured is Idt, the total amount of light emitted by the phosphor during its decay. The dependence of $\int_0^\infty Idt$ upon the pressure of the quenching gas is then given by

$$\frac{\int Idt}{\int I_0 dt}=\frac{1}{1+2cp+(cp)^2}. \tag{2}$$

In a diagram in which $1/\int Idt$ or T is plotted

against p, the curve is concave upwards; eventually it approaches a quadratic. The excitation and observation periods characteristic of the apparatus here used should give a curve which, at very low pressure is concave upwards, but not as steep as indicated by formula (2). With rising pressure of the quencher, the lifetime of the phosphor becomes smaller, and the conditions for formula (2) are rigidly fulfilled.*

As mentioned above, the observed curves have a shape very different from that expected. In the steep part at low pressures, where the sensitivity against oxygen is great, the slope, instead of increasing, decreases; in the region of higher pressures there is a rather low linear rise instead of a quadratic curve. We are therefore forced to assume that the rest phosphorescence observed at higher pressures does not come from the same source as the bulk of the phosphorescence observed at lower oxygen pressures. It is natural to assume that the second quasistable state M_2 of the trypaflavine observed by Pringsheim and Vogels is responsible for the green phosphorescence at higher pressures. According to these authors, M_2 is not sensitive to oxygen. Indeed if the slow rise of T at high pressures were caused by the small sensitivity of M_2 towards oxygen, the curve should be concave upwards. The assumption that the quenching at high pressure is due to a small sensitivity of state F toward oxygen is, however, in accord with the observations. To test this hypothesis measurements were made of the intensity of the fluorescence in vacuum and in air at atmospheric pressure.

The fluorescence was excited with ultraviolet light by irradiating a gel sample with the light of a mercury arc filtered through a Wood filter. The intensity of the fluorescent light was measured photoelectrically; a yellow filter served to absorb the scattered ultraviolet and violet light. In air at atmospheric pressure, the intensity decreased to about 40 percent of its value in vacuum. The slope of the fluorescence quenching curve is therefore, within the limits of error, the same as the slope of the phosphorescence quenching curve between 5 and 150 mm. In evaluating the errors of these measurements, it must be taken into account that they are made with different samples of the gel.

Pringsheim and Vogels assumed that M_2 contributes nothing to the green phosphorescence. But the assumption (to which we are forced in our effort to explain our quenching curves) that M_2 contributes a small percentage is not incompatible with the observations of these authors; it even explains their finding that, at room temperature, neither the decay of the green nor the decay of the yellow afterglow follows a strictly logarithmic curve. The percentage which M_2 contributes to the green fluorescence in vacuum can be calculated from the curves here obtained by extrapolating the straight line part of the curve until it cuts the axis. The intercept lies at a value of T which is 10 to 15 times higher than T_0, the starting point of the quenching curve in the absence of oxygen. Thus the contribution of M_2 in vacuum is five to ten percent of that of M_1.

QUENCHING BY WATER VAPOR

According to Kautsky, water vapor quenches the phosphorescence of the trypaflavine silica gel. This observation and the difficulty of interpreting it was mentioned in paragraph two.

In the present experiments dealing with this problem, a side tube containing a few cc of distilled water was sealed to the apparatus. Great care was taken to free the water from oxygen by boiling it while the mercury pump was running until about half of it had distilled away. The remaining water was frozen in a bath of liquid nitrogen; the gel was then heated in the usual way to 150°C in a high vacuum. Subsequently

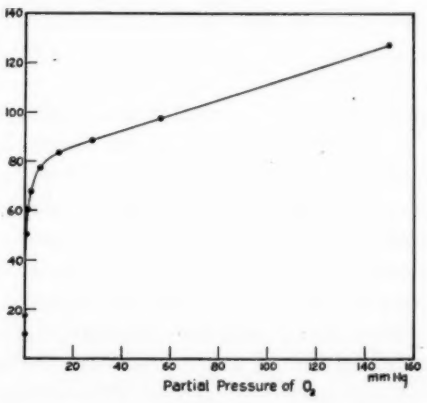

FIG. 3.

* The authors are indebted to Dr. E. Rabinowitsch for very valuable remarks, which helped greatly to clarify some points in the theoretical discussion presented above.

the side tube containing the ice container was gradually heated to temperatures between −70°C and +25° corresponding to water vapor pressures from 1.9×10^{-3} mm to 35 mm. The results were much more erratic than those obtained when oxygen was used as a quenching agent; differences in the preparation of the gels were found to cause large discrepancies.

Admission of 2×10^{-3} mm of water vapor to a freshly prepared gel quenched phosphorescence to about 25 percent of its original brightness. Freezing out the water while the pump was running immediately restored the intensity to its initial value. Repetition of the same treatment resulted in decreased quenching, even with increased water vapor pressure. The quenching influence of the water is therefore not a function of its pressure. This influence depends on the presence in the gel of a substance which is mobilized by the water and gradually removed by repeated treatment with water vapor. We suspected that oxygen adsorbed at the interfaces of the gel was displaced by water (because of the greater heat of adsorption of the latter substance) and that oxygen alone was responsible for the quenching. Experiments were therefore carried out to determine whether sufficient permanent gas to account for the quenching was evolved by admission of gas-free water to the gel. Experiments with a second air trap placed between the gel and the McLeod gauge revealed that such was indeed the fact. The first admission of water sometimes gave amounts of gas sufficient to produce a pressure of a few thousandths of a millimeter of mercury; repetition of the process gave rapidly diminishing quantities. The total output of gas was dependent on the duration of the heating period and the temperature to which the gel was heated during its preparation. In some experiments the gel was heated for three hours to 300°C (instead of the usual 150°C) without apparent destruction of the dye. In these instances, the quantity of evolved permanent gas was considerably reduced. Since oxygen is used up photochemically during the illumination, tests were made to determine whether the phosphorescence which had been partially quenched by the admission of water could be restored to its vacuum value by strong irradiation. The result corresponded to expectation. The recovery was complete as long as the pressure of the water was not too high, but only partial if water vapor of 10–30 mm pressure was used. According to Pringsheim and Vogels,[10] the polarization of the fluorescence from trypaflavine silica-gel phosphors is reduced by the presence of water vapor, because, when a water layer is formed on the surface of the gel, the dye molecules acquire a certain degree of mobility. Such an increase would also raise the probability of internal conversion, and would thus partially quench the phosphorescence, even if all oxygen were photochemically removed. The dye, after it had been submitted to irradiation in the presence of water vapor, showed the discoloration typical of oxidation. The particular gel grains directly exposed to the strongest irradiation became quite brown and permanently lost a part of their power to phosphoresce. That the water vapor did not itself take part in the photochemical reaction was shown by measurements of water pressure with a Pirani gauge before and after the irradiation.

Finally it was proved directly by a rough gas analysis that the gas evolved was at least in part oxygen. The gas was mixed with about twice its volume of hydrogen admitted through the walls of a palladium tube. The gas mixture was compressed into the capillary of the McLeod gauge until its pressure was raised to several mm of mercury. An electrodeless discharge produced by touching the capillary with an induction coil vacuum tester caused an immediate reduction of the gas volume, which indicated that $\frac{1}{2}$ of the original gas was oxygen. This amount is quite enough to have caused the observed quenching. The rest of the gas may be nitrogen, but probably some ammonia not entirely condensed in the liquid-air trap is also present.

ADSORPTION OF AMMONIA

Ammonia is adsorbed by the gel during its preparation. In Kautsky's method, iron is removed from the crude gel by a treatment with sulfuric acid. Most of this acid is then removed by rinsing the gel with distilled water; the rest is neutralized with dilute ammonia. Even if just enough ammonia to neutralize the acid in the

[10] Peter Pringsheim and H. Vogels, J. de Chim. Phys. **33**, 261 (1936).

liquid is added, the gel adsorbs considerable amounts of ammonia which cannot be removed either by rinsing with water, or by heating in vacuum to 150°C.

However, a great part of this ammonia can be removed by heating the gel (before the dye is added) in an open porcelain container for several hours at 500°C. The gas rising from the surface of the gel contains enough ammonia to color an indicator paper; the ammonia can also be detected by its smell. Excessive heating of the gel changes its structure; hence gel treated as just described was used in only a few of the experiments here reported. Ammonia contained in a gel prepared in the usual way can (like oxygen) be partially dislodged by water vapor. If the apparatus described above is used to demonstrate the evolution of oxygen, the bulk of the ammonia set free by water vapor is caught together with water in the second air trap. If the oxygen is pumped off and the liquid-air bath then removed from this trap for a short time, some of the ammonia together with a small amount of the water evaporates. When this gas is compressed into a small volume in the capillary of the McLeod gauge, pressures which much surpass the vapor pressure of water at room temperature may be measured. An electric discharge through this gas causes an expansion, due to the decomposition of ammonia into nitrogen and hydrogen.

Ammonia is more difficult than oxygen to remove from the gel. It therefore seems justified to assume that oxygen can be dislodged from the gel by ammonia in a manner similar to that in which it is liberated by water. We therefore conclude that the quenching action of ammonia observed by Kautsky like the apparent quenching by water vapor was probably due to oxygen. Since we were mainly interested in the influence of oxygen or water we performed no direct experiments to test this hypothesis.

JANUARY, 1943 JOURNAL OF CHEMICAL PHYSICS VOLUME 11

The Asymmetric Rotor

I. Calculation and Symmetry Classification of Energy Levels

GILBERT W. KING, *Arthur D. Little, Inc., Cambridge, Massachusetts,*
R. M. HAINER, AND PAUL C. CROSS, *Brown University, Providence, Rhode Island*

(Received September 30, 1942)

A table of energy level patterns for rigid asymmetric rotors is given, by means of which this approximation to the rotational energies of all molecules up to $J=10$ may be readily evaluated. The symmetry classification of each level is determined and expressed in terms of the K values of the limiting prolate- and oblate-symmetric rotors. A simple method is developed for calculating the transformation which diagonalizes the energy matrix and is applied to the derivation of perturbation formulas.

I. INTRODUCTION

THE fundamental theory of the asymmetric rotor has been discussed many times, and the equations defining the energy levels derived by various methods.[1–8] The selection rules have been satisfactorily stated, but no complete classification of the symmetry properties has been given to date. Part of the discussion to follow is accordingly devoted to the characterization of the levels by the representations of the Four-group to which their wave functions belong. The notation will be consistent with that recently proposed by Mulliken.[9] The remainder of this

[1] E. E. Witmer, Proc. Nat. Acad. Sci. **13**, 60 (1927).
[2] S. C. Wang, Phys. Rev. **34**, 243 (1929).
[3] H. A. Kramers, and G. P. Ittmann, Zeits. f. Physik **53**, 553 (1929); **58**, 217 (1929); **60**, 663 (1930).
[4] O. Klein, Zeits. f. Physik **58**, 730 (1929).
[5] H. B. G. Casimir, *Rotation of a Rigid Body in Quantum Mechanics* (J. B. Wolter's, The Hague, 1931).
[6] H. H. Nielsen, Phys. Rev. **38**, 1432 (1931).
[7] D. M. Dennison, Rev. Mod. Phys. **3**, 280 (1931).
[8] B. S. Ray, Zeits. f. Physik **78**, 74 (1932).
[9] R. S. Mulliken, Phys. Rev. **59**, 873 (1941).

paper considers in some detail the methods of calculating the energy levels. Tables of $E(\kappa)$ *vs.* κ are given to $J=10$, where κ is the convenient parameter of asymmetry introduced by Ray.[8] General methods for obtaining perturbation formulas are discussed, and the numerical coefficients for the expansions about the limiting symmetric rotors ($\kappa=\pm1$) and the "most asymmetric" rotor ($\kappa=0$) are given. The determination of the latter necessitated the evaluation of the transformations which diagonalize the energy matrix for $\kappa=0$. These transformations will later be applied to the evaluation of the Einstein coefficients of the asymmetric rotor.

II. ENERGY AND ASYMMETRY PARAMETERS

The energy of a rigid asymmetric rotor is expressed as

$$E(I_a, I_b, I_c)=\tfrac{1}{2}(P_a^2/I_a+P_b^2/I_b+P_c^2/I_c), \quad (1)$$

where P_a, P_b, P_c are the components of the angular momentum along the principle inertial axes a, b, c of the rotor with $I_a\leqslant I_b\leqslant I_c$ as the corresponding moments of inertia. For convenience, define

$$a=\hbar^2/2I_a, \quad b=\hbar^2/2I_b, \quad c=\hbar^2/2I_c, \quad (2)$$

whence

$$E(a, b, c)=(aP_a^2+bP_b^2+cP_c^2)/\hbar^2. \quad (3)$$

The matrices P_a, P_b, P_c may be any set of angular momentum matrices which satisfy the Poisson bracket relations. To examine the general properties of such a set of matrices, let us take a right-handed system of Cartesian axes x, y, z fixed in the rotor with the origin at the center of mass. (The 3! ways in which P_a, P_b, P_c may be identified with P_x, P_y, P_z are discussed in Sections III and IV, where the symmetry classification of the asymmetric rotor energy levels is determined.) The commutation rules are:

$$\begin{aligned} P_xP_y-P_yP_x&=-i\hbar P_z,\\ P_yP_z-P_zP_y&=-i\hbar P_x,\\ P_zP_x-P_xP_z&=-i\hbar P_y. \end{aligned} \quad (4)$$

A solution of these matrix equations is

$$\begin{aligned} (P_y)_{J,K;\,J,K+1}&=-i(P_x)_{J,K;\,J,K+1}\\ &=(\hbar/2)[J(J+1)-K(K+1)]^{\frac{1}{2}}, \quad (5)\\ (P_z)_{J,K;\,J,K}&=\hbar K, \end{aligned}$$

where $J\geqslant K$.

The representation used here is that which diagonalizes P_z and $P^2=P_x^2+P_y^2+P_z^2$, and which corresponds to the wave functions chosen by Wang,[2] Mulliken,[9] and Van Vleck.[10] The phase factor of these functions is such that P_y is real and positive, and P_x is imaginary, which is just the reverse of the choice made by Klein[4] and later by Dennison[7] in their matrix algebra treatment.

It follows from (5) that the squares of the angular momenta, which appear in (3), are

$$\begin{aligned} (P_y^2)_{J,K;\,J,K}&=(P_x^2)_{J,K;\,J,K}\\ &=(\hbar^2/2)[J(J+1)-K^2],\\ (P_y^2)_{J,K;\,J,K+2}&=-(P_x^2)_{J,K;\,J,K+2}\\ &=(\hbar^2/4)[\{J(J+1)-K(K+1)\}\\ &\quad\times\{J(J+1)-(K+1)(K+2)\}]^{\frac{1}{2}}, \quad (6)\\ (P_z^2)_{J,K;\,J,K}&=\hbar^2K^2, \end{aligned}$$

whence

$$(P^2)_{J,K;\,J,K}=\hbar^2J(J+1). \quad (7)$$

The calculation of the energy levels is greatly facilitated by the change of variables proposed by Ray.[8] This is given here in some detail since his paper contains several misprints. Let σ and ρ be scalar factors. Then

$$\begin{aligned} &E(\sigma a+\rho, \sigma b+\rho, \sigma c+\rho)\\ &\quad=[(\sigma a+\rho)P_a^2+(\sigma b+\rho)P_b^2+(\sigma c+\rho)P_c^2]/\hbar^2\\ &\quad=[\sigma(aP_a^2+bP_b^2+cP_c^2)+\rho(P_a^2+P_b^2+P_c^2)]/\hbar^2, \end{aligned}$$

which by (3) and (7) reduces to

$$=\sigma E(a, b, c)+\rho J(J+1). \quad (8)$$

[10] J. H. Van Vleck, Phys. Rev. **33**, 467 (1929). We may, therefore, make use of the symmetry determinations of Mulliken in our work. The actual phases of the symmetric rotor wave functions do not affect the energy, but must be clearly defined when symmetry is concerned. The confusion resulting from the many arbitrary choices of signs, phases, and "Eulerian" angles in the different quantum mechanical formulations has been cleared up by Van Vleck, especially in footnotes 9, 20, 21, 25, and 29. The phase to be determined here has only to be consistent with that of previous work which we wish to use.

From the rigid phase relation between P_x and P_y given by (5), we see that P_x has the same real, imaginary, or complex character as P_x+iP_y. This quantity is very simply expressed in the Eulerian angles used by Mulliken

$$P_x+iP_y=\hbar e^{-i\phi}[\csc\theta(\partial/\partial\chi)-\cot\theta(\partial/\partial\phi)-i(\partial/\partial\theta)]. \quad (5a)$$

Applying this operator to the symmetric rotor wave functions used by Mulliken and first clearly defined by Van Vleck, we find P_x+iP_y, and hence P_x, to be imaginary. The complex conjugate must be taken on the first factor.

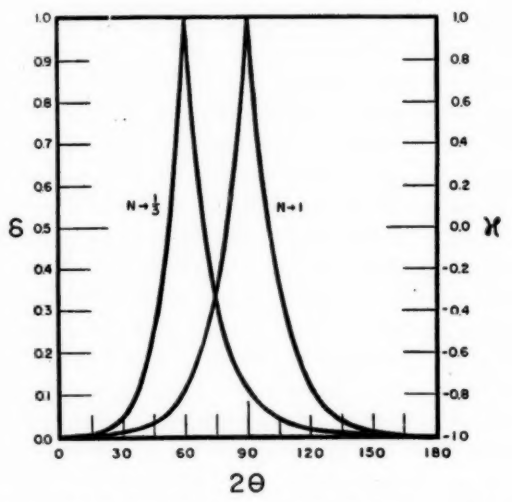

FIG. 1. Variation of δ and of κ with the valence angle of symmetrical triatomic molecules. The cases illustrated are $m=M(N\rightarrow\frac{1}{3})$ and $m\ll M(N\rightarrow 1)$.

Ray now chooses

$$\begin{aligned}\sigma&=2/(a-c),\\ \rho&=-(a+c)/(a-c),\end{aligned}\tag{9}$$

so that

$$\begin{aligned}\sigma a+\rho&=1,\\ \sigma b+\rho&=(2b-a-c)/(a-c),\\ \sigma c+\rho&=-1.\end{aligned}\tag{10}$$

He then defines the parameter of asymmetry κ as

$$\kappa=(2b-a-c)/(a-c),\tag{11}$$

so that $-1\leqslant\kappa\leqslant 1$. This parameter κ results naturally from Ray's choice of diagonalizing P_b, the angular momentum about the intermediate axis of inertia. The chief value of using κ is apparent from the relation, proved by Ray,[8]

$$E_\tau^J(\kappa)=-E_{-\tau}^J(-\kappa),\tag{12}$$

which gives the energies for positive κ from the energies for negative κ. The limit $\kappa=-1$ or $b=c$ is Mulliken's prolate-symmetric rotor, while the limit $\kappa=+1$ or $b=a$ is his oblate-symmetric rotor.

Substituting (9), (10), (11), into (8) we obtain

$$E(1,\kappa,-1)=E(\kappa)=[2/(a-c)]E(a,b,c)-[(a+c)/(a-c)]J(J+1),$$

which on rearrangement yields for the energy of any asymmetric rotor

$$2E(a,b,c)=(a-c)E(\kappa)+(a+c)J(J+1).\tag{13}$$

This relation, and that of (12), show that if the energy levels $E(\kappa)$ for values of κ between -1 and 0 are determined, once and for all, the energy levels of any asymmetric rotor can be calculated by simple multiplication and addition.

It is often more convenient to employ a parameter of asymmetry δ, defined as

$$\delta=(\kappa+1)/2=(b-c)/(a-c).\tag{14}$$

It follows that $0\leqslant\delta\leqslant 1$ and $\kappa=2\delta-1$.

Rigid Planar Molecules

For rigid planar molecules δ has a very simple form. The axes of I_a and I_b must be in the plane of the molecule and the moments of inertia must satisfy the relation

$$I_c=I_a+I_b.\tag{15}$$

Combination of (2), (14), and (15) gives

$$\delta=I_a^2/I_b^2=b^2/a^2.\tag{16}$$

Rigid Symmetrical Triatomic Molecules

For a symmetrical triatomic molecule, δ is easily expressed in terms of the structural parameters of the molecule (assuming a model of point masses in a rigid configuration). Let the central mass be M, each attached mass m, the valence angle 2θ, and the bond distance r. Also introduce $N=M/(M+2m)$. Then

$$\begin{aligned}I_\sigma&=2mNr^2\cos^2\theta,\\ I_\pi&=2mr^2\sin^2\theta,\\ I_\perp&=2mr^2(N\cos^2\theta+\sin^2\theta).\end{aligned}\tag{17}$$

As 2θ is varied from 0 to π, δ varies from 0 to 1 to 0. The principal axes of inertia in the plane of the molecule are respectively parallel (π) and perpendicular (σ) to the symmetry axis. Furthermore, $I_a=I_b=I_\sigma=I_\pi$ and $\delta=1$ when $\theta=\tan^{-1}N^{\frac{1}{2}}$. Since we require $I_a\leqslant I_b\leqslant I_c$, $I_a=I_\sigma$ if $\theta>\tan^{-1}N^{\frac{1}{2}}$ and $I_a=I_\pi$ if $\theta<\tan^{-1}N^{\frac{1}{2}}$. The angles corresponding to the most asymmetric rotors, $\delta=\frac{1}{2}$, are $\theta=\cot^{-1}(2N^2)^{-\frac{1}{4}}>\tan^{-1}N^{\frac{1}{2}}$ and $\theta=\tan^{-1}(N^2/2)^{\frac{1}{4}}<\tan^{-1}N^{\frac{1}{2}}$. The variation of δ with θ is illustrated in Fig. 1. From the above identification of the least moment of inertia with I_σ or I_π one obtains from (16) and (17)

$$\begin{aligned}\delta&=N^2\cot^4\theta \quad \text{for} \quad \theta>\tan^{-1}N^{\frac{1}{2}},\\ \delta&=N^{-2}\tan^4\theta \quad \text{for} \quad \theta<\tan^{-1}N^{\frac{1}{2}}.\end{aligned}\tag{18}$$

TABLE I.

J / n	1	2	3	4	5	6	7	8	9	10	11	12	13	14	15	16	17	18	19	20	21	22	23	24	25	26	27	28	29	30	J / n
0	1^2																														0
1		3	6^3	10^2	15^2	21^2	28^2	36^2	45^2	55^2	66^2	78^2	91^2	105^2	120^2	136^2	153^2	171^2	190^2	210^2	231^2	253^2	276^2	300^2	325^2	351^2	378^2	406^2	435^2	465^2	1
2		12	60	100	420	840	1512	2520	3960	5940	8580	12012	16380	21840	28560	36720	46512	58140	71820	87780	106260	127512	151800	179400	210600	245700	285012	326880	377580	431820	2
3			15	63	108	360	675	1155	1848	2808	4095	5775	7920	10608	13923	17965	22800	28560	35343	43263	52440	63000	75075	88803	104328	121800	141375	163215	187488	214368	3
4				28	108	270	550	990	1638	2548	3780	5400	7480	10098	13338	17290	22050	27720	34408	42228	51300	61750	73710	87318	102718	120060	139500	161200	185328	212058	4
5					45	165	396	780	1365	2205	3360	4896	6885	9405	12540	16380	21021	26565	33120	40800	49725	60021	71820	85260	100485	117645	136896	158400	182325	208845	5
6						66	234	546	1050	1800	2856	4284	6156	8550	11550	15246	19734	25116	31500	39000	47736	57834	69426	82650	97650	114576	133584	154836	178500	204750	6
7							91	315	720	1360	2295	3591	5320	7560	10395	13915	18216	23400	29575	36855	45360	55216	66555	79515	94240	110880	129591	150535	173880	199800	7
8								120	408	918	1710	2850	4410	6468	9108	12420	16500	21460	27378	34398	42630	52200	63240	75888	90288	106590	124950	145530	168498	194028	8
9									153	513	1140	2100	3465	5313	7728	10800	14625	19305	24948	31668	39585	48825	59520	71808	85833	101745	119700	139860	162393	187473	9
10										190	630	1386	2530	4140	6300	9100	12636	17010	22330	28710	36270	45136	55440	67320	80920	96390	113886	133570	155610	180180	10
11											231	756	1656	3000	4875	7371	10584	14616	19575	25575	32736	41184	51051	62475	75600	90576	107559	126711	148200	172200	11
12												276	900	1953	3510	5670	8528	12180	16740	22320	29040	37026	46410	57330	69930	84360	100776	119340	140220	163590	12
13													325	1053	2206	4060	6525	9765	13888	19008	25245	32725	41580	51948	63973	77805	93600	111520	131733	154413	13
14														378	1218	2610	4650	7440	11088	15708	21420	28350	36630	46398	57798	70980	86100	103320	122808	144738	14
15															435	1395	2976	5280	8415	12495	17640	23976	31635	40755	51480	63960	78351	94815	113520	134640	15
16																496	1584	3366	5950	9450	13986	19684	26676	35100	45100	56826	70434	86086	103950	124200	16
17																	561	1785	3780	6660	10545	15561	21840	29520	38745	49665	62436	77220	94185	113505	17
18																		630	1998	4218	7410	11700	17220	24108	32508	42570	54450	68310	84318	102648	18
19																			703	2223	4680	8200	12915	18963	26488	35640	46575	59455	74448	91728	19
20																				780	2460	5165	9030	14190	20790	28980	38916	50760	64680	80850	20
21																					861	2709	5676	9900	15525	22701	31584	42336	55125	70125	21
22																						946	2970	6210	10810	16920	24696	34300	45900	59670	22
23																							1035	3243	6768	11760	18375	26775	37128	49608	23
24																								1128	3528	7350	12750	19890	28938	40068	24
25																									1225	7956	13780	21465	31185	25
26																										1326	8586	14850	23100	26
27																											1431	9240	15960	27
28																												1540	9918	28
29																													1653	5133	29
30																														1770	

Values of
$f(J, n)=\frac{1}{4}[J(J+1)-n(n+1)]\,[J(J+1)-n(n-1)]$
$=\frac{1}{4}(J-n+1)(J+n)(J+n+1)$.

The factor 2 which always occurs with $f(J, 1)$ in the factored secular equations has been included in calculating the entries in the table. These values are therefore set apart by the use of bold face type.

Note that for symmetrical triatomic molecules, the asymmetry parameter δ (or κ) is independent of r, i.e., the energy level "pattern" $E(\kappa)$ is dependent only on the valence angle 2θ and not on the interatomic distance r. Of course, the actual energy levels $E(a, b, c)$ are functions of the moments of inertia and therefore of r.

For most triatomic molecules the valence angle is considerably greater than $2\tan^{-1}N^{\frac{1}{2}}$. Reference to Fig. 1 shows that, as a result of the fourth power in (18), δ tends to zero rapidly as 2θ deviates from $2\tan^{-1}N^{\frac{1}{2}}$. This accounts for the fact that most triatomic molecules are essentially symmetric rotors even though the valence angles are markedly different from the limiting linear-symmetric case, $2\theta=180°$.[11] The preponderance of δ values near zero makes it a natural parameter of asymmetry for use in the application of perturbation theory.

III. REPRESENTATIONS OF THE MATRIX $E(\kappa)$

Notation and Elements of the Energy Matrices

The 3! ways of identifying P_a, P_b, P_c with P_x, P_y, P_z give six representations of the energy matrix whose elements, for a given J, are of the following general form. Since the energy is diagonal in J, the index J; J is dropped.

$$E_{K;\,K}=F[J(J+1)-K^2]+GK^2$$
$$=FJ(J+1)+(G-F)K^2, \quad (19)$$

$$E_{K;\,K+2}=E_{K+2;\,K}=H[f(J, K+1)]^{\frac{1}{2}}, \quad (20)$$

where use is made of the abbreviation

$$f(J, n)=f(J, -n)=\tfrac{1}{4}[J(J+1)-n(n+1)]\times[J(J+1)-n(n-1)]. \quad (21)$$

Values of $f(J, n)$ are given in Table I.

The values of F, G, H in terms of κ or δ depend on the particular identifications of P_a, P_b, P_c with P_x, P_y, P_z. The six resulting forms can be arranged into two sets of three each which differ only in the sign of H and hence only in the sign of the non-diagonal elements. These sets correspond to the six possible superpositions of the right- and left-handed a, b, c axes on the x, y, z axes, already defined as right-handed. A

[11] See, for example, the case of NO_2, G. W. King and L. Harris, J. Chem. Phys. **8**, 775 (1940).

difference in sign of non-diagonal elements does not affect the roots of Hermitian matrices, but the sign of H must be retained to assign the symmetry properly. To maintain consistency in the definition of H, the positive square root of f is used in (20).

The identifications of a, b, c with x, y, z are given in the first three rows of Table II. These are labeled I^r, II^r, III^r for the three permutations of right-handed, a, b, c axes and I^l, II^l, III^l for the corresponding permutations (based upon the assignment to the unique, or z, axis) of left-handed a, b, c axes. By this notation the matrices displayed by Ray[8] in his Eqs. (22a), (22b), (22c) and those corresponding to the Mulliken[9] prolate K_a and oblate K_c cases are to be identified as shown in Table II. All the above types give, of course, the same secular equations and energy levels. Each type has its own particular use for special ranges of κ.

The expressions for F, G, H in terms of κ or δ for the r types are found in Table III. To obtain the matrices of the corresponding l types, the sign of H must be changed.

Limiting Cases

In the case of the limiting oblate spheroid, $I_b \to I_a$, $b \to a$, $\kappa \to 1$, $\delta \to 1$; and with $z=c$, i.e., Type III, the energy matrix becomes diagonal, $H \to 0$. This corresponds to Mulliken's case $K=K_c$, the elements of the matrix $E(\kappa)=E(1)$ become

$$E_{K_c;\,K_c} = J(J+1) - 2K_c^2. \tag{22}$$

Substitution into (13) yields the usual expression for the energy levels of the oblate-symmetric rotor,

$$E(a,b,c) = E(a,a,c) = aJ(J+1) - (a-c)K_c^2. \tag{23}$$

For κ or δ in the neighborhood of $+1$, Type III is nearly diagonal and thus is the most convenient type to use in determining the energy levels.

Table II.

x	b	c	c	a	a	b
y	c	b	a	c	b	a
z	a	a	b	b	c	c
Type	I^r	I^l	II^r	II^l	III^r	III^l
Ray	—	22a	—	22b	—	22c
Mulliken	—	K_a	—	—	K_c	—
Wang	—	$I_x<I_z$	—	—	$I_z>I_x$	—
Dennison	—	—	—	—	—	*

Table III.

	κ			δ		
Type	I^r	II^r	III^r	I^r	II^r	III^r
F	$\frac{1}{2}(\kappa-1)$	0	$\frac{1}{2}(\kappa+1)$	$\delta-1$	0	δ
G	1	κ	-1	1	$2\delta-1$	-1
H	$-\frac{1}{2}(\kappa+1)$	1	$\frac{1}{2}(\kappa-1)$	$-\delta$	1	$\delta-1$
$G-F$	$-\frac{1}{2}(\kappa-3)$	κ	$-\frac{1}{2}(\kappa+3)$	$-(\delta-2)$	$2\delta-1$	$-(\delta+1)$
$F+G-H$	$\kappa+1$	$\kappa-1$	0	2δ	$2(\delta-1)$	0
$F+G+H$	0	$\kappa+1$	$\kappa-1$	0	2δ	$2(\delta-1)$

For the limiting prolate spheroid, $I_b \to I_c$, $b \to c$, $\kappa \to -1$, $\delta \to 0$. With $z=a$, i.e., Type I, the energy matrix is again diagonal corresponding to Mulliken's $K=K_a$, the elements being

$$E_{K_a;\,K_a} = -J(J+1) + 2K_a^2, \tag{24}$$

$$E(a,b,c) = E(a,c,c) = cJ(J+1) + (a-c)K_a^2. \tag{25}$$

Type I, being nearly diagonal for κ nearly -1, or for δ nearly 0, is the most convenient form to use under these conditions.

Type II never becomes diagonal. It is useful for the case of maximum asymmetry, $\kappa=0$, when its main diagonal elements are all zero.

IV. SYMMETRY PROPERTIES

Irreducible Representations of the Asymmetric Rotor Wave Functions

The energy of a rotor is invariant under the operations of an external rotation group which has infinitely many representations characterized by the quantum numbers J and M. In the absence of external fields, one need not examine these any further than to note the resulting $2J+1$ degeneracy of the energy levels.

The wave functions of the symmetric rotor, which are used as the basis functions in the calculations of the asymmetric rotor energies, belong also to an internal rotation group $\mathbf{D}_\infty$. This group has infinitely many representations characterized by the quantum numbers J and K. They are denoted by $\Sigma_1(K=0,\ J \text{ even})$, $\Sigma_2(K=0,\ J \text{ odd})$, $\Pi(K=1,\ \cdots)$, $\Delta(K=2,\ \cdots)$, etc. On the other hand, the wave functions of the asymmetric rotor belong to the Four-group $\mathbf{V}(a,b,c)$, defined by the three rotation operators C_2^a, C_2^b, C_2^c. The character table for this group

TABLE IV.

	E	C_2^c	C_2^b	C_2^a
A	1	1	1	1
B_c	1	1	−1	−1
B_b	1	−1	1	−1
B_a	1	−1	−1	1

TABLE V. Correlation of the species classification of symmetric rotor and asymmetric rotor wave functions.

		Parity of		Rep. of	Representations of $\mathbf{V}(a, b, c)$					
K	$\mathbf{D}_\infty(z)$	K	$J+\gamma$	$\mathbf{V}(x, y, z)$	I^r	I^l	II^r	II^l	III^r	III^l
0	Σ_1	e	e	A	A	A	A	A	A	A
0	Σ_2	e	o	B_z	B_a	B_a	B_b	B_b	B_c	B_c
1	Π	o	e	B_y	B_c	B_b	B_a	B_c	B_b	B_a
1	Π	o	o	B_x	B_b	B_c	B_c	B_a	B_a	B_b
2	Δ	e	e	A	A	A	A	A	A	A
2	Δ	e	o	B_z	B_a	B_a	B_b	B_b	B_c	B_c
—	—	—	—	—	—	—	—	—	—	—

is given in Table IV. The notation for the representations shows directly the axis of rotation for which the character is +1.

However, the symmetric rotor basis functions[12] commonly used, $\psi^\times(J, K, M)$, do not belong to this Four-group, but, as pointed out by Mulliken,[9] the Wang[2] linear combinations of them do belong to the Four-group.

$$S(J, K, M, \gamma)=2^{-\frac{1}{2}}[\psi^\times(J, K, M) +(-1)^\gamma\psi^\times(J, -K, M)], \quad (26)$$

where γ is odd or even, say 1 or 0. For $K=0$, only γ even ($\gamma=0$) exists and

$$S(J, 0, M, 0)=\psi^\times(J, 0, M). \quad (27)$$

In general these new basis functions $S(J, K, M, \gamma)$ have been constructed relative to arbitrary axes x, y, z and not relative to the axes a, b, c of the molecule as here defined. They are, therefore, characterized by the representations A, B_z, B_y, B_x of the Four-group $\mathbf{V}(x, y, z)$. Here, too, the representations have been labeled to show directly the axis of rotation for which the character is +1. This makes very easy the correlation of the representations of $\mathbf{V}(a, b, c)$ with those of $\mathbf{V}(x, y, z)$. A always corresponds to A, and B_a, B_b, B_c correspond to B_x, B_y, B_z, according to the same permutation as that identifying a, b, c with x, y, z. These correlations are given on the right side of Table V. The left side of this table gives Mulliken's identification of the representations of the Group $\mathbf{D}_\infty(z)$ (to which the $S(J, K, M, \gamma)$ also belong) with the representations of the group $\mathbf{V}(x, y, z)$.[13]

[12] See Mulliken, reference 9, Eq. (3), and Van Vleck, reference 10, footncte 25.

Factors of the Energy Matrix $\mathbf{E}(\kappa)$ in the $S(J, K, M, \gamma)$ Representation

For a given J the energy matrix $E(\kappa)$ in any representation based upon the $\psi^\times(J, K, M)$'s, which may be readily obtained from (19), (20), (21) and Table III, is of the order $2J+1$ since[14] $-J\leqslant K\leqslant J$. The transformation to a representation based upon the $S(J, K, M, \gamma)$'s enables further factoring of $E(\kappa)$ into four submatrices, i.e.,

$$X'E(\kappa)X=E^+\dot{+}E^-\dot{+}O^+\dot{+}O^-, \quad (28)$$

where

$$X=X'=2^{-\frac{1}{2}}\begin{Vmatrix} \cdots & & & & \cdots \\ & -1 & & 1 & \\ & & -1 & 1 & \\ & & & 2^{\frac{1}{2}} & \\ & & 1 & 1 & \\ & 1 & & & 1 \\ \cdots & & & & \cdots \end{Vmatrix}_{2J+1} \quad (29)$$

is the Wang transformation, $\psi^\times=XS$. The orders from the top left corner are $\psi^\times(J, -J, M)$, $\psi^\times(J, -J+1, M)$, $\cdots\psi^\times(J, J, M)$, and $S(J, J, M, 1)$, $S(J, J-1, M, 1)$, $\cdots S(J, 1, M, 1)$, $S(J, 0, M, 0)$, $\cdots S(J, J, M, 0)$. These submatrices, in terms of the original elements of $E(\kappa)$, may be displayed in the form

$$E^+=\begin{Vmatrix} E_{00} & 2^{\frac{1}{2}}E_{02} & 0 & \cdots \\ & \cdots\cdots\cdots\cdots & & \\ 2^{\frac{1}{2}}E_{02} & E_{22} & E_{24} & \cdots \\ 0 & E_{24} & E_{44} & \cdots \\ \cdots & \cdots & \cdots & \cdots \end{Vmatrix}, \quad (30)$$

E^- has the same elements as E^+ after removal of the first row and first column, as indicated by

[13] See Mulliken, reference 9, Appendix I and Table III. The identifications are made by examining the behavior of the $S(J, K, M, \gamma)$ under the operations C_2^x, C_2^y, C_2^z of the group $\mathbf{V}(x, y, z)$

$$C_2^zS=(-1)^KS,$$
$$C_2^yS=(-1)^{J+\gamma}S,$$
$$C_2^xS=(-1)^{K+J+\gamma}S.$$

[14] It may, however, be displayed as two submatrices whose indices involve, respectively, only even and only odd K's.

the dotted lines, and

$$O^{\pm}=\begin{Vmatrix} (E_{11}\pm E_{-11}) & E_{13} & 0 & \cdots \\ E_{13} & E_{33} & E_{35} & \cdots \\ 0 & E_{35} & E_{55} & \cdots \\ \cdots & \cdots & \cdots & \cdots \end{Vmatrix}. \quad (31)$$

Use has been made of the relations

$$E_{KK}=E_{-K-K} \quad (32)$$

and

$$E_{K,K+2}=E_{K+2,K}=E_{-K,-K-2}=E_{-K-2,-K}. \quad (33)$$

These submatrices are identified by the symbols,[5] E^+, E^-, O^+, O^- in which E and O refer to the even- or oddness of the K values in the matrix elements and $+$ and $-$ to the even- or oddness of γ. Thus, these four species of submatrices together with the six original representations of $E(\kappa)$ give twenty-four different submatrices

$$\begin{array}{cccc} \mathrm{I}^rE^+ & \mathrm{I}^rE^- & \mathrm{I}^rO^+ & \mathrm{I}^rO^- \\ \mathrm{I}^lE^+ & \mathrm{I}^lE^- & \mathrm{I}^lO^+ & \mathrm{I}^lO^- \\ \cdots & \cdots & \cdots & \cdots \\ \mathrm{III}^lE^+ & \mathrm{III}^lE^- & \mathrm{III}^lO^+ & \mathrm{III}^lO^- \end{array}$$

which belong to the four symmetry species. Each submatrix of one type, e.g., I^rE^+, corresponds to the same set of energy levels as some submatrix of each of the other types. This correlation is accomplished by determining the symmetry classification of each submatrix.

Symmetry of the Submatrices

The Wang functions $S(J, K, M, \gamma)$ which occur in any submatrix must all belong to the same irreducible representation of the Four-group $\mathbf{V}(x, y, z)$. These representations may therefore be used to classify the submatrices. From the submatrix designation we know the parity of K and $J+\gamma$ for a given J. Thus by reference to Table V one can construct Table VI. The corresponding classification of E^+, E^-, O^+, O^- for the Types I^r, $\cdots\mathrm{III}^l$ under the group $\mathrm{V}(a, b, c)$ follows at once from Table V.

The symmetry species of any given energy level can be found from the classification of the submatrix from which the level was obtained. To distinguish one level from the other levels of a given J it has been found very convenient to label it by the values of K to which it corresponds in the limiting cases $\kappa=-1$, prolate-symmetric rotor, and $\kappa=+1$, oblate-symmetric rotor. This notation has the added attraction that the symmetry classification under $\mathbf{V}(a, b, c)$ may be found directly from the odd- or evenness of the two K's in question. That is, the four species A, B_c, B_b, B_a are indicated, respectively, by the bipartite indices *ee*, *oe*, *oo*, *eo* in which the first symbol gives the parity of K for $\kappa=-1$ and the second for $\kappa=+1$.[15]

The classification of the submatrices to the symmetry species A, B_c, B_b, B_a in terms of the parities of the limiting K_{-1}, K_1 symmetric rotor cases is given in Table VII.

The prevalent method of labeling energy levels is by J_τ, where J specifies the J-set and τ takes on the $2J+1$ values $-J\leqslant\tau\leqslant J$; the lowest energy level being J_{-J} and τ increasing with increasing energy to give the highest energy level as J_J. This is satisfactory since there are no crossings of energy levels in the entire range $-1\leqslant\kappa\leqslant 1$, but it gives no indication of symmetry. The proposed method of labeling by two subscripts; the first K_{-1}, being[16] 0, 1, 1, 2, 2$\cdots$ from *lowest to highest* energy levels and the second, K_1, being 0, 1, 1, 2, 2$\cdots$ from *highest to lowest* energy levels, gives not only the symmetry through the parity of the indices but also τ, or the rank, through the relation

$$\tau=K_{-1}-K_1. \quad (34)$$

The submatrix which contains any designated level in any type of representation, $\mathrm{I}^r\cdots\mathrm{III}^l$,

TABLE VI. Symmetry classification of the submatrices in $\mathbf{V}(x, y, z)$. (Note that as $J\rightarrow J\pm1$, the $\pm$ matrices interchange symmetry.)

			$J+\gamma$		Species Representation	
Submatrix	K	γ	J even	J odd	J even	J odd
E^+	*e*	*e*	*e*	*o*	A	B_z
E^-	*e*	*o*	*o*	*e*	B_z	A
O^+	*o*	*e*	*e*	*o*	B_y	B_x
O^-	*o*	*o*	*o*	*e*	B_x	B_y

[15] That the symmetry classification in $\mathbf{V}(a, b, c)$ is given uniquely in terms of the parity of K_{-1}, K_1 follows from the assignments of a, b, c to x, y, z for these cases ($z=a$, and $z=c$, respectively). From Tables VI and V, K_{-1} even requires the symmetry A or $B_z\rightarrow A$ or B_a, K_{-1} odd, B_x or $B_y\rightarrow B_b$ or B_c. On the other hand, K_1 even requires A or $B_z\rightarrow A$ or B_c, K_1 odd, B_x or $B_y\rightarrow B_a$ or B_b. Hence it must follow that $A=ee$, $B_z=oe$, $B_b=oo$, and $B_a=eo$. It is immaterial whether right- or left-handed Types I and III are chosen for the prolate and oblate representations.

[16] We are using K_{-1} and K_1 as the absolute magnitude of the corresponding limiting K values, as is customary in the labeling of symmetric rotor energy levels.

TABLE VII. Symmetry classification of the submatrices in $\mathbf{V}(a, b, c)$ by the parity of K_{-1}, K_1. $ee=A$, $oe=B_c$, $oo=B_b$, $eo=B_a$.

	I^r		I^l		II^r		II^l		III^r		III^l	
Sub-mat.	J even	J odd	J even	J odd	J even	J odd	J even	J odd	J even	J odd	J even	J odd
E^+	ee	eo	ee	eo	ee	oo	ee	oo	ee	oe	ee	oe
E^-	eo	ee	eo	ee	oo	ee	oo	ee	oe	ee	oe	ee
O^+	oe	oo	oo	oe	eo	oe	oe	eo	oo	eo	eo	oo
O^-	oo	oe	oe	oo	oe	eo	eo	oe	eo	oo	oo	eo

TABLE VIII. Species classification.

Group theory Mulliken	KK $(K_{-1}K_1)$	Dennison	Mecke	Ray	$J+\gamma$
A	ee	$++$	(ABC)	abc	e
B_c	oe	$+-$	(AB)	c	o
B_b	oo	$--$	(AC)	b	e
B_a	eo	$-+$	(BC)	a	o

is readily determined from the parity of the subscripts and Table VII. All the levels from a given submatrix of a given type of representation may be listed by writing the first subscripts as a descending series of numbers having the parity of the first index (from Table VII), $J \geqslant K \geqslant 0$, then writing the second subscripts as an ascending series having the parity of the second index $(0 \leqslant K \leqslant J)$, with the exception that the zero must be omitted from an even series unless it is paired with K_{-1} (or K_1) $=J$. See also Table XI.

To illustrate the foregoing, the level 7_{43} has the symmetry eo or B_a; $\tau=4-3=1$, so this level is seventh-high for $J=7$. If, for example, a III^r representation is used, Table VII shows that the level is in the O^+ submatrix. The levels from the E^- submatrix of $J=7$, Type III^r, which has the symmetry ee, are 7_{62}, 7_{44}, 7_{26}. The zero subscript does not occur here, since ee cannot contain the maximum K for J odd.

The correlation of the numerous notations for specifying the symmetry species is given in Table VIII. The parity of $J+\gamma$ is included. Note that it is the parity of the sum, $K_{-1}+K_1$.

Submatrix Symmetry by Order and Trace Equivalence

The identification of the symmetries of the submatrices in the KK notation, as displayed in Table VII, may also be obtained from the following considerations.

One of the four submatrices for a given J has an order different from that of the other three, as shown in Table IX. For all types of representation, this submatrix of unique order must obviously belong to the same symmetry class and be either E^+ (J even) or E^- (J odd). Hence, in the KK notation it must belong to the symmetry class ee.

For a given J all the submatrices of Types $I^r \cdots III^l$, having a given symmetry, must have the same roots, and hence, the same trace. This fact may be employed to complete the identification of the symmetries. The traces of the submatrices have the values shown in Table X. The explicit expressions for the different Types $I^r \cdots III^l$ are readily obtained by combination with Table III.

One submatrix has the same trace as the submatrix of symmetry ee for all values of κ. This follows from the vanishing of $(F+G+H)$, F, and $(F+G-H)$ for Types I, II, and III, respectively. For Types I and III, this submatrix is always $O^\pm$ and hence its KK symmetry is oo.

In the limits $\kappa=\pm 1$, three of the submatrices have the same trace and one has a unique trace. The unique trace for $\kappa=-1$ is $E^\pm$ for Type I representation and $O^\pm$ for Type III, and hence the submatrix has the symmetry eo.

The remaining submatrix must have symmetry oe. This can be determined directly by noting that the unique trace at $\kappa=+1$ is $O^\pm$ for Type I and $E^\pm$ for Type III.

V. ENERGY CALCULATIONS

Energy Equations

The energy levels of the rigid rotor are the roots of the characteristic equations of the four

TABLE IX. Order of submatrices.

Submatrix	J even	J odd
E^+	$\frac{1}{2}(J+2)$	$\frac{1}{2}(J+1)$
E^-	$\frac{1}{2}J$	$\frac{1}{2}(J-1)$
O^+	$\frac{1}{2}J$	$\frac{1}{2}(J+1)$
O^-	$\frac{1}{2}J$	$\frac{1}{2}(J+1)$

TABLE X. Traces of submatrices.

Submatrix	J even	J odd
E^+	$\kappa\Gamma$	$\kappa\Gamma'+\Im F$
E^-	$\kappa\Gamma-\Im F$	$\kappa\Gamma'$
O^+	$\kappa\Gamma-\frac{1}{2}\Im(F+G-H)$	$\kappa\Gamma'+\frac{1}{2}\Im(F+G+H)$
O^-	$\kappa\Gamma-\frac{1}{2}\Im(F+G+H)$	$\kappa\Gamma'+\frac{1}{2}\Im(F+G-H)$

$\Im=J(J+1)$, $\Gamma=\frac{1}{4}J(J+1)(J+2)$, $\Gamma'=\frac{1}{4}J(J+1)(J-1)$.

submatrices of any Type $I^r \cdots III^l$, chosen for convenience. By inspection of (30) and (31), it is seen that these submatrices are of the Jacobian form

$$E=\begin{Vmatrix} k_0 & b_1^{\frac{1}{2}} & 0 & \cdots \\ b_1^{\frac{1}{2}} & k_1 & b_2^{\frac{1}{2}} & \cdots \\ 0 & b_2^{\frac{1}{2}} & k_2 & \cdots \\ \cdots & \cdots & \cdots & \cdots \end{Vmatrix}. \quad (35)$$

A more convenient form is

$$D=L^{-1}EL=\begin{Vmatrix} k_0 & 1 & 0 & \cdots \\ b_1 & k_1 & 1 & \cdots \\ 0 & b_2 & k_2 & \cdots \\ \cdots & \cdots & \cdots & \cdots \end{Vmatrix}, \quad (36)$$

where L is the transformation given by (51). The values of the k_i's and b_i's for each submatrix may be obtained from the proper forms of (37) and (38).

$$E^{\pm};\ D=\begin{Vmatrix} F\Im & 1 & 0 & \cdots \\ \cdots & \cdots & \cdots & \cdots \\ 2H^2f(J,1) & 4(G-F)+F\Im & 1 & \cdots \\ 0 & H^2f(J,3) & 16(G-F)+F\Im & \cdots \\ \cdots & \cdots & \cdots & \cdots \end{Vmatrix}, \quad (37)$$

$$O^{\pm};\ D=\begin{Vmatrix} (G-F)+F\Im \pm Hf^{\frac{1}{2}}(J,0) & 1 & 0 & \cdots \\ H^2f(J,2) & 9(G-F)+F\Im & 1 & \cdots \\ 0 & H^2f(J,4) & 25(G-F)+F\Im & \cdots \\ \cdots & \cdots & \cdots & \cdots \end{Vmatrix}, \quad (38)$$

where $\Im=J(J+1)$. Values of $f(J,n)$ and F, G, and H are found in Tables I and III, respectively.

Continued Fraction Form of the Energy Equations

The solution of a secular determinant $|D-\lambda I|=0$ is greatly facilitated by the fact that the determinant is a continuant equivalent to the continued fraction

$$(k_0-\lambda)-\cfrac{b_1}{(k_1-\lambda)-[b_2/(k_2-\lambda)-\cdots]}=0. \quad (39)$$

By the use of (37), (38), Table I and Table III, the continued fraction form of any submatrix in terms of J and κ may be written by inspection.

In general, the secular equations must be solved by approximation methods. It is important, therefore, to choose the Type I, II, or III representation which gives the most rapid convergence of the successive approximations, as discussed in Section III. Furthermore, it is advantageous to approximate the mth root of a given equation by a form of the continued fraction which has k_m as the leading term, as given by (40) and as suggested by the method of Crawford and Cross.[17]

$$\lambda_m=k_m-\cfrac{b_m}{(k_{m-1}-\lambda_m)-[b_{m-1}/(k_{m-2}-\lambda_m)-\cdots]}$$
$$-\cfrac{b_{m+1}}{(k_{m+1}-\lambda_m)-[b_{m+2}/(k_{m+2}-\lambda_m)-\cdots]}. \quad (40)$$

The relation $\Sigma\lambda_m=\Sigma k_m$ may be used to obtain the root for which the convergence is poorest or to check the numerical accuracy of the solutions.

The τ value of the level λ_m can be determined from the K_{-1} and K_1 values. In Type I^r, the representation used for most of the calculations here reported, the K_{-1} value is that of the K which enters as K^2 in the main diagonal element k_m determined from (37) or (38). The values of K_1 and of τ for $K_{-1}=n$ are given in Table XI.

Energy Table

By the use of the above outlined procedure, the table of characteristic roots $E(\kappa)$ given in Appendix I has been computed. From this table

[17] B. L. Crawford and P. C. Cross, J. Chem. Phys. **5**, 621 (1937).

TABLE XI.

Representation					
Submatrix	J even	J odd	K_1	τ
$I^r E^+$	A ee	B_a eo	$J-n$	$2n-J$
$I^r E^-$	B_a eo	A ee	$J-n+1$	$2n-J-1$
$I^r O^+$	B_c oe	B_b oo	$J-n+1$	$2n-J-1$
$I^r O^-$	B_b oo	B_c oe	$J-n$	$2n-J$

In the first row, $n=0, 2, \cdots J$ (or $J-1$); in the second row, $n=2, 4, \cdots J$ (or $J-1$); in the last two rows, $n=1, 3, \cdots J-1$ (or J).

the energy levels of rigid asymmetric rotors up to $J=10$ may be readily evaluated by (13) for κ values from -1 to 0 by intervals of 0.1. Values of $E(\kappa)$ for κ values from 0 to 1 with similar intervals are readily obtained from the relation given in (12). For other values of κ a fairly accurate estimation of the energies may be obtained by interpolation. The calculations were carried to five decimal places in order to permit the use of the rigid approximation to a molecular rotor as the first approximation in a more complete treatment of its dynamical properties.

Although in general $E(\kappa)$ cannot be given in explicit form, roots which are derived from linear or quadratic factors may be expressed explicitly and are given in Table XII.

Polynomial Form of the Energy Equations

The usual polynomial form of a characteristic equation is obtained most easily by expanding the determinant $|D-\lambda I|=0$ in terms of the first principal minors p_i, of order $i+1$, by means of the recursion formulas[17a]

$$\begin{aligned} &p_0=k_0-\lambda, \\ &p_1=(k_1-\lambda)p_0-b_1, \\ &\cdots\cdots \\ &p_i=(k_i-\lambda)p_{i-1}-b_ip_{i-2}. \end{aligned} \tag{41}$$

If the order of D is $n+1$,

$$(-1)^{n+1}p_n=0 \tag{42}$$

is the usual form of the characteristic equation expressed as a polynomial in λ, with λ^{n+1} the leading term:

$$\begin{aligned} &\lambda-k_0=0, \\ &\lambda^2-\lambda(k_1+k_0)+k_1k_0-b_1=0, \\ &\lambda^3-\lambda^2(k_2+k_1+k_0)+\lambda(k_2k_1+k_2k_0+k_1k_0 \\ &\quad -b_2-b_1)-k_2k_1k_0+k_2b_1+k_0b_2=0, \text{ etc.} \end{aligned} \tag{43}$$

[17a] J. J. Sylvester, Phil. Mag. [4] **5**, 446 (1853).

With the aid of (36) and (37) or (38) the characteristic equations of any submatrix may be systematically developed. Type II representations, having the simplest forms of k_i and b_i, give these equations most readily. The true energies of a given rotor are then determined by the substitution of the roots λ_τ (or $E(\kappa)$) of these equations into (13).

The numerical coefficients of these characteristic equations in the parameter κ can be obtained from those given by Nielsen[18] by the substitution of λ/κ for his W and of $1/\kappa$ for his b.

VI. DIAGONALIZATION OF THE ENERGY MATRICES

To determine transition intensities, or to apply perturbation theory to the energy calculations over small ranges of the parameter κ, it is necessary to find a transformation T which

TABLE XII. Explicit solutions of $E(\kappa)$.

$JK_{-1}K_1$	$\lambda(\kappa)$
0_{00}	0
1_{10}	$\kappa+1$
1_{11}	0
1_{01}	$\kappa-1$
2_{20}	$2[\kappa+(\kappa^2+3)^{\frac{1}{2}}]$
2_{21}	$\kappa+3$
2_{11}	4κ
2_{12}	$\kappa-3$
2_{02}	$2[\kappa-(\kappa^2+3)^{\frac{1}{2}}]$
3_{30}	$5\kappa+3+2(4\kappa^2-6\kappa+6)^{\frac{1}{2}}$
3_{31}	$2[\kappa+(\kappa^2+15)^{\frac{1}{2}}]$
3_{21}	$5\kappa-3+2(4\kappa^2+6\kappa+6)^{\frac{1}{2}}$
3_{22}	4κ
3_{12}	$5\kappa+3-2(4\kappa^2-6\kappa+6)^{\frac{1}{2}}$
3_{13}	$2[\kappa-(\kappa^2+15)^{\frac{1}{2}}]$
3_{03}	$5\kappa-3-2(4\kappa^2+6\kappa+6)^{\frac{1}{2}}$
4_{40}	- - - -
4_{41}	$5\kappa+5+2(4\kappa^2-10\kappa+22)^{\frac{1}{2}}$
4_{31}	$10\kappa+2(9\kappa^2+7)^{\frac{1}{2}}$
4_{32}	$5\kappa-5+2(4\kappa^2+10\kappa+22)^{\frac{1}{2}}$
4_{22}	- - - -
4_{23}	$5\kappa+5-2(4\kappa^2-10\kappa+22)^{\frac{1}{2}}$
4_{13}	$10\kappa-2(9\kappa^2+7)^{\frac{1}{2}}$
4_{14}	$5\kappa-5-2(4\kappa^2+10\kappa+22)^{\frac{1}{2}}$
4_{04}	- - - -
5_{42}	$10\kappa+6(\kappa^2+3)^{\frac{1}{2}}$
5_{24}	$10\kappa-6(\kappa^2+3)^{\frac{1}{2}}$

[18] H. H. Nielsen, Phys. Rev. **38**, 1432 (1931), corrected and extended through $J=11$ by H. M. Randall, D. M. Dennison, Nathan Ginsburg, and Louis R. Weber, Phys. Rev. **52**, 160 (1937).

diagonalizes each energy submatrix. Since E is Hermitian, T can be chosen orthonormal,[18a] so that

$$T'ET=\|\lambda_\tau\|=\Lambda, \tag{44}$$

where Λ is diagonal. Here τ is not a running index, but refers to the τ values occurring in the submatrix E under consideration. The asymmetric rotor wave functions, $A(J,\tau,M,\gamma)$ are expressed as linear combinations of the Wang functions by

$$A(J,\tau,M,\gamma)=\sum_K t_{K\tau}S(J,K,M,\gamma). \tag{45}$$

The summation over K is over only those K's which occur as squares in the main diagonals of the submatrix, as determined by (37) and (38). The value of γ is fixed for each submatrix.

The orthonormal matrix T can be found in a fairly simple way if one first examines the diagonalization of D. There is a matrix V, diagonalizing D, i.e.,

$$V^{-1}DV=\Lambda, \tag{46}$$

which can be computed from the last columns of $adj|D-\lambda_\tau I|$. Let such a column, which is the column of V corresponding to the root λ_τ, be denoted by v_τ. The components of v_τ can be easily evaluated by substituting λ_τ in the recursion formula (41). Denoting $p_i(\lambda_\tau)$ as $p_{i\tau}$, one obtains

$$v_\tau=(1,\ -p_{0\tau},\ p_{1\tau},\ -p_{2\tau},\ \cdots). \tag{47}$$

Thus if $v_{i\tau}$ is the $(i+1)$th element of this column, then

$$V=\|v_{i\tau}\|,\quad i=0 \text{ to } n, \tag{48}$$

with

$$\begin{aligned} v_{0\tau}&=1,\\ v_{i\tau}&=(-1)^i p_{i-1,\tau}. \end{aligned} \tag{49}$$

The relation between V and T can be found from the relation between the original Hamiltonian E, (35), and the continuant matrix D of (36), i.e.,

$$D=L^{-1}EL, \tag{50}$$

with

$$L=\|l_{ii}\|=\begin{Vmatrix} 1 & 0 & 0\\ 0 & b_1^{-\frac{1}{2}} & 0\\ 0 & 0 & b_1^{-\frac{1}{2}}b_2^{-\frac{1}{2}} \end{Vmatrix}. \tag{51}$$

Substitution of (50) into (46) gives

$$V^{-1}L^{-1}ELV=\Lambda. \tag{52}$$

The transformation LV is orthogonal[18a] and can be normalized by post-multiplication by the diagonal matrix

$$N=\|n_{\tau\tau}\|=\|[\textstyle\sum_i (l_{ii}v_{i\tau})^2]^{-\frac{1}{2}}\|. \tag{53}$$

The transformation T required in (44) is then

$$T=LVN=\begin{Vmatrix} 1 & & & \\ & b_1^{-\frac{1}{2}} & & \\ & & b_1^{-\frac{1}{2}}b_2^{-\frac{1}{2}} & \\ & & & \cdots \end{Vmatrix}\begin{Vmatrix} 1 & 1 & 1 & \cdots\\ -p_{0\tau} & -p_{0\tau'} & -p_{0\tau''} & \cdots\\ p_{1\tau} & p_{1\tau'} & p_{1\tau''} & \cdots\\ \cdots & \cdots & \cdots & \cdots \end{Vmatrix}\begin{Vmatrix} n_{\tau\tau} & & & \\ & n_{\tau'\tau'} & & \\ & & n_{\tau''\tau''} & \\ & & & \cdots \end{Vmatrix}. \tag{54}$$

VII. ENERGY CALCULATION BY PERTURBATION METHODS

Perturbation theory may be applied to the calculation of the roots $E(\kappa+d\kappa)$, provided the roots $E(\kappa)$ are known. For a given value of κ, the transformation T, which diagonalizes a given submatrix, may be evaluated by the methods of Section VI. The diagonalized submatrix $\Lambda^{(0)}$ has for main diagonal elements the roots $E(\kappa)$, which for convenience we have called $\lambda_\tau^{(0)}$. Application of this transformation to a submatrix E for a slightly different asymmetry parameter $\kappa+d\kappa$ gives

$$T'ET=\Lambda^{(0)}+E'd\kappa=\|\lambda_\tau^{(0)}\|+\|e'_{\tau\tau'}\|d\kappa, \tag{55}$$

where $E'd\kappa$ is the perturbation matrix. In general, for $\kappa\neq\pm1$, none of the elements of E' is zero, and (55) no longer has the continuant form.

The second-order perturbation formulas giving approximate expressions for the perturbed ener-

[18a] The term "orthonormal" as used here means that the rows and columns are orthogonal and normalized. The term "orthogonal" as used here means that the columns are orthogonal but not normalized (hence the rows are *not* orthogonal).

gies $\lambda_\tau^{(2)}$ may now be written by inspection:

$$\lambda_\tau^{(2)}=\lambda_\tau^{(0)}+e'_{\tau\tau}d\kappa+\sum_{\tau'}\frac{e'^{\,2}_{\tau\tau'}}{\lambda_\tau^{(0)}-\lambda_{\tau'}^{(0)}}d\kappa^2. \quad (56)$$

The above procedures have been applied in the evaluation of the second-order perturbation around the most asymmetric case, $\kappa=0$, i.e., $d\kappa\rightarrow\kappa$. The coefficients of the expansion of $E(\kappa)$ as a power series in κ are given in Appendix II.

Perturbed Symmetric Rotors

In the limits $\kappa=-1$ and $\kappa=+1$, diagonal energy matrices are obtained in Type I and Type III representations, respectively, thus eliminating the preliminary evaluation of the diagonalizing transformation T. The application of perturbation theory to the calculation of approximate energies for nearly symmetric rotors is therefore greatly simplified. In addition, the use of (12) eliminates the necessity of expanding about both $\kappa=-1$ and $\kappa=1$. The following derivation yields the fifth-order perturbation formulas for the perturbed symmetric rotor $\delta\sim 0$ or $\kappa\sim -1$.

The continued fraction form of the submatrix secular equations of a Type I representation in terms of the asymmetry parameter δ is

$$\lambda_m=k_m{}^0+\delta k_m{}'-\cfrac{\delta^2 f_{m+1}}{k^0_{m+1}+\delta k'_{m+1}-\lambda_m-(\delta^2 f_{m+2}/k^0_{m+2}+\delta k'_{m+2}-\lambda_m-\cdots)}$$

$$-\cfrac{\delta^2 f_m}{k^0_{m-1}+\delta k'_{m-1}-\lambda_m-(\delta^2 f_{m-1}/k^0_{m-2}+\delta k'_{m-2}-\lambda_m-\cdots)}, \quad (57)$$

where the k^0's, k''s, and f's[19] for each submatrix are obtainable from (37) and (38) and Tables I and III. The first-order approximation to λ_m is

$$\lambda_m^{(1)}=k_m{}^0+\delta k_m{}'. \quad (58)$$

The third-order approximation is readily obtained by substitution of the $\lambda_m^{(1)}$ for λ_m on the right side of (57) and expanding the denominators as far as the linear term in δ.

$$\lambda_m^{(3)}=k_m{}^0+\delta k_m{}'-\delta^2\left[\frac{f_{m+1}}{k^0_{m+1}-k^0_m}+\frac{f_m}{k^0_{m-1}-k^0_m}\right]+\delta^3\left[\frac{(k'_{m+1}-k'_m)f_{m+1}}{(k^0_{m+1}-k^0_m)^2}+\frac{(k'_{m-1}-k'_m)f_m}{(k^0_{m-1}-k^0_m)^2}\right]. \quad (59)$$

Substituting $\lambda_m^{(3)}$ for λ_m on the right side of (57) and expanding the denominators to include all cubic terms in δ, one obtains for the fifth-order approximation:

$$\lambda_m^{(5)}=\lambda_m^{(3)}-\delta^4\left[\frac{f_{m+1}}{k^0_{m+1}-k^0_m}\left\{\left(\frac{k'_{m+1}-k'_m}{k^0_{m+1}-k^0_m}\right)^2-\alpha\right\}+\frac{f_m}{k^0_{m-1}-k^0_m}\left\{\left(\frac{k'_{m-1}-k'_m}{k^0_{m-1}-k^0_m}\right)^2-\beta\right\}\right]$$

$$+\delta^5\left[\frac{f_{m+1}}{k^0_{m+1}-k^0_m}\left\{\left(\frac{k'_{m+1}-k'_m}{k^0_{m+1}-k^0_m}\right)^3-2\alpha\left(\frac{k'_{m+1}-k'_m}{k^0_{m+1}-k^0_m}\right)+\frac{1}{k^0_{m+1}-k^0_m}\left(\frac{(k'_{m+2}-k'_m)f_{m+2}}{(k^0_{m+2}-k^0_m)^2}-\gamma\right)\right\}\right.$$

$$\left.+\frac{f_m}{k^0_{m-1}-k^0_m}\left\{\left(\frac{k'_{m-1}-k'_m}{k^0_{m-1}-k^0_m}\right)^3-2\beta\left(\frac{k'_{m-1}-k'_m}{k^0_{m-1}-k^0_m}\right)+\frac{1}{k^0_{m-1}-k^0_m}\left(\frac{(k'_{m-2}-k'_m)f_{m-1}}{(k^0_{m-2}-k^0_m)^2}-\gamma\right)\right\}\right], \quad (60)$$

[19] Note that the f's used here with running subscript indices for each submatrix are not the $f(J, n)$'s of Table I, although they are closely related.

where

$$\alpha=\frac{1}{k^0_{m+1}-k^0_m}\left(\frac{f_{m+1}}{k^0_{m+1}-k^0_m}+\frac{f_m}{k^0_{m-1}-k^0_m}-\frac{f_{m+2}}{k^0_{m+2}-k^0_m}\right), \tag{61}$$

$$\beta=\frac{1}{k^0_{m-1}-k^0_m}\left(\frac{f_{m+1}}{k^0_{m+1}-k^0_m}+\frac{f_m}{k^0_{m-1}-k^0_m}-\frac{f_{m-1}}{k^0_{m-2}-k^0_m}\right), \tag{62}$$

$$\gamma=\frac{(k'_{m+1}-k'_m)f_{m+1}}{(k^0_{m+1}-k^0_m)^2}+\frac{(k'_{m-1}-k'_m)f_m}{(k^0_{m-1}-k^0_m)^2}. \tag{63}$$

Appendix III gives the numerical coefficients of $\lambda_m^{(3)}$.

VIII. CONCLUSION

In the course of the approximate calculation of the energies $E(d\kappa)$ of the perturbed most asymmetric rotor, the matrices of the transformations which diagonalize the energies of a Type II representation for $\kappa=0$ were evaluated. Some time in the future, we plan to apply these transformations to the evaluation of the elements of the direction-cosine matrices for the case $\kappa=0$. These in turn will enable the calculation of the Einstein coefficients which appear in the expressions for the intensities of rotation transitions. The evaluation of the rigid rotor approximation to the intensities for H_2O, $\kappa\sim-0.436$, and for H_2S, $\kappa\sim0.5$ are partially completed.

The authors wish to express their appreciation for the care with which Mr. E. Howard, Jr., Mr. J. E. Whitney, Mr. R. D. Mair, Mr. N. R. Larson, Mr. E. N. Marvell, Mr. W. Davis, Jr., and Miss E. Leoni performed certain numerical calculations here reported.

APPENDIX I. TABLE OF RIGID ROTOR ENERGY LEVEL PATTERNS $E(\kappa)$

The asymmetry parameter $\kappa=(2b-a-c)/(a-c)$, where a, b, c, equal $\hbar^2/2I_a$, $\hbar^2/2I_b$, $\hbar^2/2I_c$, respectively, and where the condition $I_a\leqslant I_b\leqslant I_c$ is applied in assigning the moments of inertia.

Energy level patterns for $0\leqslant\kappa\leqslant1$ may be readily obtained from the table by the use of the relation

$$E_\tau{}^J(\kappa)=-E_{-\tau}{}^J(-\kappa).$$

Rotational energy levels are given by

$$E_\tau{}^J(a,b,c)=[(a+c)/2]J(J+1)+[(a-c)/2]E_\tau{}^J(\kappa).$$

Symmetries are included in terms of the JK_{-1},K_1 notation.

J_{K_{-1},K_1} \ δ / κ	0 / −1	0.05 / −0.9	0.1 / −0.8	0.15 / −0.7	0.2 / −0.6	0.25 / −0.5	0.3 / −0.4	0.35 / −0.3	0.4 / −0.2	0.45 / −0.1	0.5 / 0	δ / κ	J_τ
$0_{0,0}$	0	0	0	0	0	0	0	0	0	0	0		0_0
$1_{1,0}$	0	0.1	0.2	0.3	0.4	0.5	0.6	0.7	0.8	0.9	1		1_1
$1_{1,1}$	0	0	0	0	0	0	0	0	0	0	0		1_0
$1_{0,1}$	−2	−1.9	−1.8	−1.7	−1.6	−1.5	−1.4	−1.3	−1.2	−1.1	−1		1_{-1}
$2_{2,0}$	2	2.10384	2.21576	2.33631	2.46606	2.60555	2.75528	2.91568	3.08712	3.26987	3.46410		2_2
$2_{2,1}$	2	2.1	2.2	2.3	2.4	2.5	2.6	2.7	2.8	2.9	3		2_1
$2_{1,1}$	−4	−3.6	−3.2	−2.8	−2.4	−2.0	−1.6	−1.2	−0.8	−0.4	0		2_0
$2_{1,2}$	−4	−3.9	−3.8	−3.7	−3.6	−3.5	−3.4	−3.3	−3.2	−3.1	−3		2_{-1}
$2_{0,2}$	−6	−5.70384	−5.41576	−5.13631	−4.86606	−4.60555	−4.35528	−4.11568	−3.88712	−3.66987	−3.46410		2_{-2}
$3_{3,0}$	6	6.15245	6.31027	6.47424	6.64530	6.82496	7.01332	7.21314	7.42586	7.65364	7.89898		3_3
$3_{3,1}$	6	6.15236	6.30949	6.47147	6.63837	6.81025	6.98717	7.16917	7.35629	7.54855	7.74597		3_2
$3_{2,1}$	−4	−3.58082	−3.12186	−2.62186	−2.08082	−1.5	−0.88175	−0.22917	0.45421	1.16476	1.89898		3_1
$3_{3,2}$	−4	−3.6	−3.2	−2.8	−2.4	−2.0	−1.6	−1.2	−0.8	−0.4	0		3_0
$3_{1,2}$	−10	−9.15245	−8.31027	−7.47424	−6.64530	−5.82496	−5.01332	−4.21314	−3.42586	−2.65364	−1.89898		3_{-1}
$3_{1,3}$	−10	−9.75236	−9.50949	−9.27147	−9.03837	−8.81025	−8.58717	−8.36917	−8.15629	−7.94855	−7.74597		3_{-2}
$3_{0,3}$	−12	−11.41918	−10.87814	−10.37814	−9.91918	−9.5	−9.11825	−8.77083	−8.45421	−8.16476	−7.89898		3_{-3}
$4_{4,0}$	12	12.20299	12.41230	12.62852	12.85233	13.08461	13.32641	13.57912	13.84441	14.12449	14.42221		4_4
$4_{4,1}$	12	12.20299	12.41227	12.62834	12.85173	13.08301	13.32279	13.57174	13.83056	14.10000	14.38083		4_3
$4_{3,1}$	−2	−1.43958	−0.85577	−0.24426	0.40000	1.08276	1.81033	2.58928	3.42587	4.32541	5.29150		4_2
$4_{3,2}$	−2	−1.44022	−0.86120	−0.26350	0.35224	0.98528	1.63481	2.30000	2.97998	3.67388	4.38083		4_1
$4_{2,2}$	−12	−11.14570	−10.18216	−9.11536	−7.95859	−6.72860	−5.44216	−4.11432	−2.75776	−1.38320	0.00000		4_0
$4_{2,3}$	−12	−11.20299	−10.41227	−9.62834	−8.85173	−8.08301	−7.32279	−6.57174	−5.83056	−5.10000	−4.38083		4_{-1}
$4_{1,3}$	−18	−16.56042	−15.14423	−13.75574	−12.40000	−11.08276	−9.81033	−8.58928	−7.42587	−6.32541	−5.29150		4_{-2}
$4_{1,4}$	−18	−17.55978	−17.13880	−16.73650	−16.35224	−15.98528	−15.63481	−15.30000	−14.97998	−14.67388	−14.38083		4_{-3}
$4_{0,4}$	−20	−19.05729	−18.23015	−17.51316	−16.89374	−16.35601	−15.88425	−15.46480	−15.08665	−14.74129	−14.42221		4_{-4}

J_{K_{-1},K_1} \ δ / κ	0 / −1	0.05 / −0.9	0.1 / −0.8	0.15 / −0.7	0.2 / −0.6	0.25 / −0.5	0.3 / −0.4	0.35 / −0.3	0.4 / −0.2	0.45 / −0.1	0.5 / 0	δ / κ	J_τ
$5_{5,0}$	20	20.25361	20.51481	20.78427	21.06273	21.35107	21.65036	21.96188	22.28725	22.62851	22.98829		5_5
$5_{5,1}$	20	20.25361	20.51481	20.78426	21.06267	21.35092	21.64990	21.96077	22.28477	22.62338	22.97825		5_4
$5_{4,1}$	2	2.71155	3.44756	4.21049	5.00354	5.83082	6.69763	7.61079	8.57900	9.61304	10.72586		5_3
$5_{4,2}$	2	2.71153	3.44727	4.20892	4.99818	5.81665	6.66583	7.54704	8.46136	9.40961	10.39230		5_2
$5_{3,2}$	−12	−10.92537	−9.79317	−8.58944	−7.29895	−5.90702	−4.40221	−2.77918	−1.04053	0.80359	2.73757		5_1
$5_{3,3}$	−12	−10.92796	−9.81475	−8.66510	−7.48387	−6.27602	−5.04632	−3.79947	−2.53993	−1.27204	0.00000		5_0
$5_{2,3}$	−22	−20.57904	−18.92805	−17.09089	−15.12406	−13.07747	−10.98945	−8.88912	−6.80000	−4.74287	−2.73757		5_{-1}
$5_{2,4}$	−22	−20.71153	−19.44727	−18.20892	−16.99818	−15.81665	−14.66583	−13.54704	−12.46136	−11.40961	−10.39230		5_{-2}
$5_{1,4}$	−28	−25.82824	−23.72164	−21.69483	−19.76369	−17.94405	−16.24815	−14.68270	−13.24672	−11.93210	−10.72586		5_{-3}
$5_{1,5}$	−28	−27.32565	−26.70006	−26.11916	−25.57880	−25.07490	−24.60358	−24.16130	−23.74484	−23.35134	−22.97825		5_{-4}
$5_{0,5}$	−30	−28.63251	−27.51951	−26.61960	−25.87948	−25.25335	−24.70818	−24.22167	−23.77900	−23.37017	−22.98829		5_{-5}
$6_{6,0}$	30	30.30423	30.61738	30.94020	31.27357	31.61849	31.97615	32.34798	32.73569	33.14140	33.56782		6_6
$6_{6,1}$	30	30.30423	30.61738	30.94020	31.27357	31.61847	31.97610	32.34782	32.73527	33.14039	33.56554		6_5
$6_{5,1}$	8	8.86322	9.75433	10.67572	11.63026	12.62142	13.65350	14.73201	15.86409	17.05926	18.33030		6_4
$6_{5,2}$	8	8.86322	9.75431	10.67561	11.62975	12.61966	13.64861	14.72012	15.83798	17.00616	18.22865		6_3
$6_{4,2}$	−10	−8.67533	−7.29809	−5.86179	−4.35735	−2.77237	−1.09071	0.70756	2.64470	4.74200	7.01437		6_2
$6_{4,3}$	−10	−8.67542	−7.29951	−5.86955	−4.38365	−2.84099	−1.24202	0.41154	2.11663	3.86897	5.66311		6_1
$6_{3,3}$	−24	−22.30159	−20.48431	−18.51309	−16.35698	−14.00000	−11.44897	−8.73201	−5.88916	−2.96181	0.00000		6_0
$6_{3,4}$	−24	−22.30932	−20.54826	−18.73335	−16 88024	−15.00321	−13.11511	−11.22733	−9.35010	−7.49261	−5.66311		6_{-1}
$6_{2,4}$	−34	−31.86770	−29.33128	−26.53537	−23.61166	−20.64988	−17.71113	−14.81213	−12.08230	−9.46494	−7.01437		6_{-2}
$6_{2,5}$	−34	−32.12881	−30.31787	−28.57065	−26.88992	−25.27748	−23.73408	−22.25936	−20.85190	−19.50936	−18.22855		6_{-3}
$6_{1,5}$	−40	−36.96163	−34.07002	−31.36263	−28.87328	−26.62142	−24.60153	−22.80000	−21.17463	−19.69445	−18.33030		6_{-4}
$6_{1,6}$	−40	−39.05391	−38.20605	−37.44226	−36.74951	−36.11645	−35.53350	−34.99279	−34.48788	−34.01355	−33.56554		6_{-5}
$6_{0,6}$	−42	−40.16120	−38.78801	−37.74304	−36.90456	−36.19624	−35.57431	−35.01341	−34.49809	−34.01816	−33.56782		6_{-6}
$7_{7,0}$	42	42.35486	42.71997	43.09619	43.48453	43.88613	44.30236	44.73481	45.18543	45.65657	46.15116		7_7
$7_{7,1}$	42	42.35486	42.71997	43.09619	43.48453	43.88613	44.30235	44.73479	45.18537	45.65638	46.15066		7_6
$7_{6,1}$	16	17.01500	18.06163	19.14256	20.26091	21.42032	22.62515	23.88066	25.19347	26.57205	28.02767		7_5
$7_{6,2}$	16	17.01500	18.06162	19.14255	20.26087	21.42013	22.62446	23.87866	25.18825	26.55961	28.00000		7_4
$7_{5,2}$	−6	−4.42312	−2.78954	−1.09415	0.66943	2.50949	4.43711	6.46744	8.62113	10.92575	13.41608		7_3
$7_{5,3}$	−6	−4.42313	−2.78962	−1.09480	0.66638	2.49918	4.40873	6.39965	8.47556	10.63855	12.88860		7_2
$7_{4,3}$	−24	−21.95606	−19.81731	−17.56836	−15.18606	−12.63901	−9.88997	−6.90390	−3.66093	−0.16798	3.53956		7_1
$7_{4,4}$	−24	−21.95636	−19.82250	−17.59639	−15.27966	−12.87783	−10.40000	−7.85829	−5.26703	−2.64204	0.00000		7_0
$7_{3,4}$	−38	−35.56370	−32.90450	−29.95229	−26.67345	−23.09517	−19.29241	−15.35524	−11.36816	−7.40649	−3.53957		7_{-1}
$7_{3,5}$	−38	−35.58293	−33.06125	−30.47630	−27.86342	−25.25166	−22.66461	−20.12130	−17.63693	−15.22320	−12.88860		7_{-2}
$7_{2,5}$	−48	−44.99890	−41.38121	−37.47756	−33.51139	−29.61371	−25.87353	−22.35690	−19.10561	−16.13111	−13.41608		7_{-3}
$7_{2,6}$	−48	−45.45864	−43.03912	−40.74616	−38.58120	−36.54230	−34.62446	−32.82037	−31.12122	−29.51757	−28.00000		7_{-4}
$7_{1,6}$	−54	−49.96804	−46.22593	−42.84975	−39.88051	−37.30045	−35.04706	−33.04701	−31.23840	−29.57583	−28.02767		7_{-5}
$7_{1,7}$	−54	−52.74881	−51.66910	−50.72509	−49.88749	−49.13365	−48.44647	−47.81314	−47.22100	−46.67173	−46.15066		7_{-6}
$7_{0,7}$	−56	−53.66004	−52.06311	−50.89664	−49.96344	−49.16761	−48.46165	−47.81986	−47.22692	−46.67296	−46.15116		7_{-7}
$8_{8,0}$	56	56.40550	56.82257	57.25221	57.69554	58.15386	58.62871	59.12189	59.63558	60.17242	60.73566		8_8
$8_{8,1}$	56	56.40550	56.82257	57.25221	57.69554	58.15386	58.62871	59.12189	59.63557	60.17238	60.73555		8_7
$8_{7,1}$	26	27.16683	28.36913	29.60991	30.89263	32.22133	33.60075	35.03654	36.53557	38.10638	39.75991		8_6
$8_{7,2}$	26	27.16683	28.36913	29.60991	30.89263	32.22131	33.60066	35.03622	36.53460	38.10367	39.75292		8_5
$8_{6,2}$	0	1.82951	3.72124	5.68052	7.71361	9.82803	12.03308	14.34073	16.76690	19.33369	22.07216		8_4
$8_{6,3}$	0	1.82951	3.72123	5.68047	7.71330	9.82667	12.02844	14.32726	16.73241	19.25327	21.89858		8_3
$8_{5,3}$	−22	−19.60431	−17.11206	−14.51381	−11.79659	−8.94181	−5.92261	−2.70132	0.77076	4.54704	8.66888		8_2
$8_{5,4}$	−22	−19.60432	−17.11240	−14.51661	−11.80954	−8.98198	−6.03922	−2.97225	0.21113	3.50079	6.88121		8_1
$8_{4,4}$	−40	−37.12871	−34.10050	−30.88066	−27.41611	−23.64282	−19.50903	−15.00742	−10.18985	−5.15070	0.00000		8_0
$8_{4,5}$	−40	−37.12961	−34.11595	−30.96275	−27.68384	−24.30158	−20.84414	−17.34256	−13.82839	−10.33195	−6.88121		8_{-1}
$8_{3,5}$	−54	−50.70574	−47.02209	−42.84192	−38.18998	−33.21092	−28.07787	−22.94146	−17.92750	−13.14274	−8.66888		8_{-2}
$8_{3,6}$	−54	−50.74775	−47.35653	−43.91096	−40.47535	−37.09670	−33.80861	−30.63410	−27.58741	−24.67532	−21.89857		8_{-3}
$8_{2,6}$	−64	−59.96219	−55.08643	−49.97556	−44.94942	−40.18548	−35.79447	−31.82321	−28.25352	−25.02598	−22.07216		8_{-4}
$8_{2,7}$	−64	−60.70539	−57.62785	−54.76993	−52.12499	−49.67895	−47.41301	−45.30659	−43.33959	−41.49370	−39.75292		8_{-5}
$8_{1,7}$	−70	−64.85679	−60.23498	−56.25418	−52.90606	−50.06860	−47.60027	−45.39376	−43.37883	−41.51068	−39.75991		8_{-6}
$8_{1,8}$	−70	−68.41477	−67.10020	−65.98234	−65.00774	−64.13963	−63.35283	−62.62987	−61.95832	−61.32914	−60.73555		8_{-7}
$8_{0,8}$	−72	−69.14410	−67.35688	−66.07651	−65.04361	−64.15359	−63.35829	−62.63199	−61.95912	−61.32943	−60.73566		8_{-8}
$9_{9,0}$	72	72.45613	72.92518	73.40825	73.90658	74.42165	74.95515	75.50910	76.08592	76.68854	77.32058		9_9
$9_{9,1}$	72	72.45613	72.92518	73.40825	73.90658	74.42165	74.95515	75.50910	76.08591	76.68853	77.32056		9_8
$9_{8,1}$	38	39.31868	40.67675	42.07753	43.52486	45.02321	46.57781	48.19485	49.88181	51.64782	53.50433		9_7
$9_{8,2}$	38	39.31868	40.67675	42.07753	43.52486	45.02321	46.57780	48.19481	49.88164	51.64726	53.50266		9_6
$9_{7,2}$	8	10.08234	12.23284	14.45731	16.76247	19.15619	21.64787	24.24891	26.97372	29.84111	32.87689		9_5
$9_{7,3}$	8	10.08234	12.23284	14.45731	16.76244	19.15603	21.64717	24.24648	26.96631	29.82081	32.82576		9_4
$9_{6,3}$	−18	−15.25136	−12.40015	−9.43737	−6.35217	−3.13080	0.24515	3.80150	7.57555	11.62086	16.00923		9_3
$9_{6,4}$	−18	−15.25136	−12.40016	−9.43761	−6.35370	−3.13740	0.22283	3.73803	7.41715	11.26493	15.27959		9_2
$9_{5,4}$	−40	−36.67904	−33.20766	−29.56890	−25.73632	−21.66848	−17.30456	−12.56784	−7.38796	−1.74182	4.31610		9_1
$9_{5,5}$	−40	−36.67907	−33.20883	−29.57856	−25.78034	−21.81221	−17.68086	−13.40321	−9.00616	−4.52484	0.00000		9_0
$9_{4,5}$	−58	−54.19095	−50.13492	−45.75802	−40.95556	−35.63960	−29.81240	−23.58911	−17.14554	−10.66402	−4.31610		9_{-1}
$9_{4,6}$	−58	−54.19330	−50.17453	−45.96402	−41.60316	−37.14601	−32.65039	−28.17155	−23.75826	−19.45078	−15.27959		9_{-2}
$9_{3,6}$	−72	−67.72006	−62.80114	−57.13828	−50.92760	−44.48261	−38.07036	−31.89729	−26.11873	−20.82173	−16.00923		9_{-3}
$9_{3,7}$	−72	−67.80326	−63.44066	−59.06273	−54.76962	−50.62458	−46.66453	−42.90671	−39.35371	−35.99794	−32.82576		9_{-4}
$9_{2,7}$	−82	−76.75116	−70.47091	−64.10763	−58.08158	−52.60633	−47.75172	−43.46093	−39.61925	−36.11803	−32.87689		9_{-5}
$9_{2,8}$	−82	−77.87402	−74.10206	−70.67590	−67.56800	−64.73980	−62.15024	−59.76129	−57.54053	−55.46141	−53.50266		9_{-6}
$9_{1,8}$	−88	−81.63937	−76.14922	−71.65838	−68.00513	−64.92675	−62.22810	−59.79288	−57.55295	−55.46610	−53.50433		9_{-7}
$9_{1,9}$	−88	−86.05614	−84.50853	−83.22427	−82.11906	−81.14089	−80.25693	−79.44566	−78.69235	−77.98656	−77.32056		9_{-8}
$9_{0,9}$	−90	−86.62521	−84.67077	−83.27451	−82.13555	−81.14648	−80.25884	−79.44631	−78.69257	−77.98663	−77.32058		9_{-9}
$10_{10,0}$	90	90.50677	91.02780	91.56430	92.11765	92.68947	93.28164	93.89638	94.53636	95.20481	95.90573		10_{10}
$10_{10,1}$	90	90.50677	91.02780	91.56430	92.11765	92.68947	93.28164	93.89638	94.53636	95.20481	95.90573		10_9
$10_{9,1}$	52	53.47056	54.98444	56.54530	58.15739	59.82560	61.55565	63.35435	65.22987	67.19213	69.25347		10_8
$10_{9,2}$	52	53.47056	54.98444	56.54530	58.15739	59.82560	61.55564	63.35434	65.22984	67.19202	69.25308		10_7

J_{K_{-1},K_1} \ δ / κ	0 / −1	0.05 / −0.9	0.1 / −0.8	0.15 / −0.7	0.2 / −0.6	0.25 / −0.5	0.3 / −0.4	0.35 / −0.3	0.4 / −0.2	0.45 / −0.1	0.5 / 0	δ / κ / J_τ
$10_{8,2}$	18	20.33528	22.74489	25.23517	27.81341	30.48810	33.26924	36.16881	39.20139	42.38529	45.74432	10_8
$10_{8,3}$	18	20.33527	22.74489	25.23517	27.81341	30.48808	33.26914	36.16840	39.19991	42.38053	45.73037	10_5
$10_{7,3}$	−12	−8.89789	−5.68593	−2.35463	1.10694	4.71202	8.47676	12.42191	16.57564	20.97829	25.68964	10_4
$10_{7,4}$	−12	−8.89789	−5.68593	−2.35468	1.10677	4.71111	8.47295	12.40876	16.53640	20.87367	25.43593	10_3
$10_{6,4}$	−38	−34.22662	−30.29839	−26.20121	−21.91700	−17.42058	−12.67461	−7.62217	−2.18038	3.75474	10.27364	10_2
$10_{6,5}$	−38	−34.22663	−30.29846	−26.20216	−21.92298	−17.44611	−12.75906	−7.85527	−2.73819	2.57523	8.05291	10_1
$10_{5,5}$	−60	−55.64584	−51.06976	−46.24088	−41.10481	−35.57362	−29.53245	−22.88752	−15.64523	−7.94325	0.00000	10_0
$10_{5,6}$	−60	−55.64594	−51.07323	−46.26924	−41.23155	−35.97438	−30.53144	−24.95372	−19.30370	−13.64837	−8.05291	10_{-1}
$10_{4,6}$	−78	−73.14002	−67.90347	−62.14553	−55.70142	−48.53948	−40.84180	−32.89913	−24.99790	−17.38959	−10.27364	10_{-2}
$10_{4,7}$	−78	−73.14548	−67.99406	−62.60214	−57.06078	−51.47118	−45.92680	−40.50444	−35.26085	−30.23225	−25.43593	10_{-3}
$10_{3,7}$	−92	−86.59725	−80.20810	−72.83972	−64.98059	−57.11839	−49.60411	−42.67271	−36.41928	−30.79761	−25.68964	10_{-4}
$10_{2,8}$	−92	−86.74965	−81.32404	−75.96389	−70.80642	−65.92196	−61.33674	−57.04805	−53.03606	−49.27319	−45.73037	10_{-5}
$10_{2,8}$	−102	−95.36420	−87.56942	−79.96900	−73.07902	−67.07495	−61.87341	−57.28235	−53.13293	−49.31110	−45.74432	10_{-6}
$10_{2,9}$	−102	−96.96993	−92.48017	−88.49517	−84.94730	−81.76026	−78.86492	−76.20507	−73.73723	−71.42832	−69.25308	10_{-7}
$10_{1,9}$	−108	−100.32958	−94.02065	−89.11005	−85.17893	−81.84560	−78.89585	−76.21603	−73.74100	−71.42956	−69.25347	10_{-8}
$10_{1,10}$	−108	−105.67708	−103.90124	−102.45750	−101.22619	−100.14037	−99.16041	−98.26134	−97.42648	−96.64413	−95.90573	10_{-9}
$10_{0,10}$	−110	−106.11121	−104.00141	−102.48373	−101.23362	−100.14256	−99.16106	−98.26154	−97.42654	−96.64415	−95.90573	10_{-10}

APPENDIX II. COEFFICIENTS OF THE SECOND-ORDER APPROXIMATION TO THE ENERGIES $E(\kappa)$ OF PERTURBED "MOST ASYMMETRIC" ROTORS $\kappa \sim 0$

J_τ	κ^0	κ^1	κ^2
0_0	0	0	0
$1_{\pm1}$	± 1	1	0
1_0	0	0	0
$2_{\pm2}$	± 3.46410	2	± 0.57735
$2_{\pm1}$	± 3	1	0
2_0	0	4	0
$3_{\pm3}$	± 7.89898	2.55049	± 1.02061
$3_{\pm2}$	± 7.74597	2	± 0.25820
$3_{\pm1}$	± 1.89898	7.44951	± 1.02061
3_0	0	4	0
$4_{\pm4}$	±14.42221	3.07691	± 1.06343
$4_{\pm3}$	±14.38083	2.86800	± 0.61053
$4_{\pm2}$	± 5.29150	10	± 3.40355
$4_{\pm1}$	± 4.38083	7.13200	± 0.61053
4_0	0	13.84615	0
$5_{\pm5}$	±22.98829	3.70146	± 1.09887
$5_{\pm4}$	±22.97825	3.63637	± 0.90921
$5_{\pm3}$	±10.72586	11.57003	± 4.66868
$5_{\pm2}$	±10.39230	10	± 1.73208
$5_{\pm1}$	± 2.73757	19.72850	± 3.56981
5_0	0	12.72720	0
$6_{\pm6}$	±33.56782	4.37860	± 1.20617
$6_{\pm5}$	±33.56554	4.36049	± 1.14046
$6_{\pm4}$	±18.33030	13.14291	± 4.63150
$6_{\pm3}$	±18.22865	12.50987	± 2.91242
$6_{\pm2}$	± 7.01437	23.62143	± 8.97291
$6_{\pm1}$	± 5.66311	18.12993	± 1.77196
6_0	0	29.71418	0
$7_{\pm7}$	±46.15116	5.07485	± 1.35549
$7_{\pm6}$	±46.15066	5.07021	± 1.33530
$7_{\pm5}$	±28.02767	14.98862	± 4.60001
$7_{\pm4}$	±28	14.77564	± 3.85550
$7_{\pm3}$	±13.41608	25.96144	±11.24935
$7_{\pm2}$	±12.88860	22.92976	± 4.23885
$7_{\pm1}$	± 3.53957	37.97507	± 8.00483
7_0	0	26.44871	0
$8_{\pm8}$	±60.73566	5.77734	± 1.52190
$8_{\pm7}$	±60.73555	5.77621	± 1.51620
$8_{\pm6}$	±39.75991	16.99343	± 4.83960
$8_{\pm5}$	±39.75292	16.92944	± 4.56773
$8_{\pm4}$	±22.07216	28.37652	±10.70308
$8_{\pm3}$	±21.89857	27.10072	± 6.58510
$8_{\pm2}$	± 8.66888	43.00657	±17.81406
$8_{\pm1}$	± 6.88121	34.19363	± 3.53356
8_0	0	51.69231	0

J_τ	κ^0	κ^1	κ^2
$9_{\pm9}$	±77.32058	6.48187	± 1.69428
$9_{\pm8}$	±77.32056	6.48161	± 1.69279
$9_{\pm7}$	±53.50433	19.06330	± 5.24270
$9_{\pm6}$	±53.50266	19.04556	± 5.15451
$9_{\pm5}$	±32.87689	31.31083	±10.19637
$9_{\pm4}$	±32.82576	30.85743	± 8.36221
$9_{\pm3}$	±16.00923	45.87258	±21.28125
$9_{\pm2}$	±15.27959	40.95446	± 7.86816
$9_{\pm1}$	± 4.31610	62.27144	±14.63618
9_0	0	45.32189	0
$10_{\pm10}$	±95.90573	7.18725	± 1.86883
$10_{\pm9}$	±95.90573	7.18721	± 1.86846
$10_{\pm8}$	±69.25347	21.15760	± 5.71802
$10_{\pm7}$	±69.25308	21.15295	± 5.69155
$10_{\pm6}$	±45.74432	34.56504	±10.32836
$10_{\pm5}$	±45.73037	34.42074	± 9.63341
$10_{\pm4}$	±25.68964	48.92328	±19.69299
$10_{\pm3}$	±25.43593	46.78521	±11.74885
$10_{\pm2}$	±10.27364	68.24765	±30.39124
$10_{\pm1}$	± 8.05291	55.45391	± 5.93853
10_0	0	79.83824	0
$11_{\pm11}$	±116.49101	7.89303	± 2.04411
$11_{\pm10}$	±116.49101	7.89302	± 2.04401
$11_{\pm9}$	±87.00484	23.26159	± 6.22114
$11_{\pm8}$	±87.00476	23.26049	± 6.21376
$11_{\pm7}$	±60.63695	37.96101	±10.86339
$11_{\pm6}$	±60.63335	37.91851	±10.62714
$11_{\pm5}$	±37.57816	52.80410	±18.19006
$11_{\pm4}$	±37.49896	52.01224	±14.56648
$11_{\pm3}$	±18.52846	71.40516	±35.23697
$11_{\pm2}$	±17.59094	64.18842	±12.69943
$11_{\pm1}$	± 5.07342	92.67506	±23.73327
11_0	0	69.45454	0
$12_{\pm12}$	±139.07639	8.59911	± 2.21982
$12_{\pm11}$	±139.07639	8.59910	± 2.21979
$12_{\pm10}$	±106.75754	25.37029	± 6.73525
$12_{\pm9}$	±106.75752	25.37001	± 6.66084
$12_{\pm8}$	±77.54083	41.41539	±11.58290
$12_{\pm7}$	±77.53995	41.40366	±11.50884
$12_{\pm6}$	±51.56206	57.21806	±17.89676
$12_{\pm5}$	±51.53914	56.95433	±16.55247
$12_{\pm4}$	±29.20920	74.88820	±31.98796
$12_{\pm3}$	±28.86916	71.66763	±18.51034
$12_{\pm2}$	±11.83982	99.41162	±47.13339
$12_{\pm1}$	± 9.18884	82.00526	± 9.02566
12_0	0	114.19496	0

APPENDIX III. COEFFICIENTS OF THE THIRD-ORDER APPROXIMATION TO THE ENERGIES $E(\delta)$ OF PERTURBED SYMMETRIC ROTORS $\delta \sim 0$, OR $\kappa \sim -1$

$J_{K-1,K1}$	δ^0	δ^1	δ^2	δ^3
$0_{0,0}$	0	0	0	0
$1_{1,0}$	0	2	0	0
$1_{1,1}$	0	0	0	0
$1_{0,1}$	−2	2	0	0
$2_{2,0}$	2	2	1.5	0.75
$2_{2,1}$	2	2	0	0
$2_{1,1}$	−4	8	0	0
$2_{1,2}$	−4	2	0	0
$2_{0,2}$	−6	6	−1.5	−0.75
$3_{3,0}$	6	3	0.9375	0.82031
$3_{3,1}$	6	3	0.9375	0.11719
$3_{2,1}$	−4	8	7.5	3.75
$3_{2,2}$	−4	8	0	0
$3_{1,2}$	−10	17	−0.9375	−0.82031
$3_{1,3}$	−10	5	−0.9375	−0.11719
$3_{0,3}$	−12	12	−7.5	−3.75
$4_{4,0-1}$	12	4	1.16667	0.58333
$4_{3,1}$	−2	11	3.9375	4.42969
$4_{3,2}$	−2	11	3.9375	−0.49219
$4_{2,2}$	−12	16	21.33333	10.66667
$4_{2,3}$	−12	16	−1.16667	−0.58333
$4_{1,3}$	−18	29	−3.9375	−4.42969
$4_{1,4}$	−18	9	−3.9375	0.49219
$4_{0,4}$	−20	20	−22.5	−11.25
$5_{5,0-1}$	20	5	1.40625	0.70313
$5_{4,1-2}$	2	14	4.5	2.25
$5_{3,2}$	−12	21	9.09375	14.39062
$5_{3,3}$	−12	21	9.09375	−5.29688
$5_{2,3}$	−22	26	48	24
$5_{2,4}$	−22	26	−4.5	−2.25
$5_{1,4}$	−28	44	−10.5	−15.09375
$5_{1,5}$	−28	14	−10.5	4.59375
$5_{0,5}$	−30	30	−52.5	−26.25
$6_{6,0-1}$	30	6	1.65	0.825
$6_{5,1-2}$	8	17	5.15625	2.57813
$6_{4,2-3}$	−10	26	9.6	4.8
$6_{3,3}$	−24	33	17.34375	38.20312
$6_{3,4}$	−24	33	17.34375	−20.85938
$6_{2,4}$	−34	38	93.75	46.875
$6_{2,5}$	−34	38	−11.25	−5.625
$6_{1,5}$	−40	62	−22.5	−40.78125
$6_{1,6}$	−40	20	−22.5	18.28125
$6_{0,6}$	−42	42	−105	−52.5
$7_{7,0-1}$	42	7	1.89583	0.94792
$7_{6,1-2}$	16	20	5.85	2.925
$7_{5,2-3}$	−6	31	10.47917	5.23958
$7_{4,3-4}$	−24	40	17.06667	8.53333
$7_{3,4}$	−38	47	29.8125	88.03125
$7_{3,5}$	−38	47	29.8125	−58.92188
$7_{2,5}$	−48	52	166.08333	83.04166
$7_{2,6}$	−48	52	−22.91667	−11.45834
$7_{1,6}$	−54	83	−42.1875	−94.21875
$7_{1,7}$	−54	27	−42.1875	52.73438
$7_{0,7}$	−56	56	−189	−94.5

$J_{K-1,K1}$	δ^0	δ^1	δ^2	δ^3
$8_{8,0-1}$	56	8	2.14286	1.07143
$8_{7,1-2}$	26	23	6.5625	3.28125
$8_{6,2-3}$	0	36	11.50714	5.75357
$8_{5,3-4}$	−22	47	17.8125	8.90625
$8_{4,4-5}$	−40	56	27.6	13.8
$8_{3,5}$	−54	63	47.8125	186.32813
$8_{3,6}$	−54	63	47.8125	−138.51563
$8_{2,6}$	−64	68	273.75	136.875
$8_{2,7}$	−64	68	−41.25	−20.625
$8_{1,7}$	−70	107	−72.1875	−198.51563
$8_{1,8}$	−70	35	−72.1875	126.32813
$8_{0,8}$	−72	72	−315	−157.5
$9_{9,0-1}$	72	9	2.39063	1.19532
$9_{8,1-2}$	38	26	7.28571	3.64286
$9_{7,2-3}$	8	41	12.60937	6.30468
$9_{6,3-4}$	−18	54	18.96429	9.48214
$9_{5,4-5}$	−40	65	27.65625	13.82813
$9_{4,5-6}$	−58	74	42	21
$9_{3,6}$	−72	81	72.84375	361.26562
$9_{3,7}$	−72	81	72.84375	−288.42188
$9_{2,7}$	−82	86	426.75	213.375
$9_{2,8}$	−82	86	−68.25	−34.125
$9_{1,8}$	−88	134	−115.5	−382.59375
$9_{1,9}$	−88	44	−115.5	267.09375
$9_{0,9}$	−90	90	−495	−247.5
$10_{10,0-1}$	90	10	2.63889	1.31945
$10_{9,1-2}$	52	29	8.01563	4.00782
$10_{8,2-3}$	18	46	13.75397	6.87698
$10_{7,3-4}$	−12	61	20.31770	10.15885
$10_{6,4-5}$	−38	74	28.60714	14.30357
$10_{5,5-6}$	−60	85	40.57292	20.28646
$10_{4,6-7}$	−78	94	61.16667	30.58333
$10_{3,7}$	−92	101	106.59375	656.57812
$10_{3,8}$	−92	101	106.59375	−549.98438
$10_{2,8}$	−102	106	636.33333	318.16666
$10_{2,9}$	−102	106	−106.16667	−53.08334
$10_{1,9}$	−108	164	−175.5	−691.03125
$10_{1,10}$	−108	54	−175.5	515.53125
$10_{0,10}$	−110	110	−742.5	−371.25
$11_{11,0-1}$	110	11	2.8875	1.44375
$11_{10,1-2}$	74	32	8.75	4.375
$11_{9,2-3}$	32	51	14.925	7.4625
$11_{8,3-4}$	−4	68	21.78571	10.89286
$11_{7,4-5}$	−34	83	30	15
$11_{6,5-6}$	−60	96	41.08929	20.54464
$11_{5,6-7}$	−82	107	57.18750	28.59375
$11_{4,7-8}$	−100	116	85.875	42.9375
$11_{3,8}$	−114	123	150.9375	1131.21094
$11_{3,9}$	−114	123	150.9375	−980.27344
$11_{2,9}$	−124	128	915	457.5
$11_{2,10}$	−124	128	−157.5	−78.75
$11_{1,10}$	−130	197	−255.9375	−1183.71094
$11_{1,11}$	−130	65	−255.9375	927.77344
$11_{0,11}$	−132	132	−1072.5	−536.25
$12_{12,0-1}$	132	12	3.13636	1.56818
$12_{11,1-2}$	86	35	9.4875	4.74375
$12_{10,2-3}$	44	56	16.11364	8.05682
$12_{9,3-4}$	6	75	23.325	11.6625
$12_{8,4-5}$	−28	92	31.64285	15.82143
$12_{7,5-6}$	−58	107	42	21
$12_{6,6-7}$	−84	120	56.20715	28.10357
$12_{5,7-8}$	−106	131	78.1875	39.09375
$12_{4,8-9}$	−124	140	117.9	58.95
$12_{3,9}$	−138	147	207.9375	1863.53906
$12_{3,10}$	−138	147	207.9375	−1655.60156
$12_{2,10}$	−148	152	1276.5	638.25
$12_{2,11}$	−148	152	−225	−112.5
$12_{1,11}$	−154	233	−360.9375	−1940.03906
$12_{1,12}$	−154	77	−360.9375	1579.10156
$12_{0,12}$	−156	156	−1501.5	−750.75

Letter to the Editor

PROMPT publication of brief reports of important discoveries in physics may be secured by addressing them to this department. The closing date for this department is the third of the month. Because of the late closing date for the section no proof can be shown to authors. The Board of Editors does not hold itself responsible for the opinions expressed by the correspondents. Communications should not in general exceed 600 words in length.

Steric Strains and the Anomalous Base Strengths of the Methylamines

HERBERT C. BROWN AND HERMAN BARTHOLOMAY, JR.
George Herbert Jones Laboratory, University of Chicago, Chicago, Illinois
November 27, 1942

THE increase in base strength resulting from the introduction of a methyl group into the ammonia molecule is ascribed to the operation of the positive inductive effect ($+I$). The further increase caused by the presence of a second methyl group is also ascribed to the same effect. A third methyl group, however, markedly reduces the strength of the resulting amine.[1]

So far no satisfactory explanation has been given for the interesting phenomenon just described. Recent studies dealing with the marked effect of steric strains on the strength of bases[2,3] suggest that such strains may be the cause of this anomalous behavior of the methylamines. The highly complex nature of the aqueous solutions of these bases, however, practically precludes any attempt to evaluate the effect of steric strains on the relative magnitudes of their dissociation constants.

TABLE I. Base dissociation constants for ammonia and the methylamines at 25°.

Amine	$K_b \times 10^5$
NH_3	1.79
$CH_3 \rightarrow NH_2$	42.5
$\begin{matrix} CH_3\searrow \\ CH_3\nearrow \end{matrix}$NH	59.9
$\begin{matrix} CH_3\searrow \\ CH_3\rightarrow \\ CH_3\nearrow \end{matrix}$N	6.31

To avoid these complications we have investigated the base strengths of ammonia and the methylamines in the vapor phase by using the trimethylboron as the reference acid. The dissociation constants of the addition compounds, obtained from equilibria represented by the following equation,

$$R_3N : B(CH_3)_3 \rightleftarrows R_3N + B(CH_3)_3$$

place the four bases in a relative order identical with that obtained by investigating their aqueous solutions by classical methods (compare Tables I and II).

The relative degrees of dissociation exhibited by these addition compounds may well be the result of two opposing effects of the methyl groups: first, the positive inductive effect which tends to increase the stability of the addition compound; second, the steric effect which tends to decrease that stability. The high base strength of monomethylamine, where the steric strain is small, can thus be attributed to the inductive effect of the methyl group. In trimethylamine, however, the steric strain resulting from the presence of three methyl groups is sufficient largely to overcome their inductive effect and markedly to decrease the strength of the base.

The agreement in the order of the amines as determined by the two different methods (Tables I and II), is probably not a matter of chance. It is reasonable to explain the identical orders in the same way—that is, by assuming the presence of large steric strain in the trimethylammonium ion even though the exact character of this strain is less obvious here than in the corresponding trimethylboron addition compounds. We shall attempt to elucidate this question in the near future, after we have completed a more intensive experimental study of the compounds in question.

TABLE II. Dissociation data of the addition compounds of trimethylboron with ammonia and the methylamines.

Compound	Temp. °C	Pressure observed, mm	Pressure calculated, mm	Degree of dissociation α	Dissociation constant, K(atmos.)
$NH_3 : B(CH_3)_3$	89.5	64.5	32.5	0.985	2.7
$CH_3NH_2 : B(CH_3)_3$	89.7	39.61	26.34	0.503	0.0176
$(CH_3)_2NH : B(CH_3)_3$	89.6	38.86	27.69	0.403	0.00991
$(CH_3)_3N : B(CH_3)_3$†	89.5	148.0	86.6	0.709	0.197

† Schlesinger, Flodin, and Burg, J. Am. Chem. Soc. **61**, 1078 (1938).

The results here given suggest many other applications of the steric strain hypothesis. For example, the high base strength of the cyclic imines[4] can be correlated with the probable absence of steric strain in these molecules as a result of their ring structure; the low coordination number of many metal ions in the complexes which they form with trimethylamine can be attributed to the large steric strains involved in packing a number of molecules of this amine about a small central atom.

We are now actively engaged in extending the steric strain hypothesis to the explanation of other puzzling phenomena.

[1] Everett and Wynne-Jones, Proc. Roy. Soc. London **177A**, 499 (1941).
[2] Brown, Schlesinger, and Cardon, J. Am. Chem. Soc. **64**, 325 (1942).
[3] Brown and Adams, J. Am. Chem. Soc. **64**, 2557 (1942).
[4] Adams and Mahan, J. Am. Chem. Soc. **64**, 2588 (1942).

THE AMERICAN INSTITUTE OF PHYSICS

INCORPORATED

ADMINISTRATIVE STAFF

HENRY A. BARTON, *Director*

MADELINE M. MITCHELL, *Publications Manager*

JOHN T. TATE, *Adviser on Publications*

Office: 175 Fifth Avenue, New York, New York

JOURNALS

THE PHYSICAL REVIEW
REVIEWS OF MODERN PHYSICS
JOHN T. TATE, *Editor (on leave)*
J. W. BUCHTA, *Acting Editor*

JOURNAL OF THE OPTICAL SOCIETY OF AMERICA
GEORGE R. HARRISON, *Editor*

THE JOURNAL OF THE ACOUSTICAL SOCIETY OF AMERICA
FLOYD A. FIRESTONE, *Editor*

AMERICAN JOURNAL OF PHYSICS
DUANE ROLLER, *Editor*

THE REVIEW OF SCIENTIFIC INSTRUMENTS
GAYLORD P. HARNWELL, *Editor*

THE JOURNAL OF CHEMICAL PHYSICS
JOSEPH E. MAYER, *Editor*

JOURNAL OF APPLIED PHYSICS
ELMER HUTCHISSON, *Editor*

GOVERNING BOARD

PAUL E. KLOPSTEG, *Chairman*
Central Scientific Company

GEORGE B. PEGRAM, *Secretary*
Columbia University

For the American Physical Society:

L. A. DUBRIDGE
University of Rochester

GEORGE B. PEGRAM
Columbia University

JOHN T. TATE
University of Minnesota

For the Optical Society:

R. C. GIBBS
Cornell University

A. C. HARDY
Massachusetts Institute of Technology

K. S. GIBSON
National Bureau of Standards

For the Acoustical Society of America:

FLOYD A. FIRESTONE
University of Michigan

HARVEY FLETCHER
Bell Telephone Laboratories

WALLACE WATERFALL
The Celotex Corporation

For the Society of Rheology:

R. B. DOW
Aberdeen Proving Ground

HERMANN MARK
Brooklyn Polytechnic Institute

N. W. TAYLOR
The Pennsylvania State College

For the American Association of Physics Teachers:

GEORGE R. HARRISON
Massachusetts Institute of Technology

PAUL E. KLOPSTEG
Central Scientific Company

A. G. WORTHING
University of Pittsburgh

The American Institute of Physics is a membership corporation of which five societies are the founding members. These five societies are the principal national societies devoted to pure and applied physics in America. Their names, and those of their representatives who form the Governing Board of the Institute, are given above. The principal activity of the Institute is the publication of journals sponsored by the societies or by itself. The names and the editors of the journals are also listed above.

The broad purpose of the Institute is to represent, in all matters of wide or common interest, the five thousand or more members and subscribers associated with the Founder Societies and the journals. It aims to advance the science and profession of physics, and to promote cooperation between pure research, the applied sciences and the industries. To achieve these aims, it is greatly in need of an endowment and is empowered by law to administer grants and funds of any kind.

CONTENTS

THE JOURNAL OF CHEMICAL PHYSICS VOL. 11, NO. 1 JANUARY, 1943

Volume Title Page i

Raman Spectra of Hydrocarbons. I. 1-Octene, *cis*+*trans* 2-Octene, *trans*-3-Octene, *trans*-4-Octene, 2-Octyne, and 1-Octyne . . . . . FORREST F. CLEVELAND 1

Activation Energy of the Reaction $CH_3+HBr=CH_4+Br$ and the Carbon-Hydrogen Bond Strength in Methane . . . . . HOLGER C. ANDERSEN AND G. B. KISTIAKOWSKY 6

Exchange of Radioactive Silver and Bromide with Silver Bromide Suspensions . . A. LANGE 11

Specific Heat of Pure Iron at Low Temperatures . . . . . K. K. KELLEY 16

Conductance of Aqueous Solutions of Potassium Bromide at Temperatures from 15° to 45°C, and the Limiting Mobility of Bromide Ion . . . H. E. GUNNING AND A. R. GORDON 18

Phosphorescence of Adsorbed Trypaflavine and Its Quenching by Oxygen . . . . . JAMES FRANCK AND PETER PRINGSHEIM 21

Asymmetric Rotor. I. Calculation and Symmetry Classification of Energy Levels . . . . . GILBERT W. KING, R. M. HAINER, AND PAUL C. CROSS 27

Letter to the Editor:

Boric Fluoride and the Comparative Base Strengths of the Methylamines . . . . . HERBERT C. BROWN AND HERMAN BERNHOLTZMAN, JR. 49

LANCASTER PRESS, INC., LANCASTER, PA.